CMB Polarization Measurements

CMB polarization (E)

- CMB photons are last scattered at recombination.
- It's a Thomson scattering, and any quadrupole anisotropy in the incoming photons produces a degree of linear polarization in the scattered photons.
- Density perturbation produce a small degree of linear polarization (E-modes)

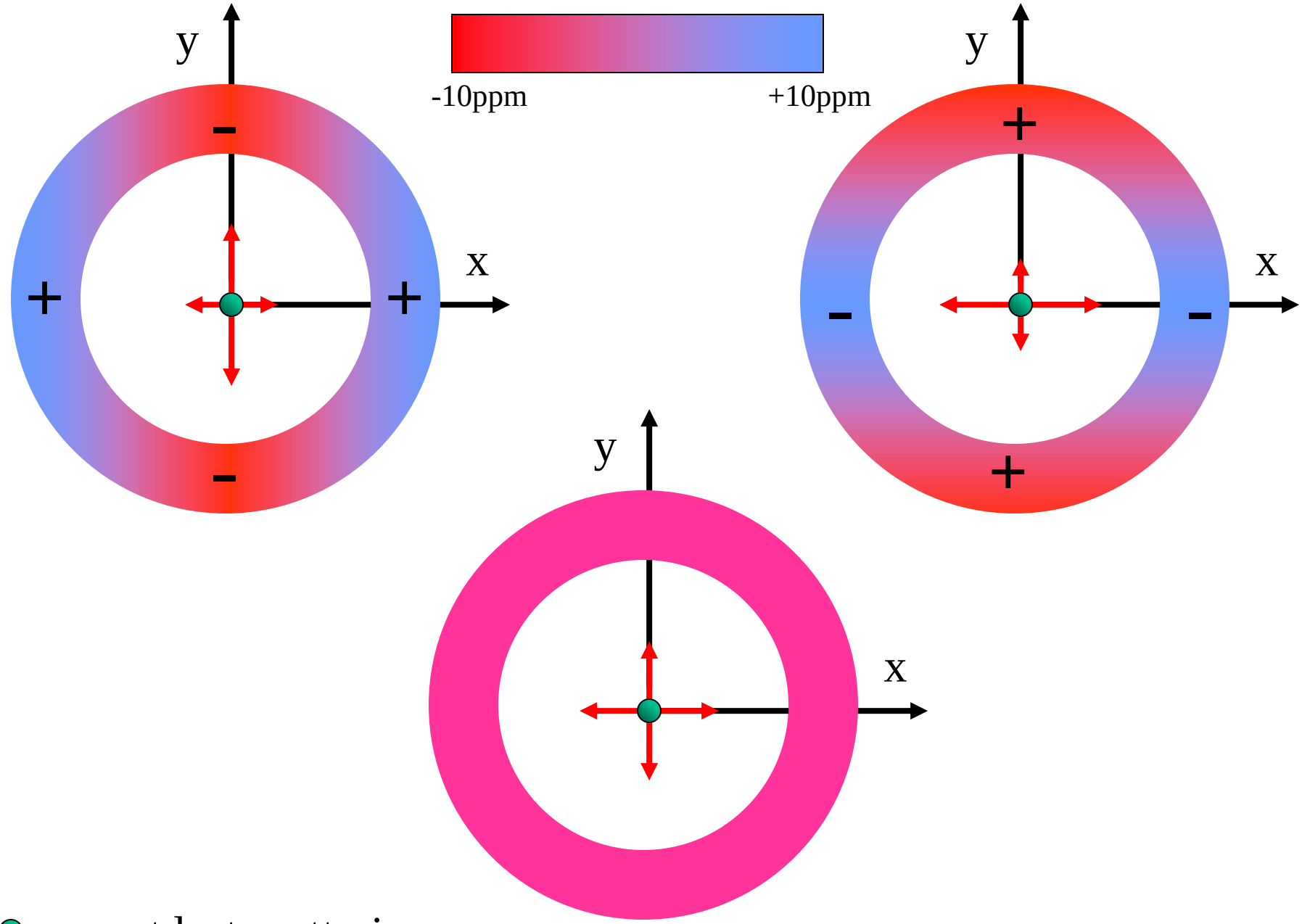

● = e^- at last scattering

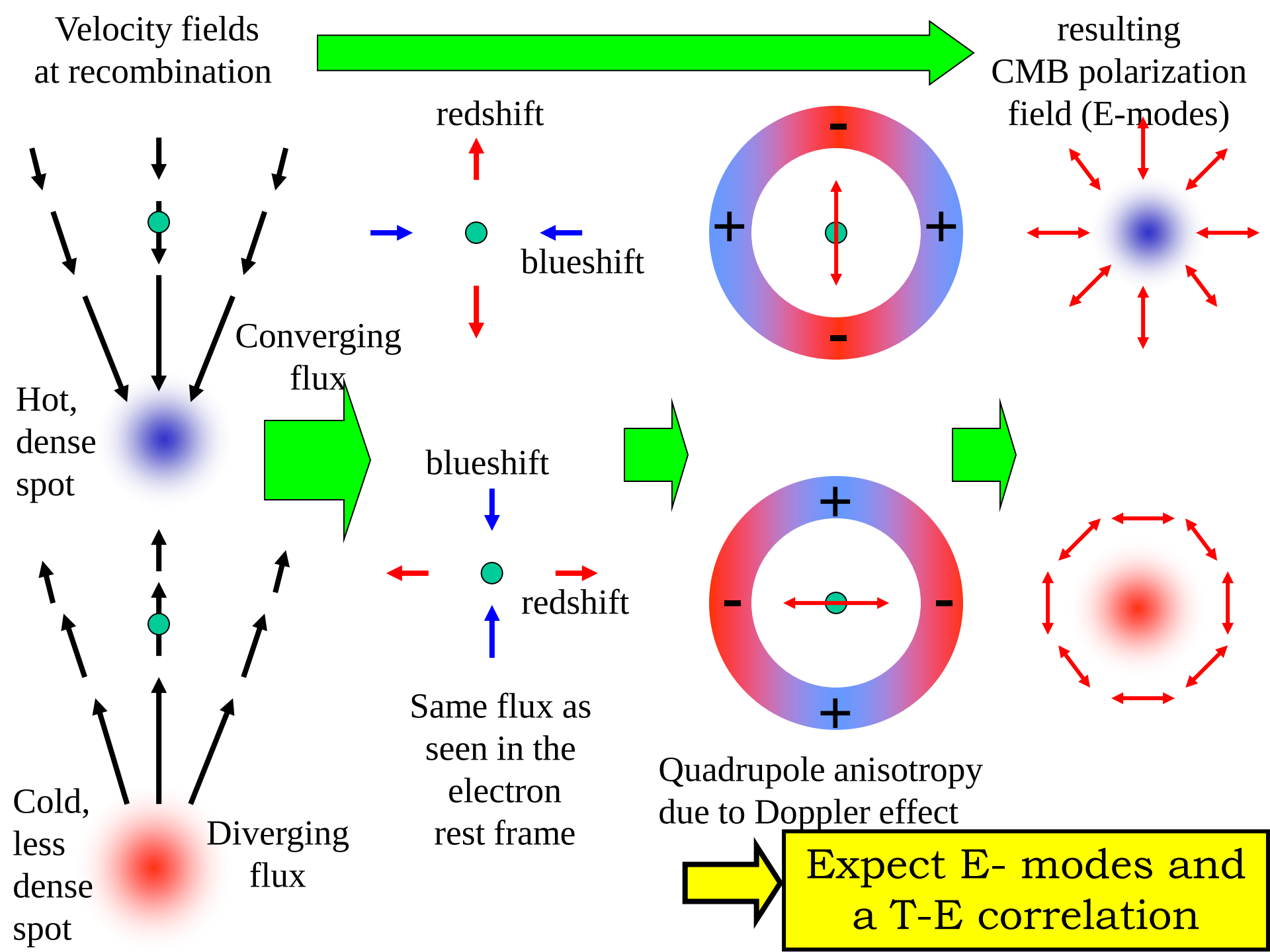
Velocity fields
at recombination
resulting
CMB polarization
field (E-modes)
redshift
blueshift
Converging
flux
Hot,
dense
spot
blueshift
redshift
Same flux as
seen in the
electron
rest frame
Quadrupole anisotropy
due to Doppler effect
Cold,
less
dense
spot
Diverging
flux
Expect E- modes and
a T-E correlation

- E-modes are irrotational
- E modes are related to velocities, while T is related mainly to density
- We expect a power spectrum of the E-modes, <EE>, with maxima and mimina in quadrature with the anisotropy power spectrum <TT>.

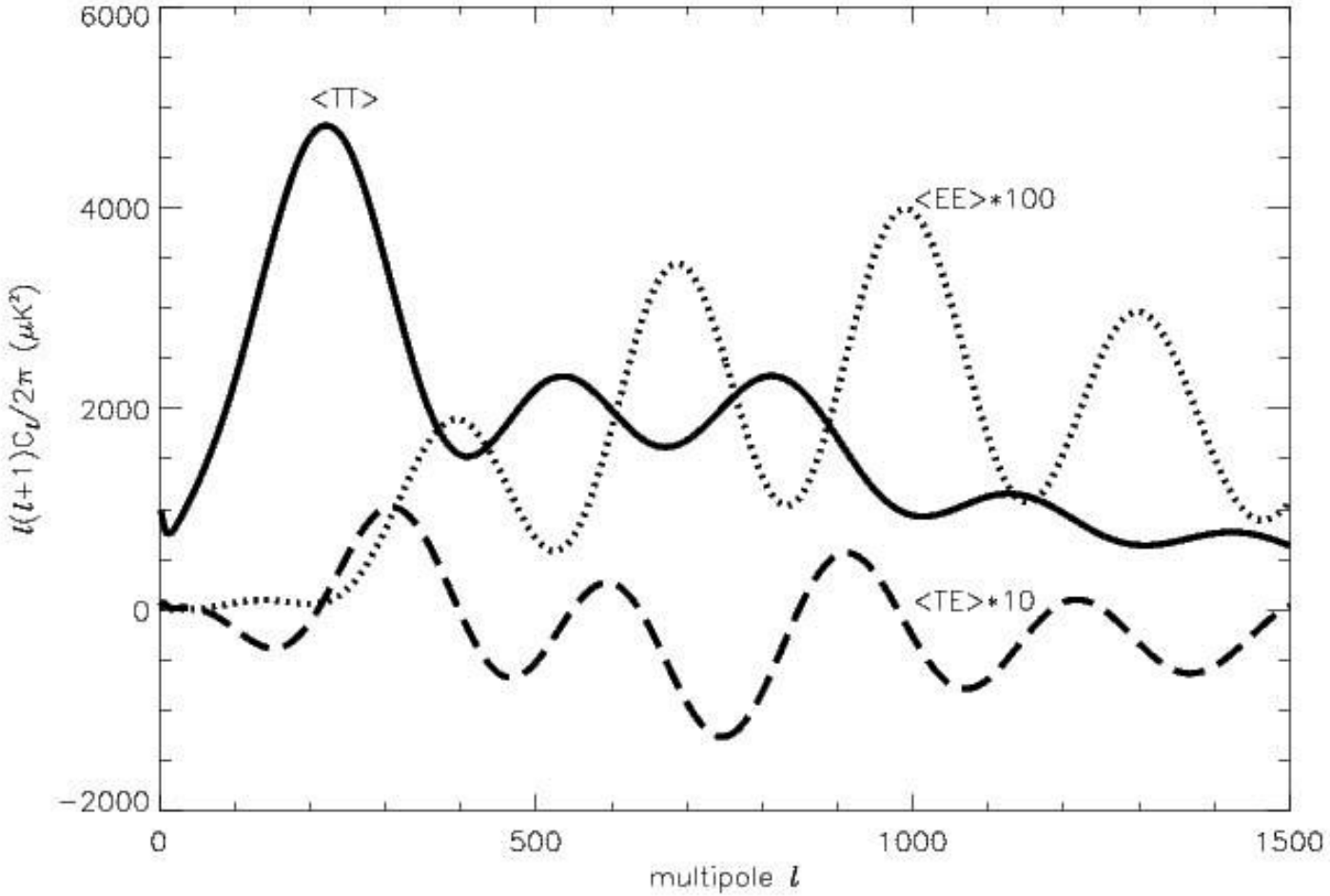

Figure 1.7: Estimated power spectra for the cosmological parameters: $\Omega_b = 0.05$, $\Omega_{cdm} = 0.3$, $\Omega_\Lambda = 0.65$, $\Omega_\nu = 0$, $H_0 = 65$ km/s/Mpc, $\tau = 0.17$. The temperature power spectrum, $\langle TT \rangle = C_\ell^T$, the E-modes power spectrum $\langle EE \rangle = C_\ell^E$ multiplied by a factor 100 to make it visible and the cross power spectrum between temperature and polarization, $\langle TE \rangle = C_\ell^{TE}$ multiplied by a factor 10. The spectra are computed using the publicly available code CMBFAST (http://www.cmbfast.org),

CMB polarization (B)

- CMB photons are last scattered at recombination.
- It's a Thomson scattering, and any quadrupole anisotropy in the incoming photons produces a degree of linear polarization in the scattered photons.
- Tensor perturbations (gravitational waves) produce a small degree of linear polarization with curl properties (B-modes)
- Also, lensing of E-modes does the same at smaller scales

If inflation really happened…

- It stretched geometry of space to nearly Euclidean
- It produced a nearly scale invariant spectrum of density fluctuations
- It produced a stochastic background of gravitational waves.

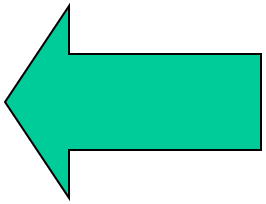

OK

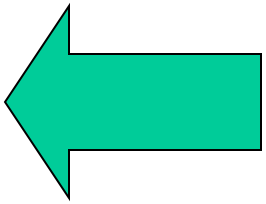

OK

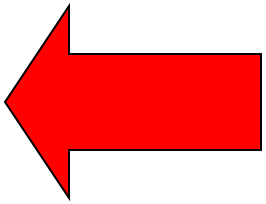

?

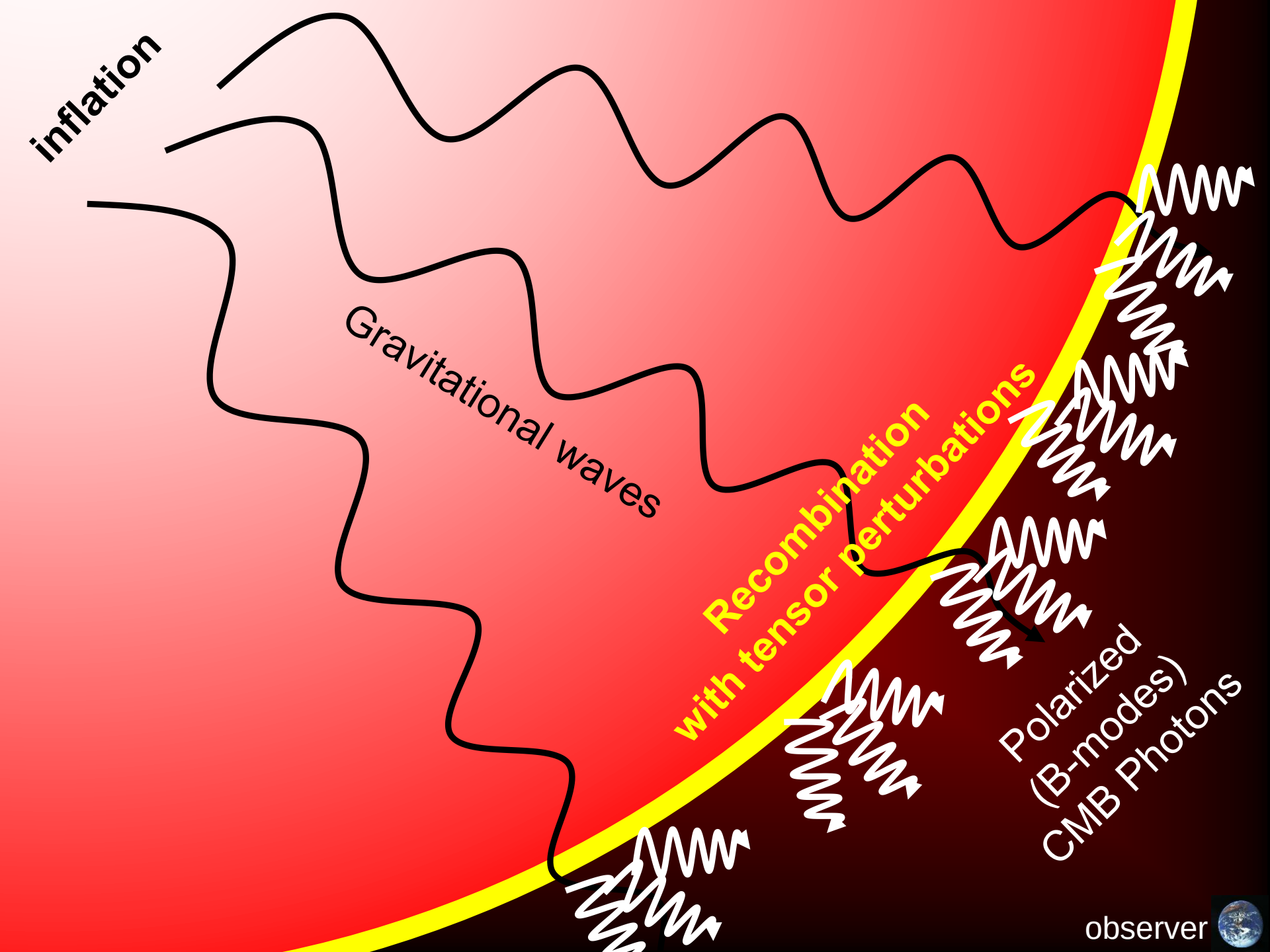
inflation
Gravitational waves
Recombination
with tensor perturbations
Polarized
(B-modes)
CMB Photons
observer

Quadrupole from P.G.W.

- If inflation really happened:
  - ✓ It stretched geometry of space to nearly Euclidean
  - ✓ It produced a nearly scale invariant spectrum of gaussian density fluctuations
  - ✓ It produced a stochastic background of gravitational waves: Primordial G.W. The background is so faint that even LISA will not be able to measure it.
- Tensor perturbations also produce quadrupole anisotropy. They generate irrotational (E-modes) **and rotational (B-modes) components** in the CMB polarization field.
- Since B-modes are not produced by scalar fluctuations, they represent a signature of inflation.

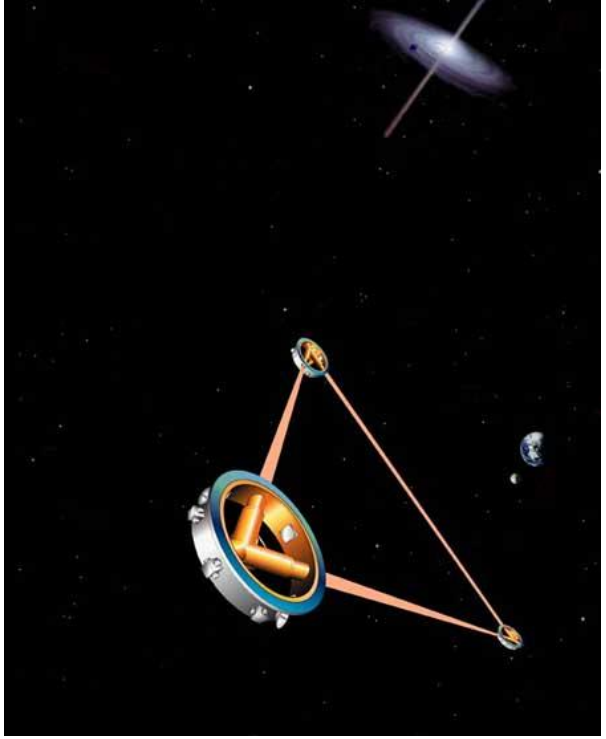

E-modes

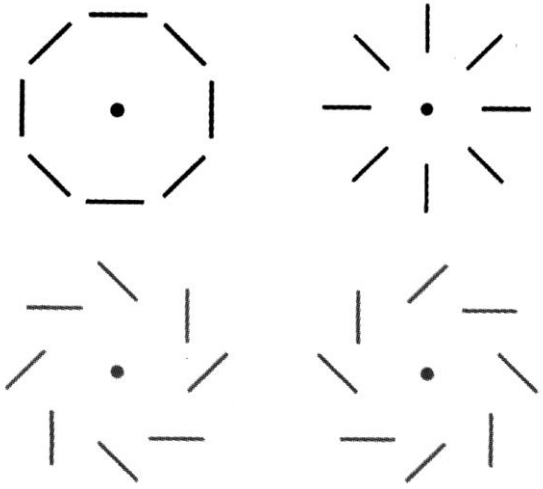

B-modes

B-modes from P.G.W.

- The amplitude of this effect is very small, but depends on the Energy scale of inflation. In fact the amplitude of tensor modes normalized to the scalar ones is:

$$\left(\frac{T}{S}\right)^{1/4} \equiv \left(\frac{C_2^{GW}}{C_2^{Scalar}}\right)^{1/4} \cong \frac{V^{1/4}}{3.7\times10^{16}\,\mathrm{GeV}}$$

← Inflation potential

- and

$$\sqrt{\frac{\ell(\ell+1)}{2\pi}C_{\ell\,\max}^{B}} \cong 0.1\mu K\left[\frac{V^{1/4}}{2\times10^{16}\,\mathrm{GeV}}\right]$$

- There are theoretical arguments to expect that the energy scale of inflation is close to the scale of GUT i.e. around 10^{16} GeV.
- The current upper limit on anisotropy at large scales gives $T/S<0.5$ (at 2σ)
- A competing effect is lensing of E-modes, which is important at large multipoles.

E-modes & B-modes

Spin-2 quantity Spin-2 basis

$$(Q \pm iU)(\vec{n}) = \sum_{\ell,m} \left(a^{E}_{\ell m} \pm i a^{B}_{\ell m} \right) {}_{\pm 2}Y_{\ell m}(\vec{n})$$

- From the measurements of the Stokes Parameters $\boldsymbol{Q}$ and $\boldsymbol{U}$ of the linear polarization field we can recover both irrotational and rotational a_{lm} by means of modified Legendre transforms:

E-modes produced by scalar and tensor perturbations

$$a^{E}_{\ell m} = \frac{1}{2} \int d\Omega W(\vec{n}) \left[(Q + iU)(\vec{n}) {}_{+2}Y_{\ell m}(\vec{n}) + (Q - iU)(\vec{n}) {}_{-2}Y_{\ell m}(\vec{n}) \right]$$

B-modes produced **only** by tensor perturbations

$$a^{B}_{\ell m} = \frac{1}{2i} \int d\Omega W(\vec{n}) \left[(Q + iU)(\vec{n}) {}_{+2}Y_{\ell m}(\vec{n}) - (Q - iU)(\vec{n}) {}_{-2}Y_{\ell m}(\vec{n}) \right]$$

The signal is extremely weak

- Nobody really knows how to detect this.
  - Pathfinder experiments are needed
- Whatever smart, ambitious experiment we design to detect the B-modes:
  - It needs to be extremely sensitive
  - It needs an extremely careful control of systematic effects
  - It needs careful control of foregrounds
  - It will need independent experiments with orthogonal systematics.
- There is still a long way to go: …

How to characterize and measure Polarization

Stokes Parameters

$$I = S_o = E_{oy}^2 + E_{ox}^2$$

$$Q = S_1 = E_{ox}^2 - E_{oy}^2$$

$$U = S_2 = 2E_{ox}E_{oy}\cos\delta$$

$$V = S_3 = 2E_{ox}E_{oy}\sin\delta$$

- If light is not purely monochromatic, the amplitudes and phases fluctuate with time.
- It can be shown that, in general,

$$S_o^2 \geq S_1^2 + S_2^2 + S_3^2$$

- The = sign is valid for ***fully polarized*** light, while the > sign is valid for ***partially polarized*** or ***unpolarized*** light. *P*=degree of polarization:

$$P = \frac{I_{pol}}{I_{total}} = \frac{\sqrt{S_1^2 + S_2^2 + S_3^2}}{S_o}$$

$$0 \leq P \leq 1$$

- The ***intensity*** is related to S_o:

$$S_o = E_{oy}^2 + E_{ox}^2$$

- The ***orientation*** of the polarization ellipse is related to S_1 and S_2:

$$\tan 2\psi = \frac{2E_{ox}E_{oy}\cos\delta}{E_{ox}^2 - E_{oy}^2} = \frac{S_2}{S_1}$$

- The ***ellipticity*** of the polarization ellipse is related to S_3:

$$\sin 2\chi = \frac{2E_{ox}E_{oy}\sin\delta}{E_{ox}^2 + E_{oy}^2} = \frac{S_3}{S_o}$$

Classical measurement of the Stokes Parameters

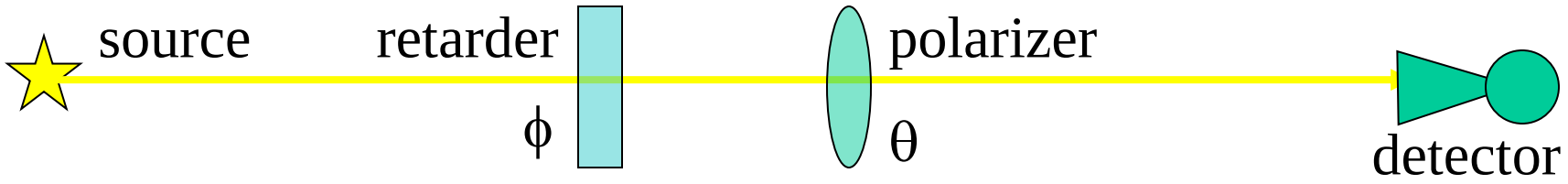

- The measurement of the 4 Stokes Parameters needs two optical components:
  - A ***retarder*** (wave plate): it is a phase-shifting element, whose effect is to advance the phase of the x component by $\phi/2$ and to retard the phase of the y component by $-\phi/2$. So the field emerging from the retarder is $E'_x = E_x e^{i\phi/2}$ and $E'_y = E_y e^{-i\phi/2}$
  - A ***polarizer***. The optical field can pass only along one axis, the transmission axis. So the total field emerging from the polarizer is $E'' = E'_x \cos\theta + E'_y \sin\theta$, where E' is the incident field and θ is the angle of the transmission axis.
- So the beam arriving on the detector is

$$E'' = E_x e^{i\phi/2} \cos\theta + E_y e^{-i\phi/2} \sin\theta$$

Classical measurement of the Stokes Parameters

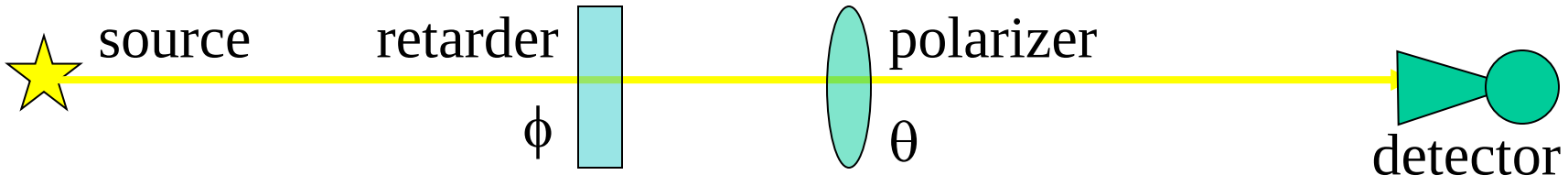

- $E'' = E_x e^{i\,\phi/2} \cos\theta + E_y e^{-i\,\phi/2} \sin\theta$
- The detector measures its intensity, i.e. $I = E''E''^*$
- So we get $I(\vartheta,\phi) = E_x E_x^* \cos^2\theta + E_y E_y^* \sin^2\theta +$

$$+ E_x^* E_y e^{-i\phi} \sin\theta\cos\theta + E_x E_y^* e^{i\phi} \sin\theta\cos\theta$$

- Which can be rewritten using the half-angle formulas:

$$\cos^2\theta = \frac{1+\cos 2\theta}{2} \qquad \sin^2\theta = \frac{1-\cos 2\theta}{2} \qquad \sin\theta\cos\theta = \frac{\sin 2\theta}{2}$$

$$I(\vartheta,\phi) = \frac{1}{2}\left[\begin{array}{l}\left(E_x E_x^* + E_y E_y^*\right) + \left(E_x E_x^* - E_y E_y^*\right)\cos 2\theta \\ + \left(E_x E_y^* + E_y E_x^*\right)\cos\phi \sin 2\theta + i\left(E_x E_y^* - E_y E_x^*\right)\sin\phi \sin 2\theta\end{array}\right]$$

$$I(\vartheta,\phi) = \frac{1}{2}\left[S_o + S_1\cos 2\theta + S_2\cos\phi\sin 2\theta + S_3\sin\phi\sin 2\theta\right]$$

Classical measurement of the Stokes Parameters

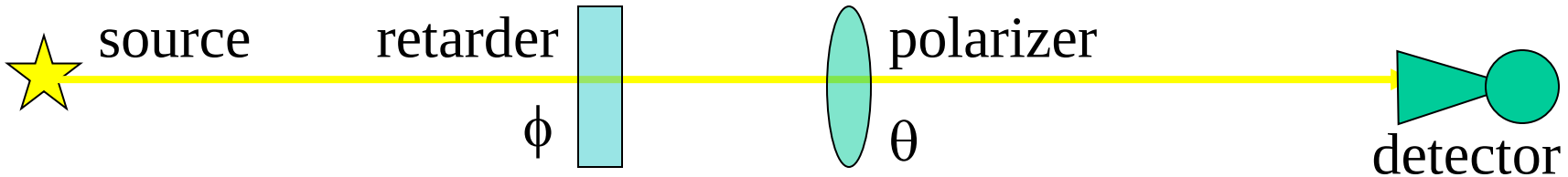

$$I(\vartheta,\phi)=\tfrac{1}{2}\left[S_o+S_1\cos 2\theta+S_2\cos\phi\sin 2\theta+S_3\sin\phi\sin 2\theta\right]$$

- This is the formula derived in 1852 by Sir George Gabriel Stokes.
- The first three parameters can be measured by removing the retarder ($\phi=0$) and measuring the intensity with three orientations of the polarizer θ=0°,45°,90°:
- The fourth parameter can be measured by inserting a 90° retarder (quarter wave plate):

$$\begin{cases} I(0^o,0^o)=\tfrac{1}{2}\left[S_o+S_1\right] \\ I(45^o,0^o)=\tfrac{1}{2}\left[S_o+S_2\right] \\ I(90^o,0^o)=\tfrac{1}{2}\left[S_o-S_1\right] \\ I(45^o,90^o)=\tfrac{1}{2}\left[S_o+S_3\right] \end{cases}$$

$$\begin{cases} S_o=I(0^o,0^o)+I(90^o,0^o) \\ S_1=I(0^o,0^o)-I(90^o,0^o) \\ S_2=2I(45^o,0^o)-I(0^o,0^o)-I(90^o,0^o) \\ S_3=2I(45^o,90^o)-I(0^o,0^o)-I(90^o,0^o) \end{cases}$$

Classical measurement of the Stokes Parameters

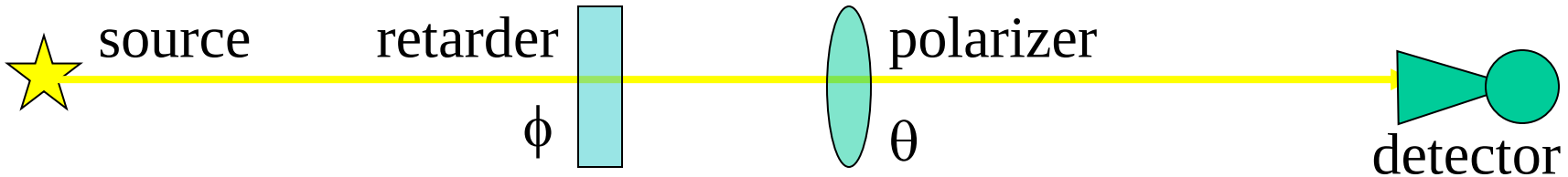

$$I(\vartheta,\phi) = \tfrac{1}{2}\left[S_o + S_1\cos 2\theta + S_2\cos\phi\sin 2\theta + S_3\sin\phi\sin 2\theta\right]$$

- The great advantage of the Stokes Parameters is that they are observable. The polarization ellipse is not (too fast).
- Moreover, the Stokes parameters can be used to describe unpolarized light: light which is not affected by the rotation of a polarized or by the presence of a retarder. Stokes was the first one to describe mathematically unpolarized and partially polarized light.
- It is evident from Stokes formula that, for unpolarized light, $S_1=S_2=S_3=0$, while $S_o>0$.
- The fully polarized light had $S_o^2 = S_1^2 + S_2^2 + S_3^2$
- The intermediate state is partially polarized light, where $S_o^2 \geq S_1^2 + S_2^2 + S_3^2$

Polarization-active optical components

- When a beam of light interacts with matter its polarization state is almost always changed.
- It can be changed by
  - changing the amplitudes → Polarizer (Diattenuator)
  - changing the phases → Wave-plate (Retarder)
  - changing the directions → Rotator

  of the orthogonal field components.
- Their effect can be described by means of the Mueller matrices: M is a 4x4 matrix such that the emerging Stokes vector is S'=M S .

1) Polarizer or Diattenuator

- It attenuates the orthogonal components of an optical beam unequally:

$$\begin{cases} E_x' = p_x E_x \\ E_y' = p_y E_y \end{cases}$$

- Using the definitions of S and S'

$$\begin{pmatrix} S_o' \\ S_1' \\ S_2' \\ S_3' \end{pmatrix} = \begin{pmatrix} E_x' E_x'^* + E_y' E_y'^* \\ E_x' E_x'^* - E_y' E_y'^* \\ E_x' E_y'^* + E_y' E_x'^* \\ i(E_x' E_y'^* - E_y' E_x'^*) \end{pmatrix} \qquad \begin{pmatrix} S_o \\ S_1 \\ S_2 \\ S_3 \end{pmatrix} = \begin{pmatrix} E_x E_x^* + E_y E_y^* \\ E_x E_x^* - E_y E_y^* \\ E_x E_y^* + E_y E_x^* \\ i(E_x E_y^* - E_y E_x^*) \end{pmatrix}$$

- And inserting the expressions for *E'* we get

$$\begin{pmatrix} S_o' \\ S_1' \\ S_2' \\ S_3' \end{pmatrix} = \frac{1}{2} \begin{pmatrix} p_x^2 + p_y^2 & p_x^2 - p_y^2 & 0 & 0 \\ p_x^2 - p_y^2 & p_x^2 + p_y^2 & 0 & 0 \\ 0 & 0 & 2p_x p_y & 0 \\ 0 & 0 & 0 & 2p_x p_y \end{pmatrix} \begin{pmatrix} S_o \\ S_1 \\ S_2 \\ S_3 \end{pmatrix}$$

2) Retarder

- It introduces a phase shift between the orthogonal components of an optical beam :

$$\begin{cases} E_x'(t) = e^{+i\varphi/2} E_x(t) \\ E_y'(t) = e^{-i\varphi/2} E_y(t) \end{cases}$$

- Using the definitions of S and S'

$$\begin{pmatrix} S_o' \\ S_1' \\ S_2' \\ S_3' \end{pmatrix} = \begin{pmatrix} E_x' E_x'^* + E_y' E_y'^* \\ E_x' E_x'^* - E_y' E_y'^* \\ E_x' E_y'^* + E_y' E_x'^* \\ i(E_x' E_y'^* - E_y' E_x'^*) \end{pmatrix} \qquad \begin{pmatrix} S_o \\ S_1 \\ S_2 \\ S_3 \end{pmatrix} = \begin{pmatrix} E_x E_x^* + E_y E_y^* \\ E_x E_x^* - E_y E_y^* \\ E_x E_y^* + E_y E_x^* \\ i(E_x E_y^* - E_y E_x^*) \end{pmatrix}$$

- And inserting the expressions for *E'* we get

$$\begin{pmatrix} S_o' \\ S_1' \\ S_2' \\ S_3' \end{pmatrix} = \begin{pmatrix} 1 & 0 & 0 & 0 \\ 0 & 1 & 0 & 0 \\ 0 & 0 & \cos\varphi & \sin\varphi \\ 0 & 0 & \sin\varphi & \cos\varphi \end{pmatrix} \begin{pmatrix} S_o \\ S_1 \\ S_2 \\ S_3 \end{pmatrix}$$

Special cases

$$\begin{pmatrix} S_o' \\ S_1' \\ S_2' \\ S_3' \end{pmatrix} = \begin{pmatrix} 1 & 0 & 0 & 0 \\ 0 & 1 & 0 & 0 \\ 0 & 0 & \cos\varphi & -\sin\varphi \\ 0 & 0 & \sin\varphi & \cos\varphi \end{pmatrix} \begin{pmatrix} S_o \\ S_1 \\ S_2 \\ S_3 \end{pmatrix}$$

- If the retarder is a quarter-wave plate (ϕ=90^o):

$$\begin{pmatrix} S_o' \\ S_1' \\ S_2' \\ S_3' \end{pmatrix} = \begin{pmatrix} 1 & 0 & 0 & 0 \\ 0 & 1 & 0 & 0 \\ 0 & 0 & 0 & -1 \\ 0 & 0 & 1 & 0 \end{pmatrix} \begin{pmatrix} S_o \\ S_1 \\ S_2 \\ S_3 \end{pmatrix}$$

- Such a retarder converts a $\pm$45^o linearly polarized beam into a right/left circularly polarized beam:

$$\begin{pmatrix} 1 \\ 0 \\ 0 \\ \pm 1 \end{pmatrix} = \begin{pmatrix} 1 & 0 & 0 & 0 \\ 0 & 1 & 0 & 0 \\ 0 & 0 & 0 & -1 \\ 0 & 0 & 1 & 0 \end{pmatrix} \begin{pmatrix} 1 \\ 0 \\ \pm 1 \\ 0 \end{pmatrix}$$

- If the retarder is a half-wave plate (ϕ=180^o):
- This reverses the ellipticity and orientation of the incomin polarization state.

$$\begin{pmatrix} S_o' \\ S_1' \\ S_2' \\ S_3' \end{pmatrix} = \begin{pmatrix} 1 & 0 & 0 & 0 \\ 0 & 1 & 0 & 0 \\ 0 & 0 & -1 & 0 \\ 0 & 0 & 0 & -1 \end{pmatrix} \begin{pmatrix} S_o \\ S_1 \\ S_2 \\ S_3 \end{pmatrix}$$

3) Rotator

- Here $\begin{cases} E_x'(t) = E_x(t)\cos\theta + E_y(t)\sin\theta \\ E_y'(t) = -E_x(t)\sin\theta + E_y(t)\cos\theta \end{cases}$

- Using the definitions of S and S'

$$\begin{pmatrix} S_o' \\ S_1' \\ S_2' \\ S_3' \end{pmatrix} = \begin{pmatrix} E_x'E_x'^* + E_y'E_y'^* \\ E_x'E_x'^* - E_y'E_y'^* \\ E_x'E_y'^* + E_y'E_x'^* \\ i(E_x'E_y'^* - E_y'E_x'^*) \end{pmatrix} \qquad \begin{pmatrix} S_o \\ S_1 \\ S_2 \\ S_3 \end{pmatrix} = \begin{pmatrix} E_xE_x^* + E_yE_y^* \\ E_xE_x^* - E_yE_y^* \\ E_xE_y^* + E_yE_x^* \\ i(E_xE_y^* - E_yE_x^*) \end{pmatrix}$$

- And inserting the expressions for *E'* we get

$$\begin{pmatrix} S_o' \\ S_1' \\ S_2' \\ S_3' \end{pmatrix} = \begin{pmatrix} 1 & 0 & 0 & 0 \\ 0 & \cos 2\theta & \sin 2\theta & 0 \\ 0 & -\sin 2\theta & \cos 2\theta & 0 \\ 0 & 0 & 0 & 1 \end{pmatrix} \begin{pmatrix} S_o \\ S_1 \\ S_2 \\ S_3 \end{pmatrix}$$

Rotated Optical Components

- We have assumed that the optical axis of the components we have considered were aligned to the coordinate system.
- If they are not (as often happens), we have to
  1. rotate the incident beam from the original coordinate system to the one aligned with the component: $S' = M_R(\theta) S_{in}$
  2. Multiply S' by the Mueller matrix M_C of the optical component $S'' = M_C S'$
  3. Rotate the output beam back into the original coordinate system:

     $S_{out} = M_R(-\theta)\, S''$
- So we have:

  $S_{out} = M_R(-\theta)\, M_C\, M_R(\theta)\, S_{in}$

  Where θ is the rotation on the optical component C.

$$M_R(\theta) = \begin{pmatrix} 1 & 0 & 0 & 0 \\ 0 & \cos 2\theta & \sin 2\theta & 0 \\ 0 & -\sin 2\theta & \cos 2\theta & 0 \\ 0 & 0 & 0 & 1 \end{pmatrix} \underset{def}{=} \begin{pmatrix} 1 & 0 & 0 & 0 \\ 0 & c_2 & s_2 & 0 \\ 0 & -s_2 & c_2 & 0 \\ 0 & 0 & 0 & 1 \end{pmatrix}$$

Linear Polarimeter

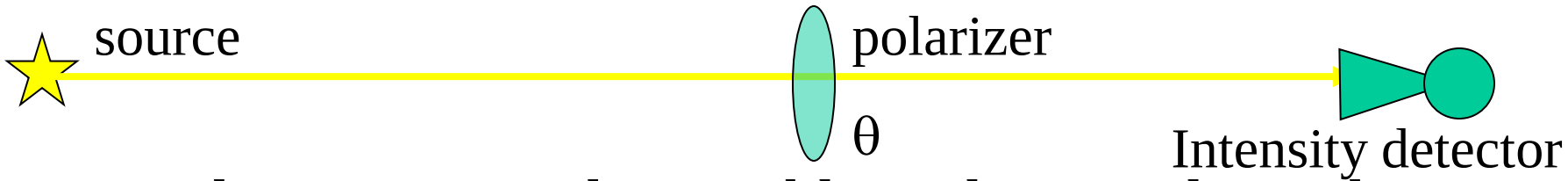

- A polarimeter is a device able to detect polarized light and measure its polarization characteristics.
- The simplest polarimeter we can imagine is a linear polarimeter, which can be built with a rotating polarizer in front of an intensity detector.
- An intensity detector is represented by a Stokes vector D=(1,0,0,0). The power detected by the detector from an optical beam with Stokes vector S is simply $w=DS=S_o$
- If we put a polarizer in front of the detector, the polarizer is called analyzer, and the power detected will be $w(\theta) = DM_P(\theta)S$

Linear Polarimeter

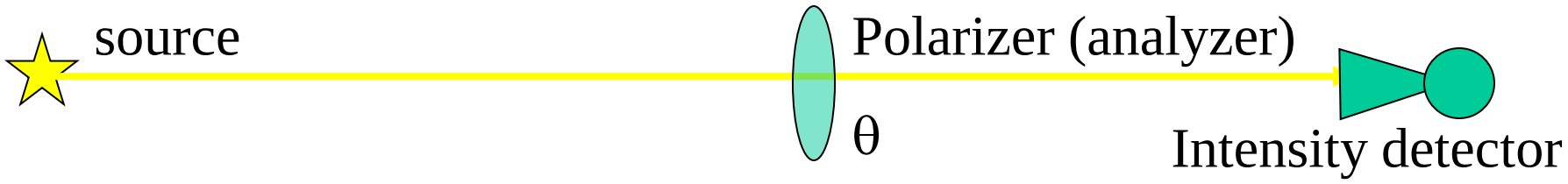

$$w = DM_P(\theta)S = (1,0,0,0)\frac{1}{2}\begin{pmatrix} \Sigma & c_2\Delta & s_2\Delta & 0 \\ c_2\Delta & c_2^2\Sigma + s_2^2 X & s_2 c_2(\Sigma - X) & 0 \\ s_2\Delta & s_2 c_2(\Sigma - X) & s_2^2\Sigma + c_2^2 X & 0 \\ 0 & 0 & 0 & X \end{pmatrix}\begin{pmatrix} S_o \\ S_1 \\ S_2 \\ S_3 \end{pmatrix} \Rightarrow$$

$$w = \tfrac{1}{2}\left(\Sigma S_o + \Delta S_1 \cos 2\theta + \Delta S_2 \sin 2\theta\right)$$

This polarimeter is not sensitive to circular polarization (no S_3).
It is sensitive to linear polarization (S_1 and S_2) and to unpolarized light (S_o).

If the polarizer is ideal: $\Delta = 1 \;\; ; \;\; \Sigma = 1 \;\; ; \;\; X = 0$

$$w = \tfrac{1}{2}\left(S_o + S_1 \cos 2\theta + S_2 \sin 2\theta\right)$$

Linear Polarimeter

- If we are interested to the linear polarized component only, we can rotate continuously the polarizer: $\theta=\omega t$ and look only for the AC signal at frequency 2ω.
- This allows to reject the unpolarized component, even if it is dominant, and to remove all the noise components at frequencies different than 2ω (synchronous demodulation).

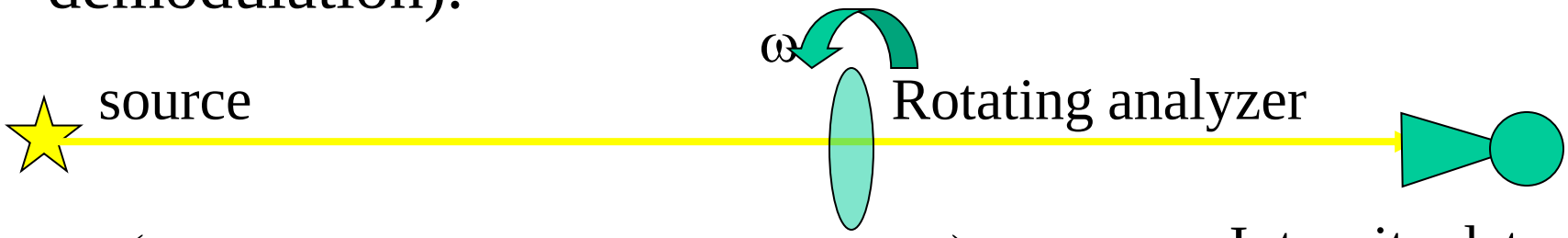

$$w = \tfrac{1}{2}\left(\Sigma S_o + \Delta S_1 \cos 2\omega t + \Delta S_2 \sin 2\omega t\right)$$

$$V(t) = Rw(t) + N(t) = \tfrac{1}{2} R\left[\Sigma S_o + \Delta\left(S_1 \cos 2\omega t + S_2 \sin 2\omega t\right)\right] + N(t)$$

detector responsivity

constant signal (DC)

modulated signal (AC)

noise (AC)

Linear Polarimeter

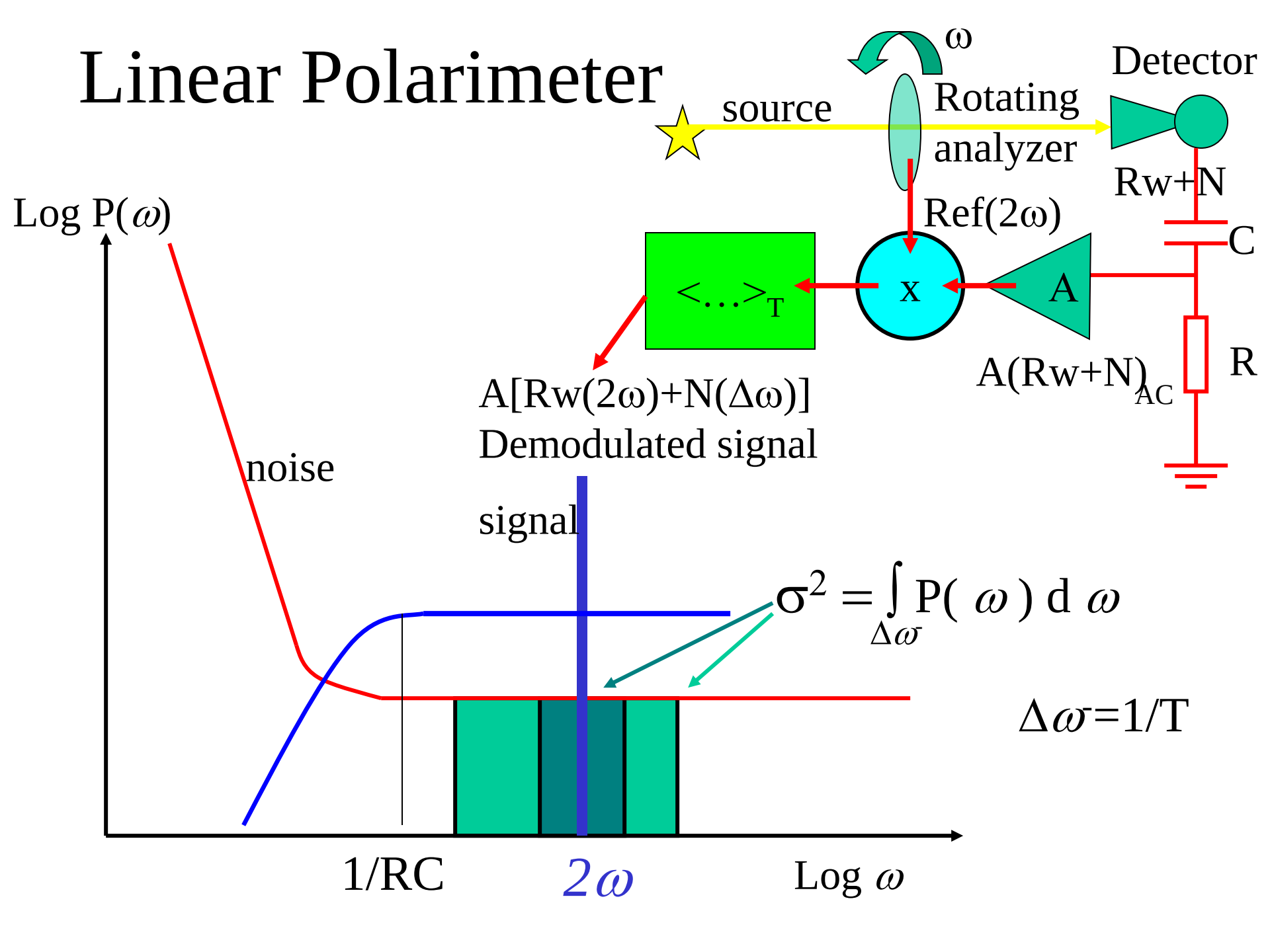

How do we separate S_1 and S_2

$$V(t) = Rw(t) + N(t) = \tfrac{1}{2} R\left[\Sigma S_o + \Delta\left(S_1 \cos 2\omega t + S_2 \sin 2\omega t\right)\right] + N(t)$$

- Neglecting the stochastic effect of noise (we integrate enough that N becomes negligible) and of the constant term (which we remove with the AC decoupling)

$$V(t) = Rw(t) = \tfrac{1}{2} R\left[\Delta\left(S_1 \cos 2\omega t + S_2 \sin 2\omega t\right)\right]$$

- We measure V and we want to estimate S_1 and S_2. We can use two reference signals, out of phase by T/8 and synchronously demodulate with them:

How do we separate S_1 and S_2

$$X = \frac{1}{T}\int_0^T V(t)\sin 2\omega t dt = \frac{1}{2}\frac{R\Delta}{T}\left[S_1 \int_0^T \cos 2\omega t \sin 2\omega t dt + S_2 \int_0^T \sin 2\omega t \sin 2\omega t dt \right]$$

$$Y = \frac{1}{T}\int_0^T V(t)\cos 2\omega t dt = \frac{1}{2}\frac{R\Delta}{T}\left[S_1 \int_0^T \cos 2\omega t \cos 2\omega t dt + S_2 \int_0^T \sin 2\omega t \cos 2\omega t dt \right]$$

$$X = \frac{1}{8} R\Delta S_2$$

$$Y = \frac{1}{8} R\Delta S_1$$

- So the double linear polarimeter is insensitive to S_o and it is easy to calibrate.
- Is this a troubleless instrument ? No !
- It is inefficient (factor 1/8 from modulation and demodulation)
- It can be microphonic.
- And, as all polarimeters, needs a telescope.

Systematics of the linear polarimeter

- The main disadvantage of the linear polarimeter, in its naive implementation consisiting in a rotating polarizer in front of an intensity detector, is the spurious polarization produced by any polarization sensitivity of the detector.

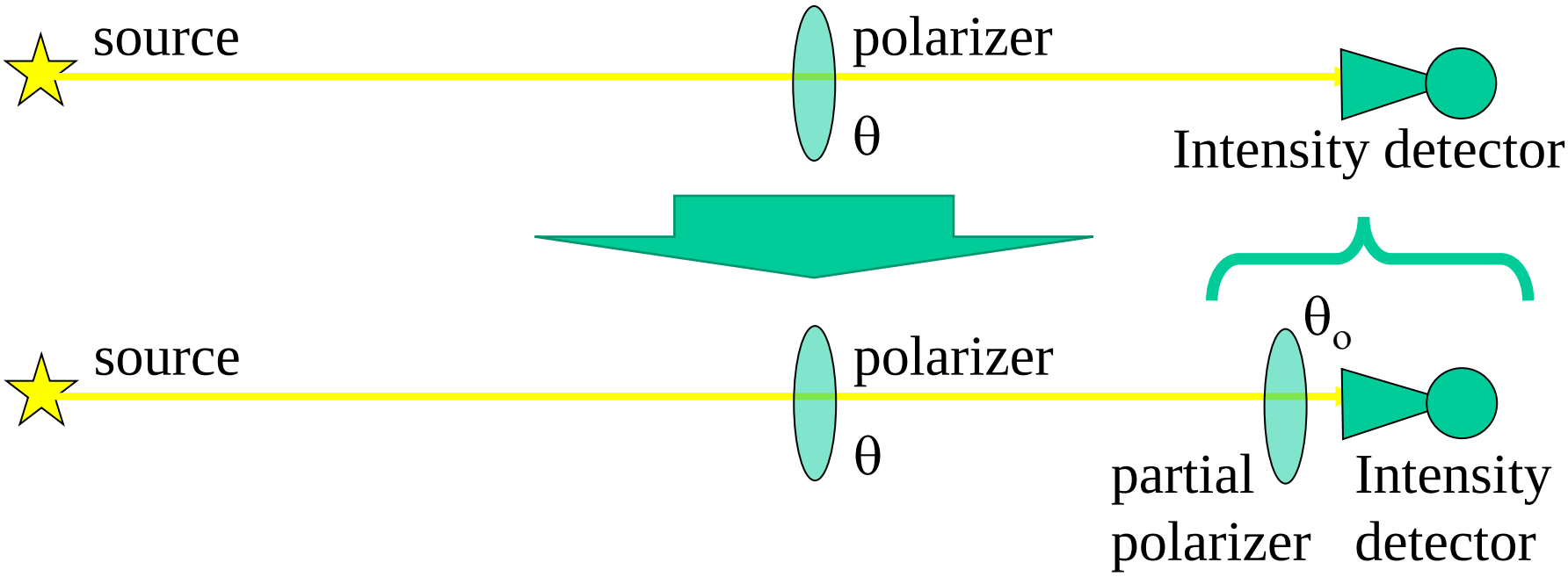

Systematics of the linear polarimeter

- A possible solution of the problem is the joint rotation of both the polarizer and the detector.

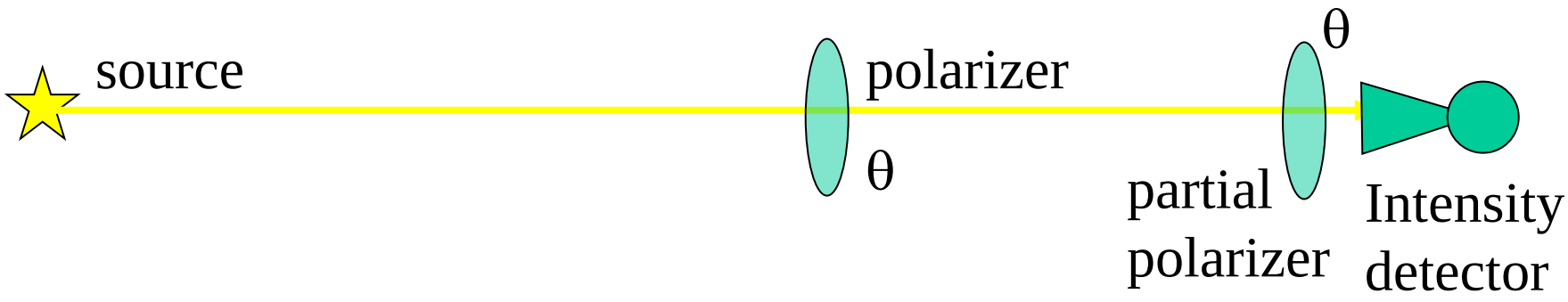

- This solves the problem with the polarization sensitivity of the detector, but another problem remains: if the source is anisotropic, and the detector beam is elliptical, a spurious polarization is detected even if the source is unpolarized.

Systematics of the linear polarimeter

- If an unpolarized source is anisotropic or off axis, and the detector beam is elliptical, a signal mimiking a polarized source (spurious polarization) is detected, even if the source is unpolarized.
- This is called intensity to polarization leakage.

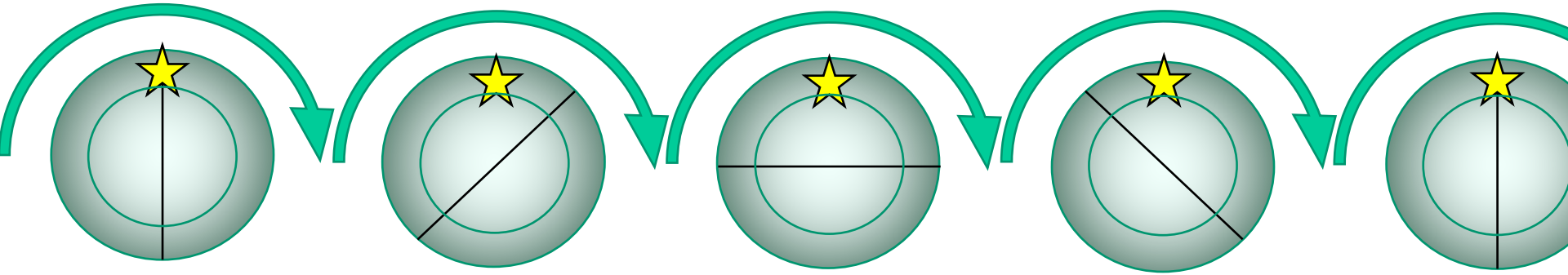

Circular beam: constant signal from an unpolarized off-axis/anisotropic source

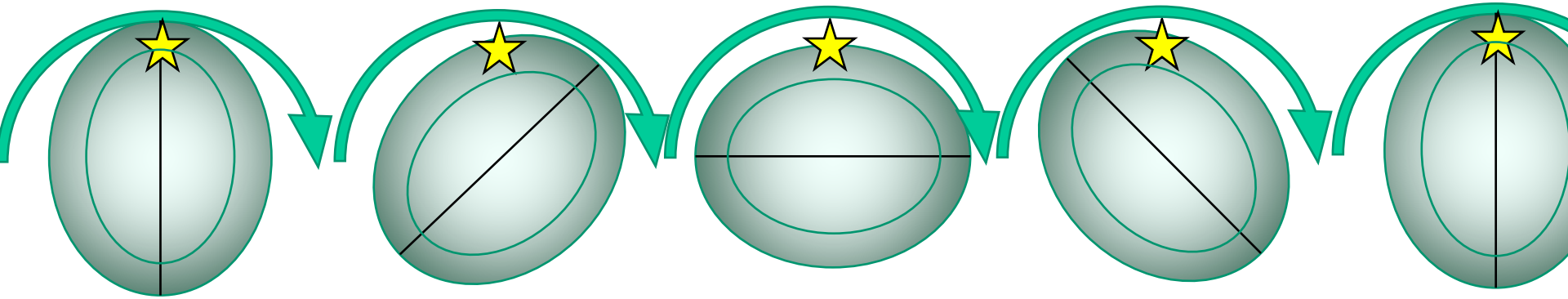

Elliptical beam: modulated signal from an unpolarized off-axis/anisotropic source, mimiking a polarized source

HWP polarimeter

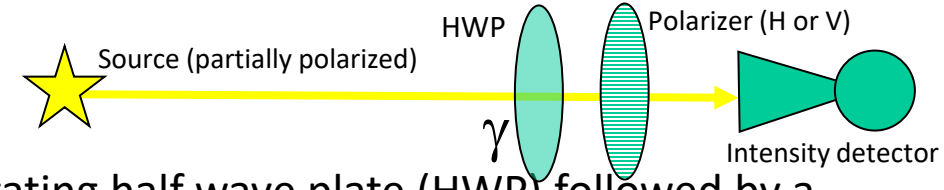

- Imagine a Stokes Polarimeter, including a rotating half wave plate (HWP) followed by a steady polarizer and two focal planes (one illuminated by radiation transmitted by the polarizer, the other illuminated by radiation reflected by the polarizer) filled with power detectors (intrinsically insensitive to polarization).
- The power reaching each power detector is :

$$W_{V,H} = D \cdot P_{V,H} \cdot R(-\gamma) \cdot H \cdot R(\gamma) \cdot S$$

where :

S is the Stokes parameters vector of the radiation being analyzed, in the reference frame of the instrument *i ;*

R is the rotation matrix, and γ is the rotation angle of the principal axis of the HWP,

H is the Mueller matrix of a vertical HWP,

P_H is the Mueller matrix of a horizontal polarizer while P_V is the Mueller matrix of a horizontal polarizer. These apply to the reflected and transmitted focal planes, respectively

$$D = \begin{pmatrix} 1 & 0 & 0 & 0 \end{pmatrix} \quad P_H = \frac{1}{2}\begin{pmatrix} 1 & 1 & 0 & 0 \\ 1 & 1 & 0 & 0 \\ 0 & 0 & 0 & 0 \\ 0 & 0 & 0 & 0 \end{pmatrix} \quad P_V = \frac{1}{2}\begin{pmatrix} 1 & -1 & 0 & 0 \\ -1 & 1 & 0 & 0 \\ 0 & 0 & 0 & 0 \\ 0 & 0 & 0 & 0 \end{pmatrix}$$

$$R(\gamma) = \begin{pmatrix} 1 & 0 & 0 & 0 \\ 0 & c_2(\gamma) & s_2(\gamma) & 0 \\ 0 & -s_2(\gamma) & c_2(\gamma) & 0 \\ 0 & 0 & 0 & 1 \end{pmatrix} \quad H = \begin{pmatrix} 1 & 0 & 0 & 0 \\ 0 & 1 & 0 & 0 \\ 0 & 0 & -1 & 0 \\ 0 & 0 & 0 & -1 \end{pmatrix} \quad S = \begin{pmatrix} I_i \\ Q_i \\ U_i \\ V_i \end{pmatrix}$$

$$s_2(\gamma) = \sin(2\gamma)$$

$$c_2(\gamma) = \cos(2\gamma)$$

HWP polarimeter

We compute the Mueller matrix of the rotated HWP first:

$$H(\gamma)=R(-\gamma)HR(\gamma)=\begin{pmatrix}1&0&0&0\\0&c_2(\gamma)&-s_2(\gamma)&0\\0&s_2(\gamma)&c_2(\gamma)&0\\0&0&0&1\end{pmatrix}\begin{pmatrix}1&0&0&0\\0&1&0&0\\0&0&-1&0\\0&0&0&-1\end{pmatrix}\begin{pmatrix}1&0&0&0\\0&c_2(\gamma)&s_2(\gamma)&0\\0&-s_2(\gamma)&c_2(\gamma)&0\\0&0&0&1\end{pmatrix}=\begin{pmatrix}1&0&0&0\\0&c_4(\gamma)&s_4(\gamma)&0\\0&s_4(\gamma)&-c_4(\gamma)&0\\0&0&0&-1\end{pmatrix}$$

So we get:

$$W_H=D\cdot P_H\cdot H(\gamma)\cdot S=\frac{1}{2}\left[I_i+c_4(\gamma)Q_i+s_4(\gamma)U_i\right]$$

$$W_V=D\cdot P_V\cdot H(\gamma)\cdot S=\frac{1}{2}\left[I_i-c_4(\gamma)Q_i-s_4(\gamma)U_i\right]$$

The Stokes parameters in the reference frame of the sky S_s are related to the Stokes parameters in the reference frame of the instrument S_i by a rotation. If the vertical axis of the instrument is rotated by an angle θ with respect to the meridian, we have:

$$S_i=\begin{pmatrix}I_i\\Q_i\\U_i\\V_i\end{pmatrix}=R(\theta)S_s=\begin{pmatrix}1&0&0&0\\0&c_2(\theta)&s_2(\theta)&0\\0&-s_2(\theta)&c_2(\theta)&0\\0&0&0&1\end{pmatrix}\begin{pmatrix}I_s\\Q_s\\U_s\\V_s\end{pmatrix}=\begin{pmatrix}I_s\\c_2(\theta)Q_s+s_2(\theta)U_s\\-s_2(\theta)Q_s+c_2(\theta)U_s\\V_s\end{pmatrix}$$

HWP polarimeter

$$W_H = D \cdot P_H \cdot H(\gamma) \cdot S = \frac{1}{2}\left[I_i + c_4(\gamma) Q_i + s_4(\gamma) U_i\right]$$

$$W_V = D \cdot P_V \cdot H(\gamma) \cdot S = \frac{1}{2}\left[I_i - c_4(\gamma) Q_i - s_4(\gamma) U_i\right]$$

$$S_i = \begin{pmatrix} I_i \\ Q_i \\ U_i \\ V_i \end{pmatrix} = R(\theta) S_s = \begin{pmatrix} 1 & 0 & 0 & 0 \\ 0 & c_2(\theta) & s_2(\theta) & 0 \\ 0 & -s_2(\theta) & c_2(\theta) & 0 \\ 0 & 0 & 0 & 1 \end{pmatrix} \begin{pmatrix} I_s \\ Q_s \\ U_s \\ V_s \end{pmatrix} = \begin{pmatrix} I_s \\ c_2(\theta) Q_s + s_2(\theta) U_s \\ -s_2(\theta) Q_s + c_2(\theta) U_s \\ V_s \end{pmatrix}$$

So we get the power on the detector as a function of the Stokes vector of the sky signal:

$$W_H = \frac{1}{2}\left[I_s + c_4(\gamma) c_2(\theta) Q_s + c_4(\gamma) s_2(\theta) U_s - s_4(\gamma) s_2(\theta) Q_s + s_4(\gamma) c_2(\theta) U_s\right] =$$

$$= \frac{1}{2}\left[I_s + Q_s\left[c_4(\gamma) c_2(\theta) - s_4(\gamma) s_2(\theta)\right] + U_s\left[c_4(\gamma) s_2(\theta) + s_4(\gamma) c_2(\theta)\right]\right] \quad \rightarrow$$

$$\Rightarrow \quad W_H = \frac{1}{2}\left[I_s + Q_s \cos(4\gamma + 2\theta) + U_s \sin(4\gamma + 2\theta)\right]$$

$$\Rightarrow \quad W_V = \frac{1}{2}\left[I_s - Q_s \cos(4\gamma + 2\theta) - U_s \sin(4\gamma + 2\theta)\right]$$

The linearly polarized fraction of the sky brightness is modulated at 4 times the rotation frequency of the HWP

CMB Polarimeters

PHYSICAL REVIEW D VOLUME 17, NUMBER 8 15 APRIL 1978

Polarization of the microwave background radiation. II. An infrared survey of the sky

N. Caderni
Istituto di Fisica Teorica, University of Florence, Italy

R. Fabbri
Istituto di Fisica Superiore, University of Florence, Italy

B. Melchiorri, F. Melchiorri, and V. Natale
Infrared Group of Istituto di Ricerca sulle Onde Elettromagnetiche-Consiglio Nazionale delle Ricerche, Florence, Italy

(Received 10 August 1977)

The linear polarization degree of the cosmological background has been investigated at angular scales ranging between 0.5° and 40° by means of a balloon-borne far-infrared polarimeter. An upper limit has been found of 8×10^{-4} at 40° (at one standard deviation). Some cosmological implications are discussed.

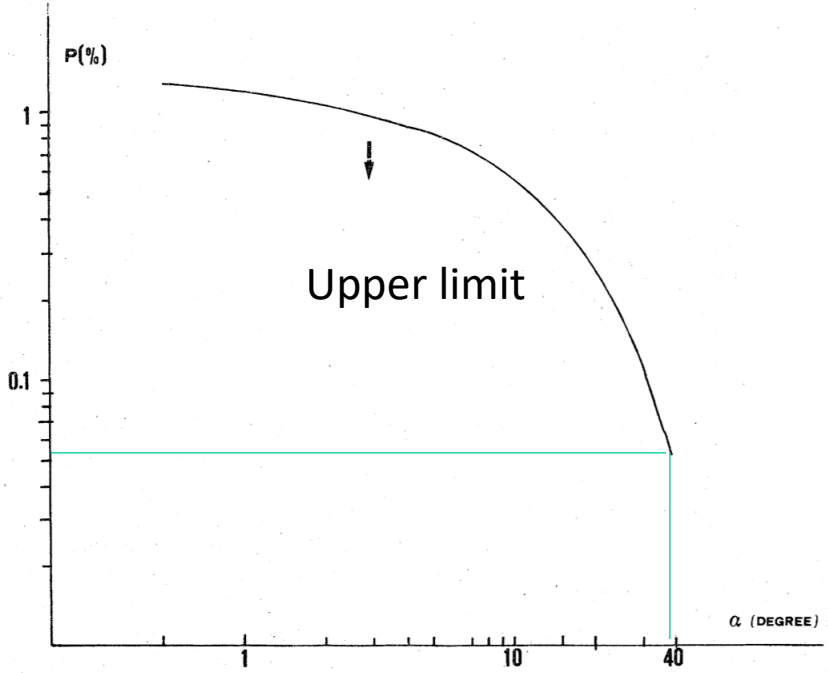

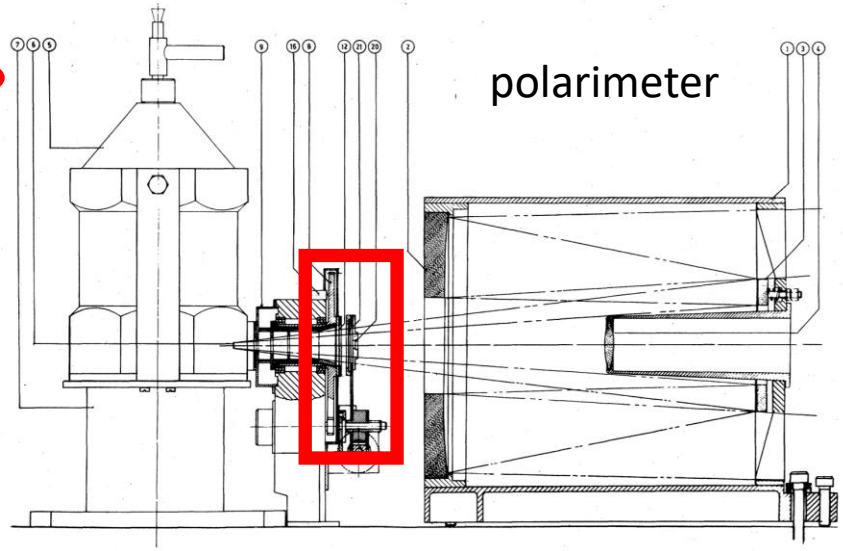

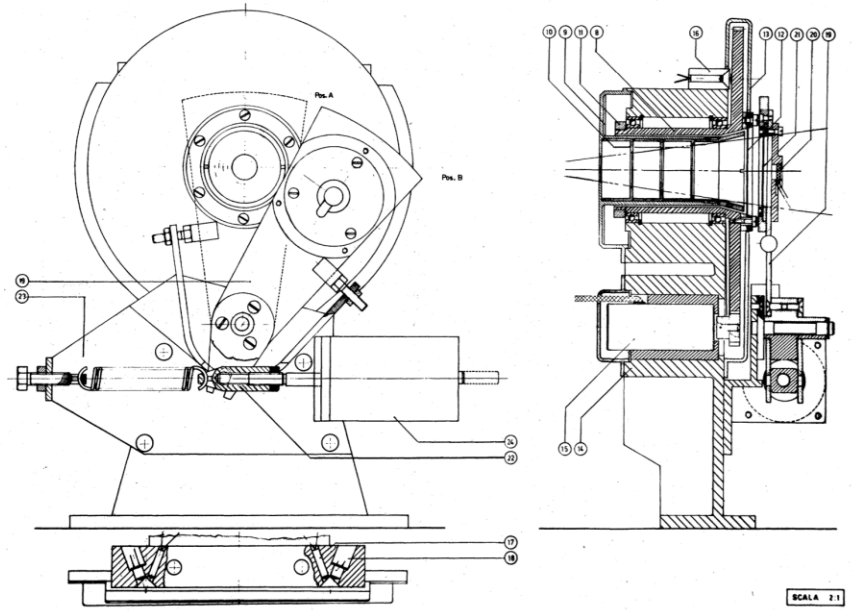

First detection of CMB polarization

2002

articles

Detection of polarization in the cosmic microwave background using DASI

J. M. Kovac*†‡, E. M. Leitch§†‡, C. Pryke§†‡||, J. E. Carlstrom§*†‡||, N. W. Halverson¶† & W. L. Holzapfel¶†

* Department of Physics; † Center for Astrophysical Research in Antarctica; ‡ Center for Cosmological Physics; § Department of Astronomy & Astrophysics and || Enrico Fermi Institute, University of Chicago, 5640 South Ellis Avenue, Chicago, Illinois 60637, USA
¶ Department of Physics, University of California at Berkeley, Le Conte Hall, California 94720, USA

The past several years have seen the emergence of a standard cosmological model, in which small temperature differences in the cosmic microwave background (CMB) radiation on angular scales of the order of a degree are understood to arise from acoustic oscillations in the hot plasma of the early Universe, arising from primordial density fluctuations. Within the context of this model, recent measurements of the temperature fluctuations have led to profound conclusions about the origin, evolution and composition of the Universe. Using the measured temperature fluctuations, the theoretical framework predicts the level of polarization of the CMB with essentially no free parameters. Therefore, a measurement of the polarization is a critical test of the theory and thus of the validity of the cosmological parameters derived from the CMB measurements. Here we report the detection of polarization of the CMB with the Degree Angular Scale Interferometer (DASI). The polarization is deteced with high confidence, and its level and spatial distribution are in excellent agreement with the predictions of the standard theory.

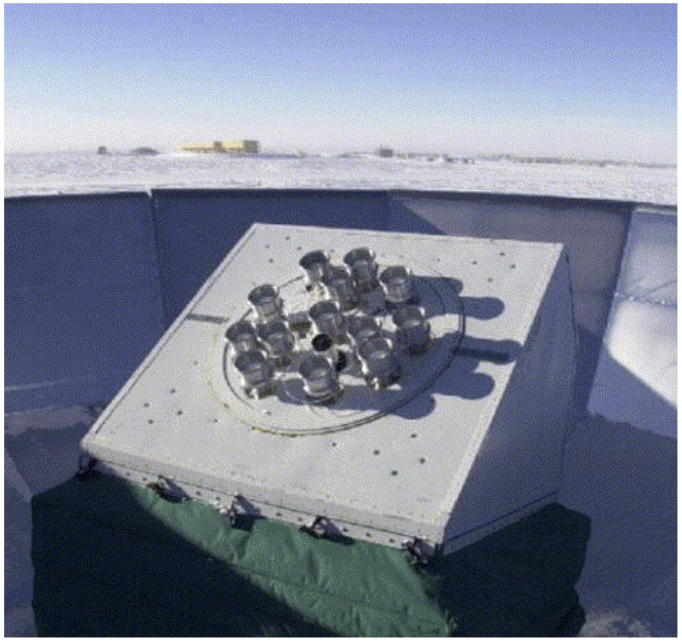

Coherent Polarimeters

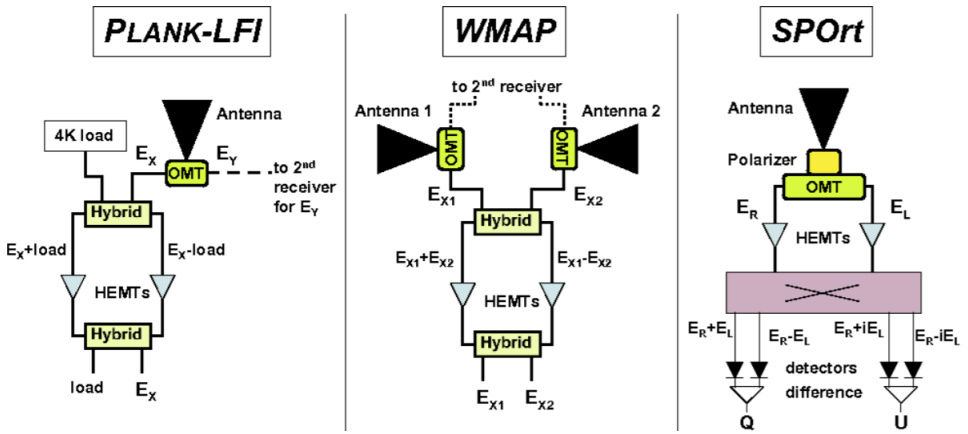

Figure 35.2: Schemes of *Planck*–LFI, *WMAP*, and SPOrt receivers.

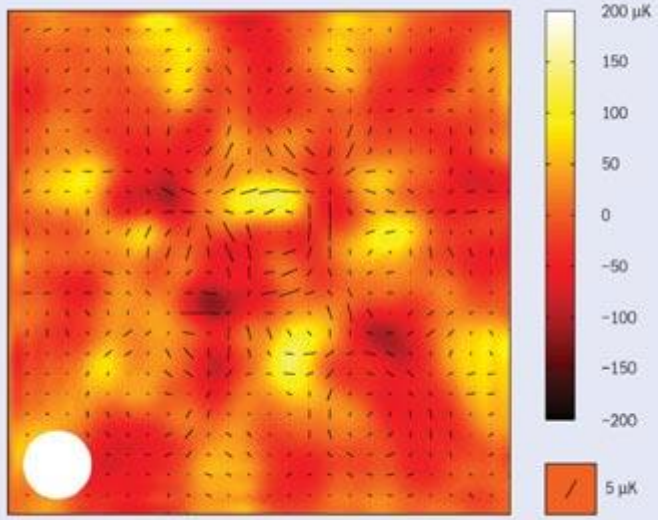

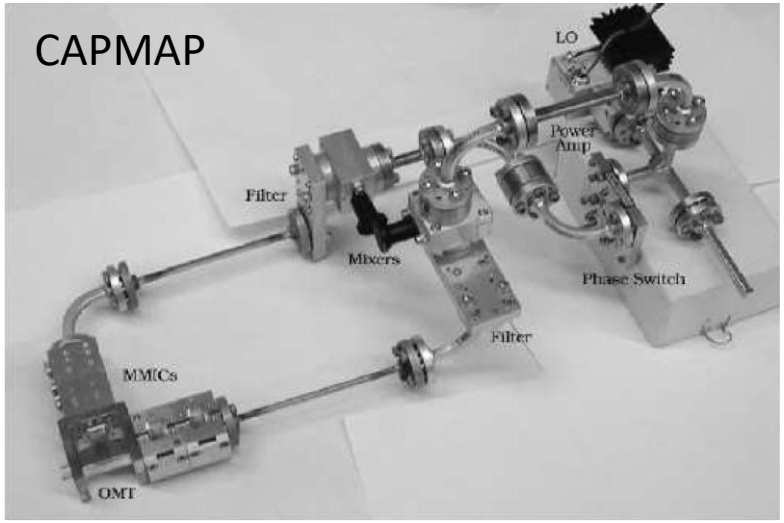

Coherent polarimetric receivers are very clean and performing, but suffer for a scalability problem:

- Complexity (mitigated by MMIC)
- Cost
- Power dissipation

The largest current one is STRIP on LSPE.

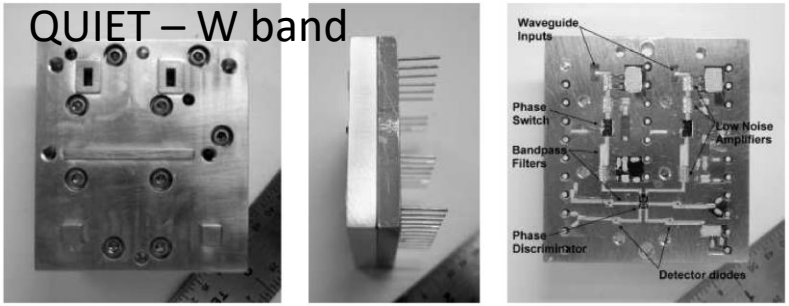

But most of current CMB polarimeters are based on bolometer/TES arrays (since replicating them in large arrays does not change the dissipated power) with quasi-optical polarization modulators, as described above.

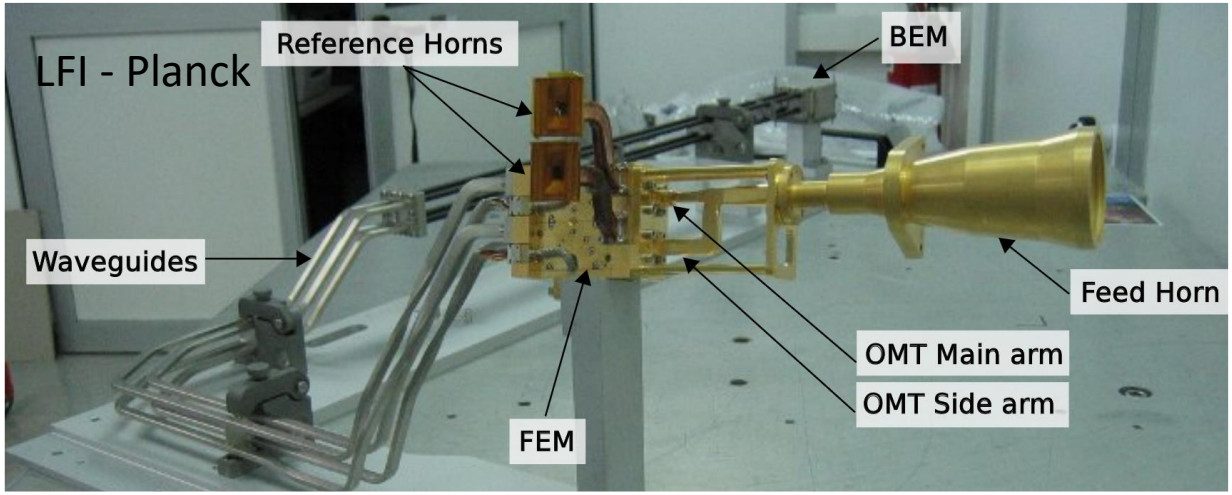

BOOMERanG as a polarimeter

A&A 458, 687–716 (2006)
DOI: 10.1051/0004-6361:20053891
© ESO 2006

Astronomy & Astrophysics

Masi & 2006

Instrument, method, brightness, and polarization maps from the 2003 flight of BOOMERanG

S. Masi[1], P. A. R. Ade[2], J. J. Bock[3], J. R. Bond[4], J. Borrill[5,6], A. Boscaleri[7], P. Cabella[8], C. R. Contaldi[4,9], B. P. Crill[10], P. de Bernardis[1], G. De Gasperis[8], A. de Oliveira-Costa[11], G. De Troia[1], G. Di Stefano[12], P. Ehlers[13], E. Hivon[10], V. Hristov[14], A. Iacoangeli[1], A. H. Jaffe[9], W. C. Jones[14], T. S. Kisner[15,16], A. E. Lange[14], C. J. MacTavish[17], C. Marini Bettolo[1], P. Mason[14], P. D. Mauskopf[2], T. E. Montroy[15], F. Nati[1], L. Nati[1], P. Natoli[8,18], C. B. Netterfield[13,17], E. Pascale[17], F. Piacentini[1], D. Pogosyan[4,19], G. Polenta[1], S. Prunet[20], S. Ricciardi[1], G. Romeo[12], J. E. Ruhl[15], P. Santini[1], M. Tegmark[11], E. Torbet[16], M. Veneziani[1], and N. Vittorio[8,18]

$$s = \frac{1}{2}\left[(1+\epsilon)\,\mathcal{I} + (1-\epsilon)\left(\mathcal{Q}\,cos(2\psi) + \mathcal{U}\,sin(2\psi)\right)\right]$$

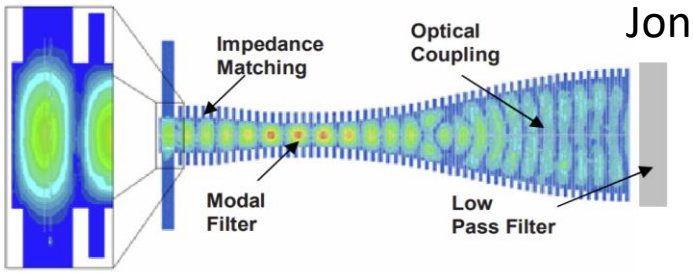

Jones & 2003: **PSB**

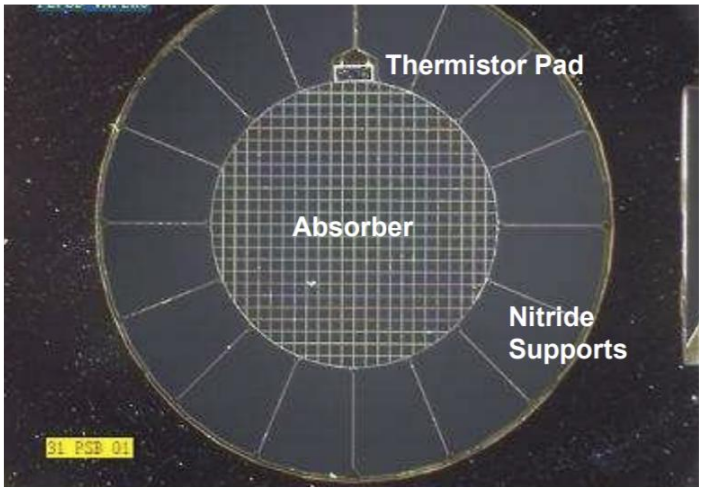

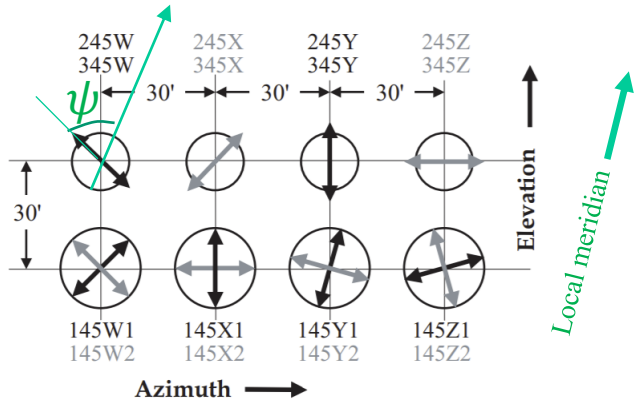

Fig. 5. Focal Plane Schematic. 2-color photometers with band centers at 245 GHz and 345 GHz populate the upper row. Each photometer is only sensitive to one polarization. The lower row has 4 pairs of PSB's. The elements in a PSB pair are sensitive to orthogonal polarizations. The circles representing the pixels show relative beams sizes: ~7′ for both photometer channels and 9.5′ for the PSB's. The arrows through the circles show the orientation of the principal axis of polarization. The photometer and PSB rows are separated by 30′ in elevation, while the pixels in a row are separated by 30′ in cross-elevation. The labels of the two bolometers used for each pixel are also reported.

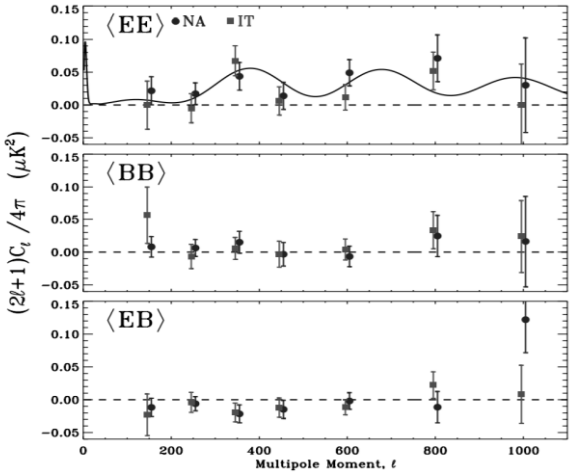

Montroy & 2006

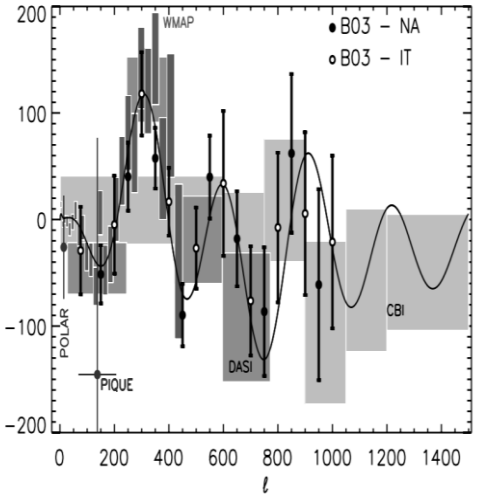

Piacentini & 2006

Planck HFI as a polarimeter

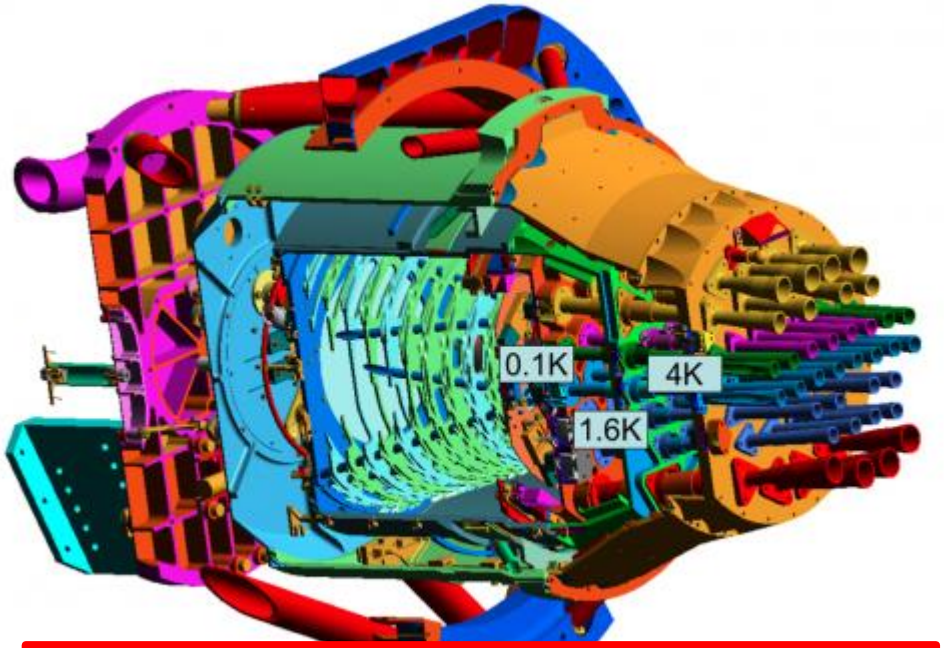

$$s = \frac{1}{2}\Big[(1+\epsilon)\,\mathcal{I} + (1-\epsilon)\Big(\mathcal{Q}\,cos(2\psi) + \mathcal{U}\,sin(2\psi)\Big)\Big]$$

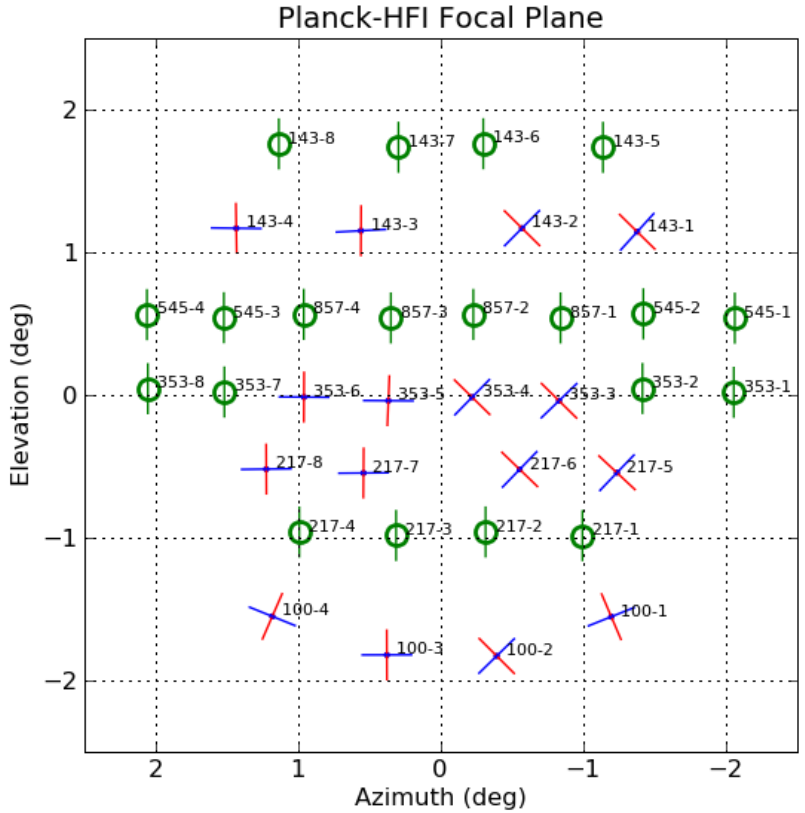

- Planck HFI uses combination of orthogonal detectors to get Q and U (PSBs a la B03), while LFI uses coherent detectors.
- The measurement is challenging - any differential calibration error between pairs of detectors causes leakage of total intensity into the polarization maps (such as gain calibration error or different spectral transmissions)
- the response of each detector to polarization is difficult to calibrate (due to the lack of celestial standard sources)

Planck as a polarimeter

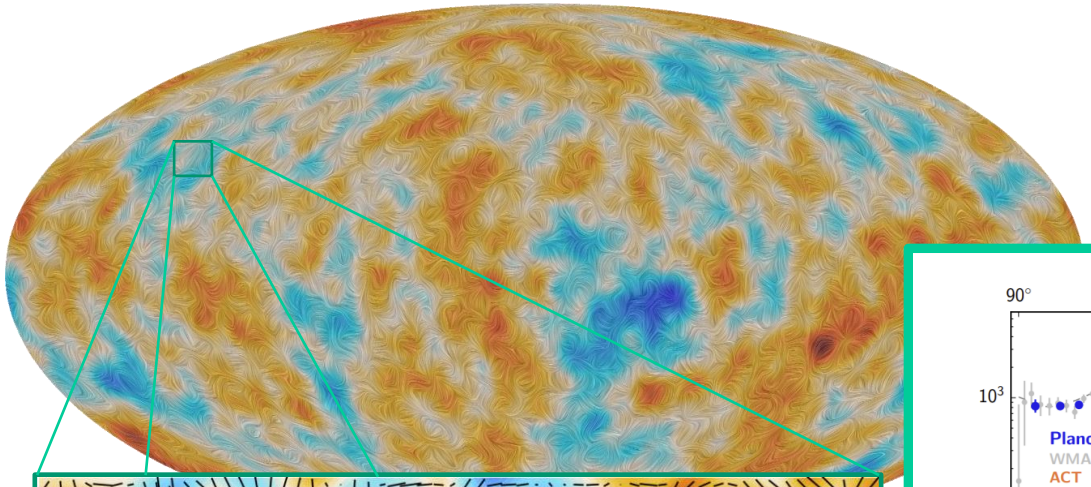

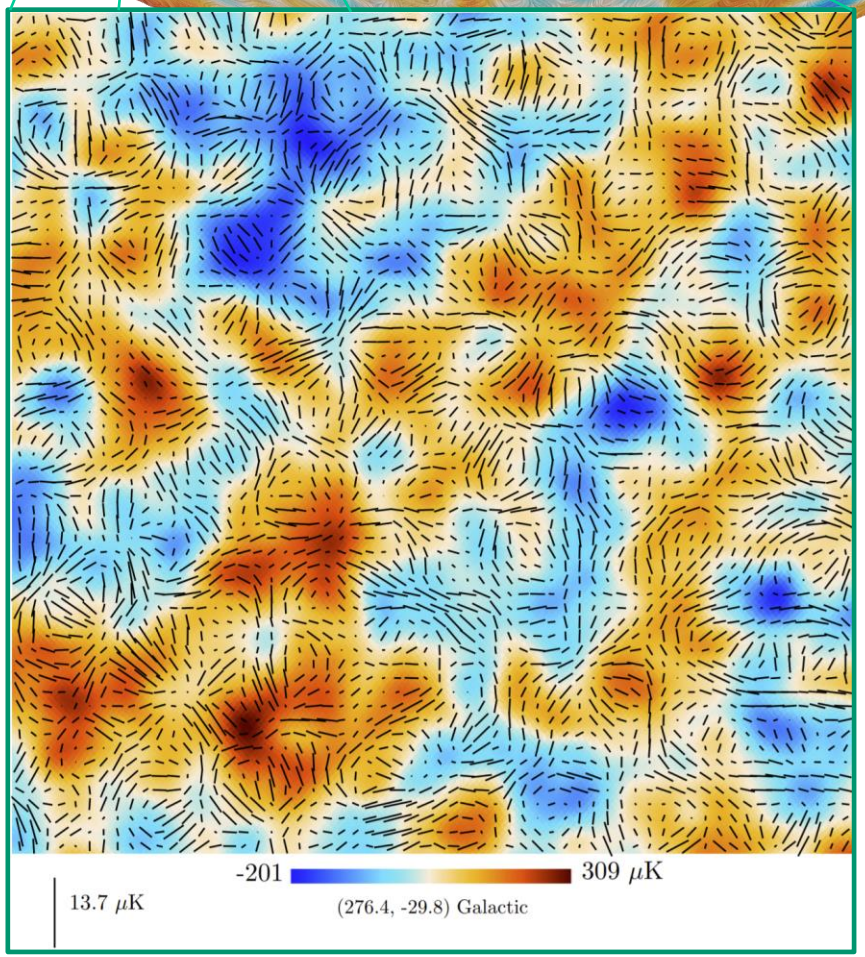

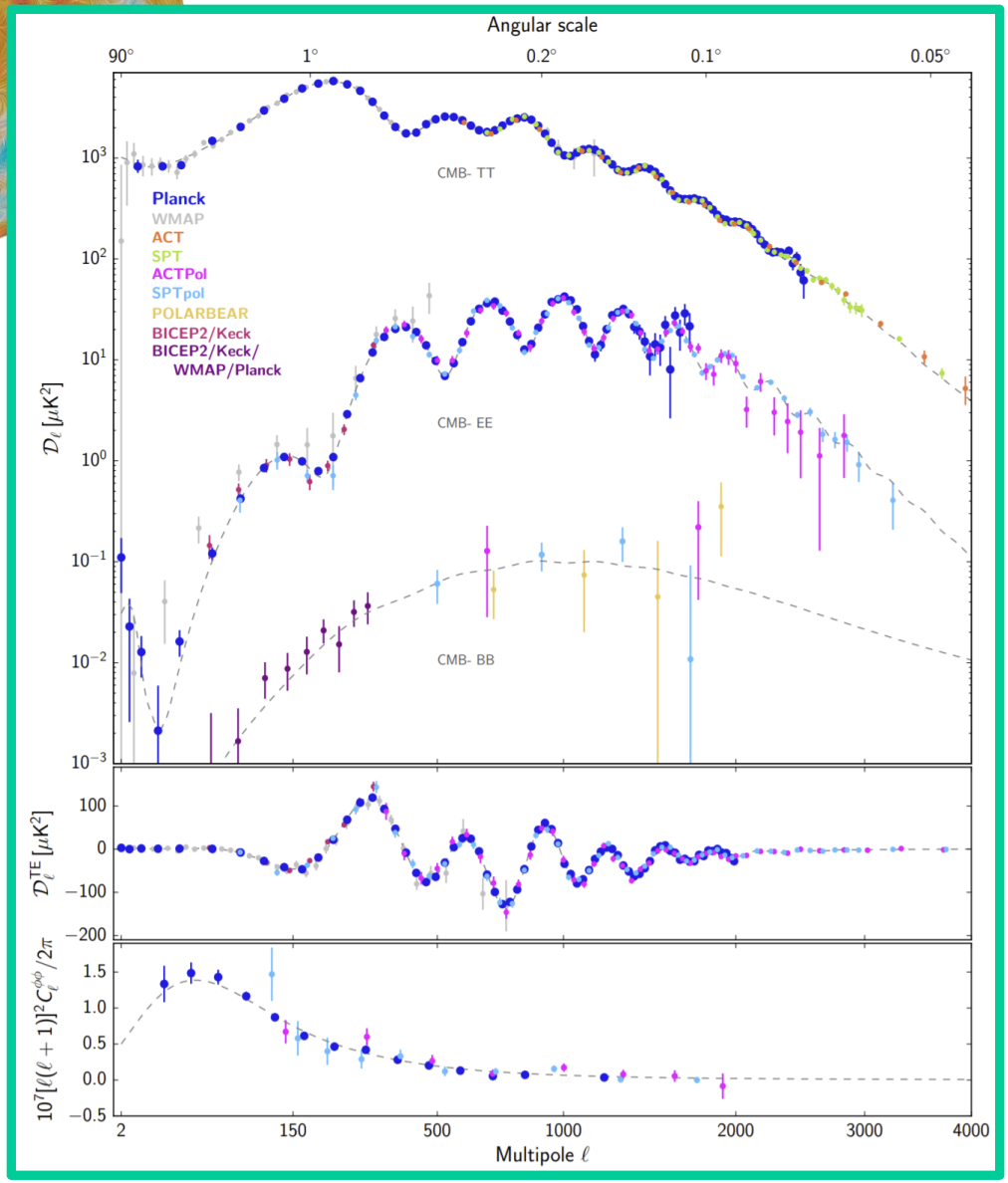

BICEP Keck

BICEP-3 (100 GHz)

- Ground based instruments (Atmospheric emission is not linearly polarized)
- South pole (the best site on Earth ?) in the Antarctic winter for high transmission and stability - Heavily filter the data to remove large-scale fluctuations
- Massive increase in the number of detectors to boost the survey speed

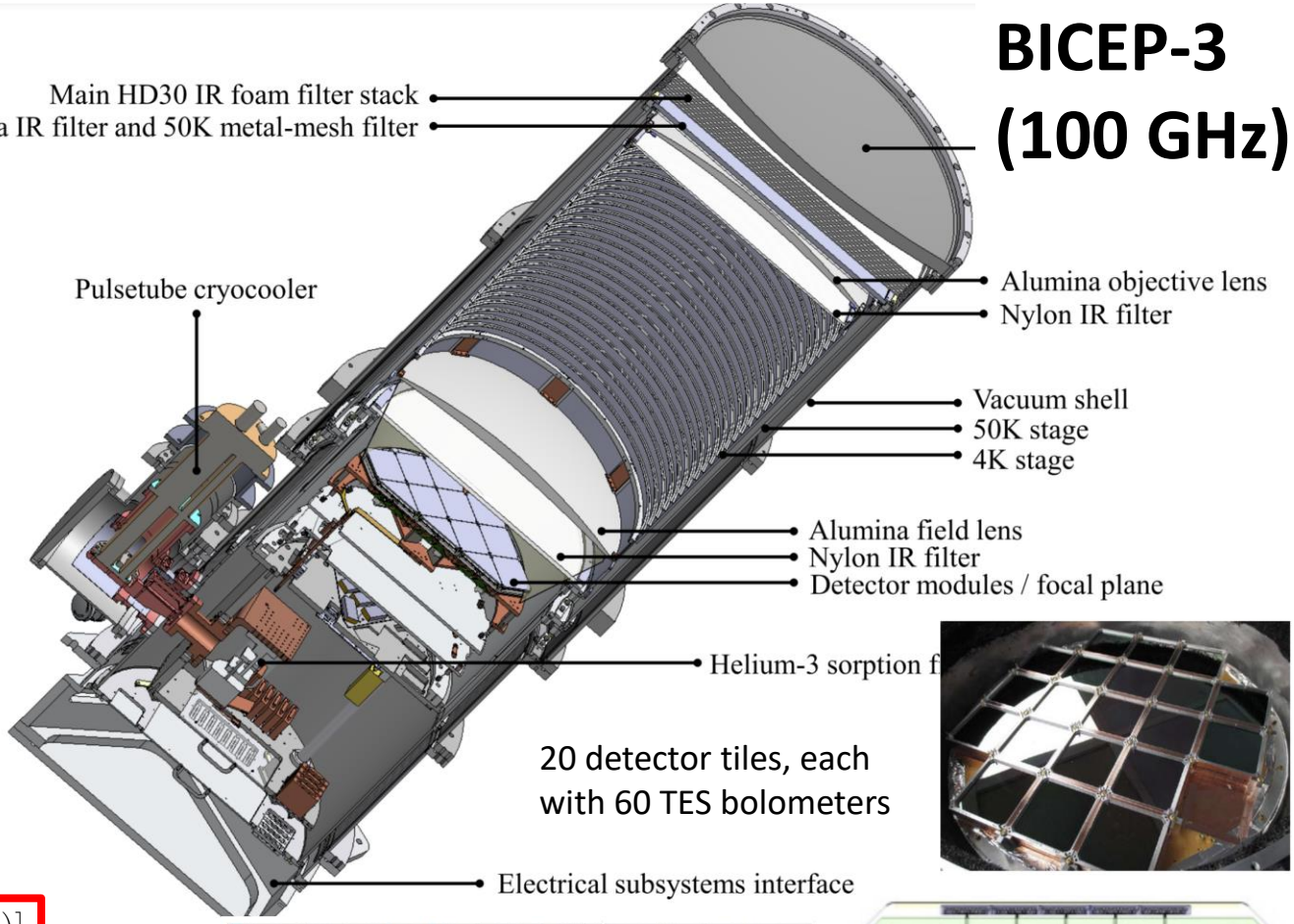

20 detector tiles, each with 60 TES bolometers

$$s = \frac{1}{2}\Big[(1+\epsilon)\,\mathcal{I} + (1-\epsilon)\Big(\mathcal{Q}\,cos(2\psi) + \mathcal{U}\,sin(2\psi)\Big)\Big]$$

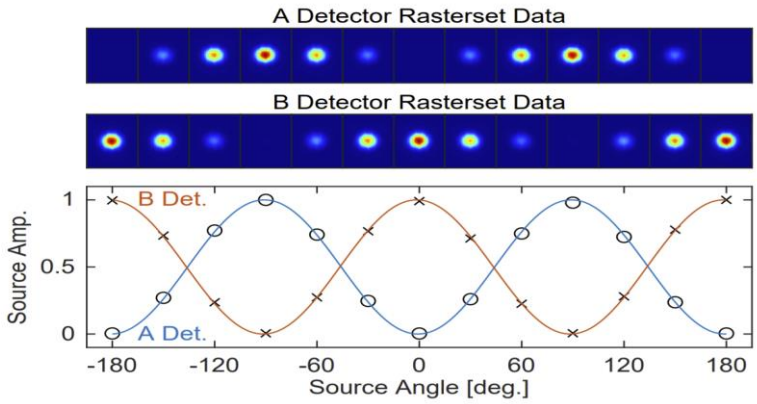

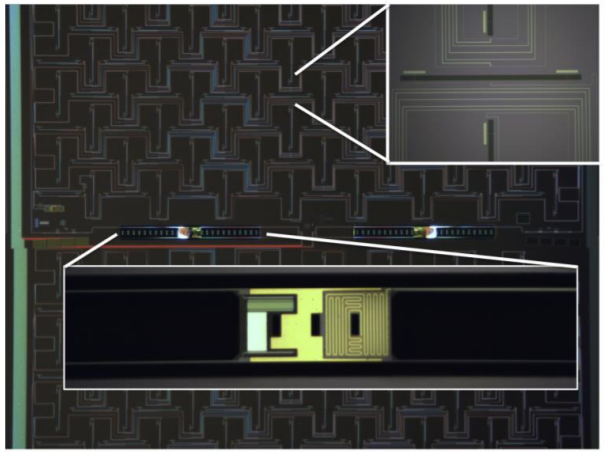

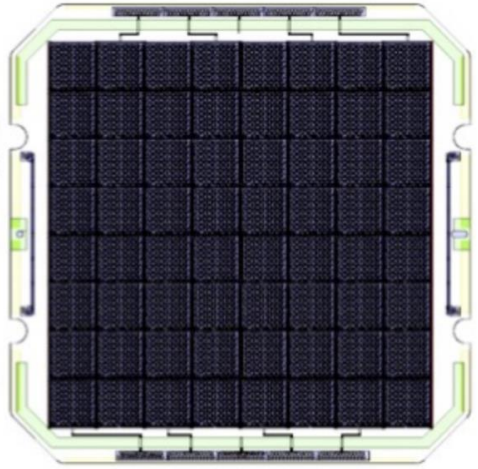

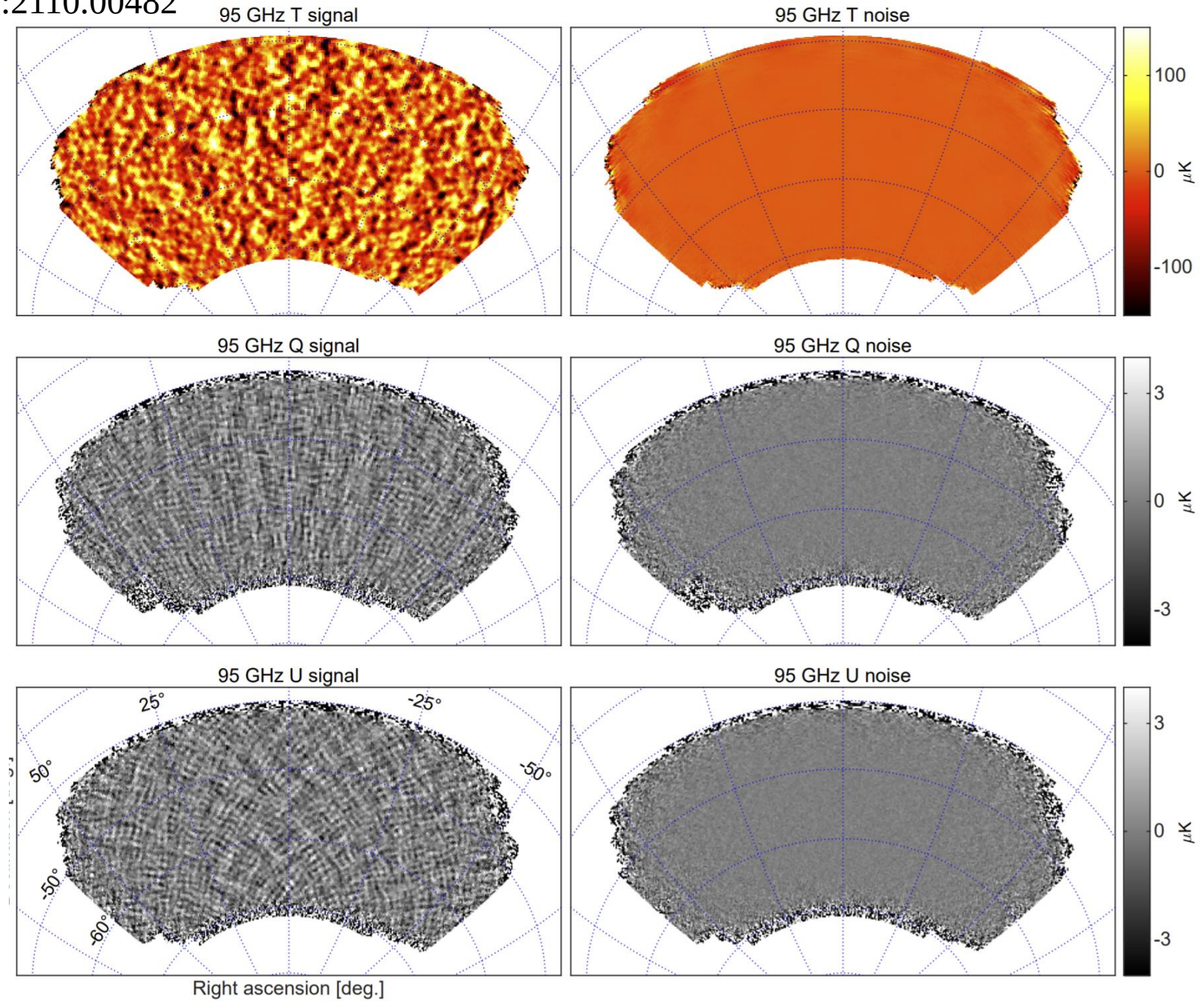

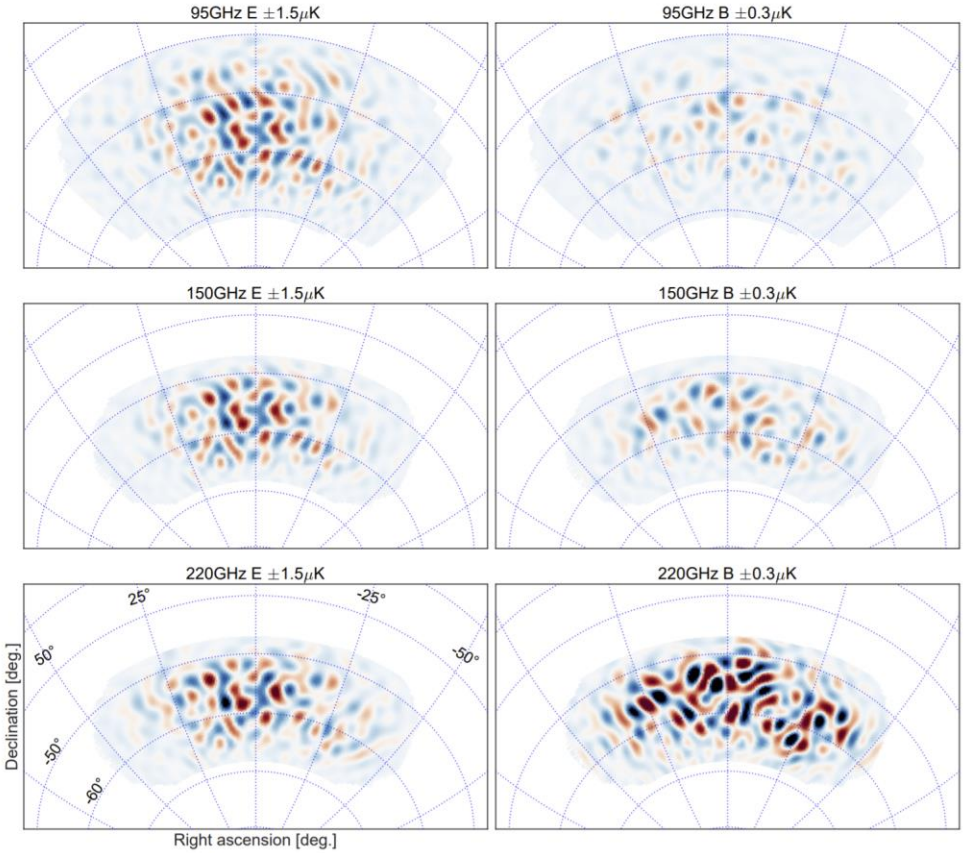

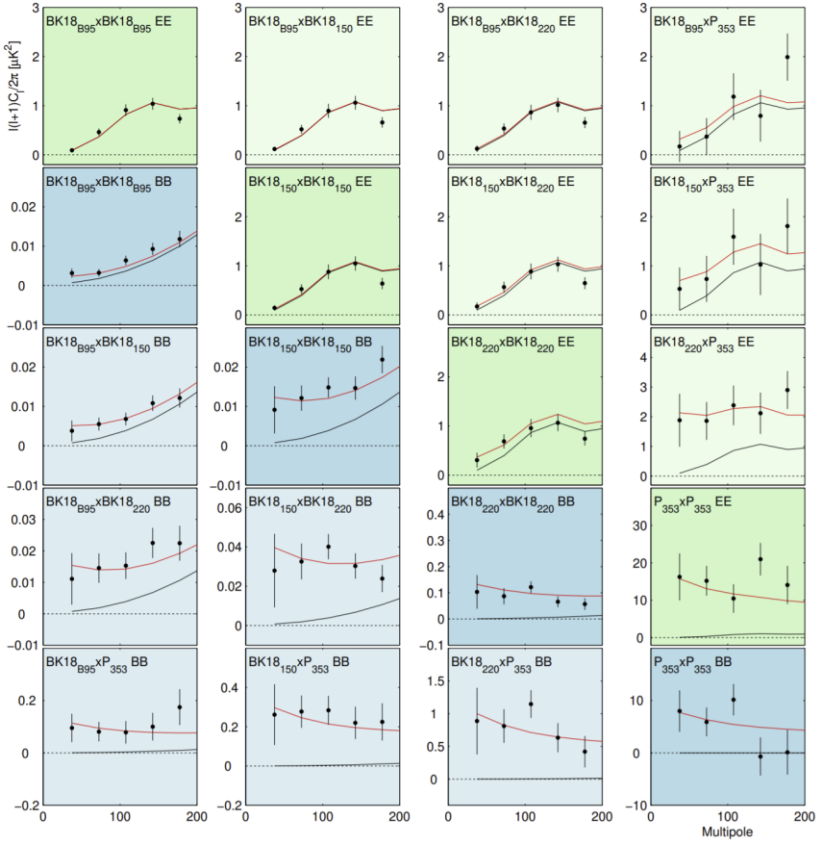

arXiv:2110.00483

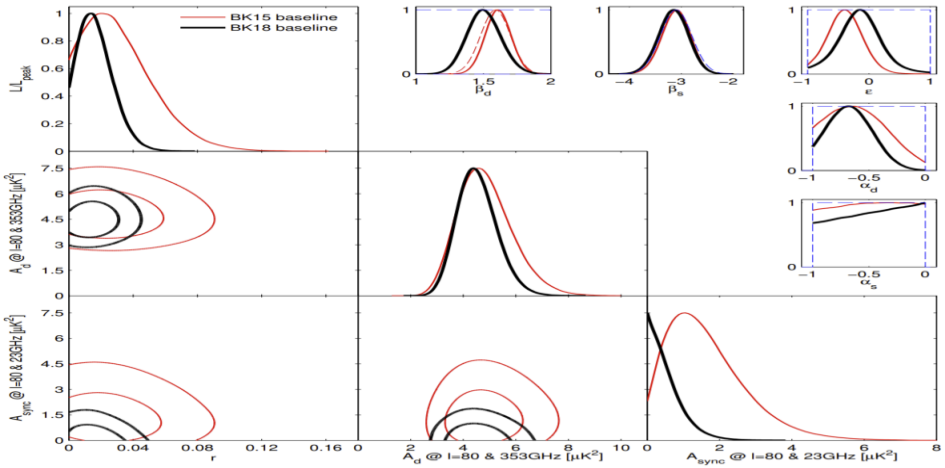

The LSPE collaboration

Addamo	G.
Farooqui	Z.
Lumia	M.
Paonessa	F.
Peverini	O.A.
Virone	G.
Battaglia	P.
Bersanelli	M.
Caccianiga	B.
Caprioli	S.
Cavaliere	F.
Colombo	L.
Franceschet	C.
Incardona	F.
Maino	D.
Mandelli	S.
Mandelli	L.
Mennella	A.
Paradiso	S.
Pezzotta	F.
Realini	S.
Tomasi	M.
Viganò	D.
Baschirotto	A.
Baù	A.
De Matteis	M.
Gervasi	M.
Ghigna	T.
Mainini	R.
Nati	F.
Passerini	A.
Pincella	C.
Tartari	A.
Zannoni	M.
Cuttaia	F.
De Rosa	A.
Morgante	G.
Ricciardi	S.
Sandri	M.
Terenzi	L.
Villa	F.

Gregorio	A.
Maris	M.
Sartor	S.
Zacchei	A.
Hill-Valler	J.
Jew	L.
Jones	M.
Taylor	A.
Watkins	B.
Gaier	T.
Soria	M.
Cleary	K.
Genova-Santos	R.
González Escalera	V.
Hoyland	R.
Perez	A.
Rebolo	R.
Rubiño-Martin	J. A.
Mena	P.
Pizarro	J.
Reyes	N.
Tapia	V.
Amico	G.
Battistelli	E. S.
Columbro	F.
Coppi	G.
Coppolecchia	A.
D'Alessandro	G.
de Bernardis	P.
De Petris	M.
Lamagna	L.
Marchetti	T.
Masi	S.
Paiella	A.
Panico	F.
Piacentini	F.
Presta	G.
Schillaci	A.
Boscaleri	A.

Biasotti	M.
Boragno	C.
Ceriale	V.
Corsini	D.
Fontanelli	F.
Fumagalli	E.
Gatti	F.
Giovannini	M.
Grosso	D.
Siri	B.
Baldini	A. M.
Cei	F.
Galli	L.
Grassi	M.
Incagli	M.
Moggi	A.
Nicolò	D.
Piendibene	M.
Signorelli	G.
Spinella	F.
Tartari	D.
Vaccaro	D.
Ade	P.A.R.
Pisano	G.
Tucker	C.
Coppi	G.
Martinis	L.
May	A.
McCulloch	M.
Melhuish	S.
Piccirillo	L.
Baccigalupi	C.
Farsian	F.
Krachmalnicoff	N.
Puglisi	G.
Matarrese	S.

Matarrese	S.
Forastieri	F.
Gruppuso	A.
Iacobellis	G.
Lattanzi	M.
Molinari	D.
Natoli	P.
Pagano	L.
Polastri	L.
Zavattini	G.
Bazzicchi	A.
Buzzelli	A.
Cabella	P.
Cesarini	E.
Cifaldi	M.
Coccia	E.
D'Antonio	S.
De Gasperis	G.
Fafone	V.
Haridasu	S.
Lorenzini	M.
Lukovich	V.
Migliaccio	M.
Rocchi	A.
Vittorio	N.
Polenta	G.
Tommasi	E.
Volpe	A.

Scientists from institutions in Italy, UK, USA, Spain, Chile:

- CNR-TO
- UniMI, INFN-MI
- UniMIB, INFN-MIB
- INAF-BO
- INAF-OAT
- UniTS
- Oxford
- JPL
- Caltech
- IAC
- UniChile
- UniGE, INFN Ge
- INFN Pi
- Sapienza Roma, INFN Roma
- IFAC CNR
- UniCardiff
- UniManchester
- SISSA
- UniPD
- UniFE, INFN Fe
- Tor Vergata, INFN RM2
- ASI

LSPE in a nutshell

- The **Large-Scale Polarization Explorer** is an experiment to measure the polarization of the CMB at large angular scales.
- **Science drivers / targets** :
  - The B-modes from inflation are mainly at large scales (*r*)
  - Polarization signatures from reionization (τ) are mainly at large scales
  - Rotation of the polarization angles (related to new physics)
  - Sensitive polarized dust survey at *f* close to the CMB ones
  - Sensitive polarized synchrotron survey at *f* close to the CMB ones
- **Instrumental approach** :
  - Frequency coverage: 40 – 250 GHz (5 bands)
  - 2 instruments covering the same northern sky
  - **STRIP** is a ground-based instrument working at 43 and 90 GHz
  - **SWIPE** works from near-space (balloon) at 145, 210, 240 GHz

LSPE : frequency coverage

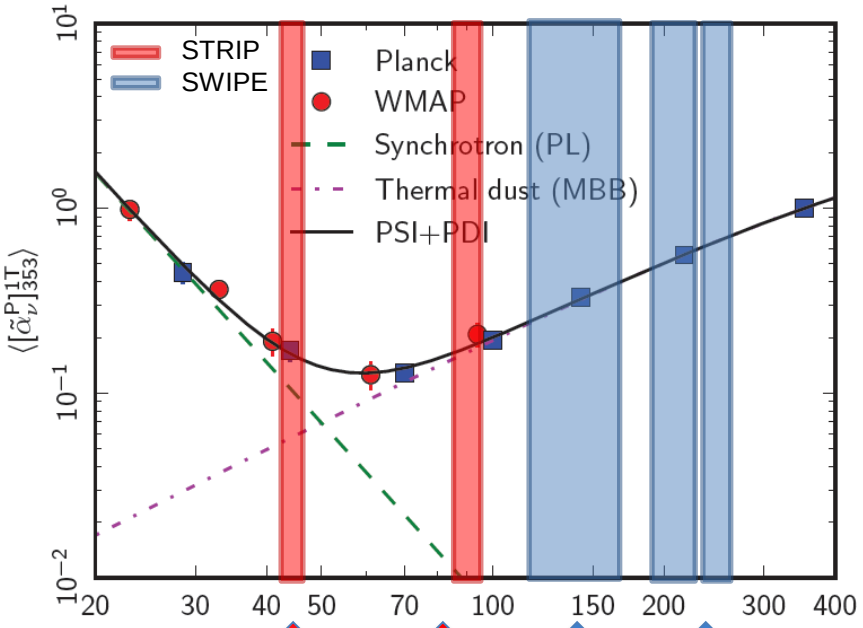

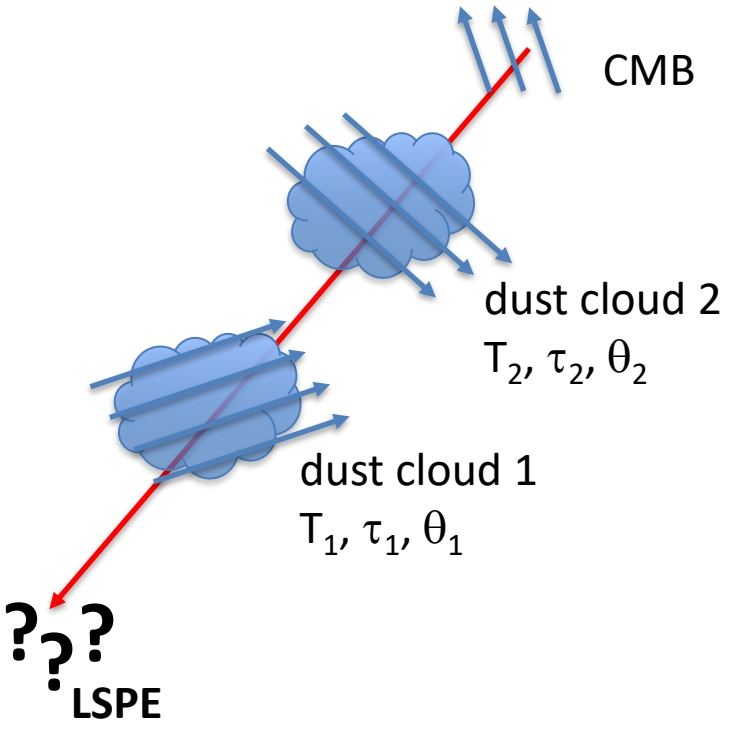

43 GHz (ground)
Monitor polarized synchrotron

90 GHz (ground)
Atmospheric monitor

145 GHz (balloon)
Main CMB channel

210 + 240 GHz (balloon)
Monitor **level, slope and possible rotation with frequency** of polarized dust emission.
To date: extrapolated from single frequency (Planck 353 GHz)

LSPE : Sky Coverage

STRIP

Ground telescope at 43 and 95 GHz located in Tenerife. Will measure for two years. Based on coherent polarimeters

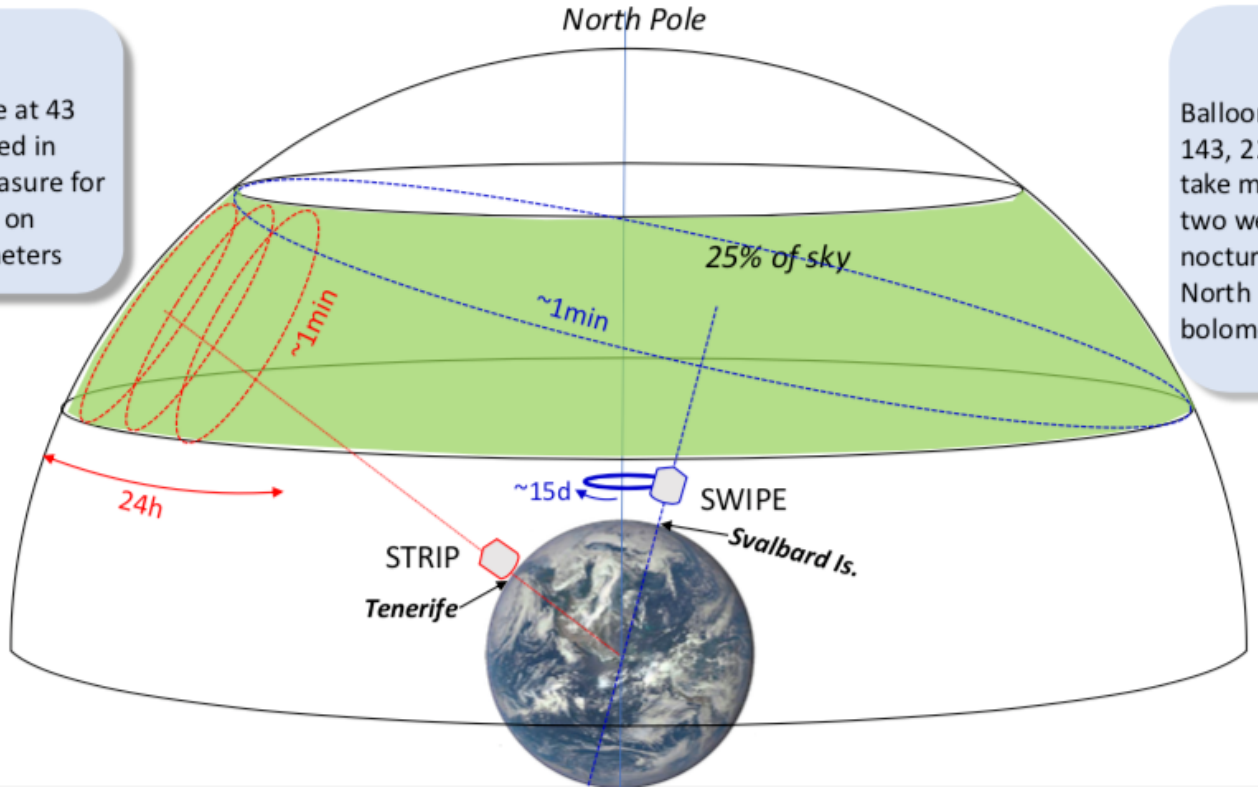

SWIPE

Balloon borne telescope at 143, 220 and 240 GHz. Will take measurements for two weeks during a LDB nocturnal flight around the North Pole. Based on TES bolometers

Credit A. Mennella

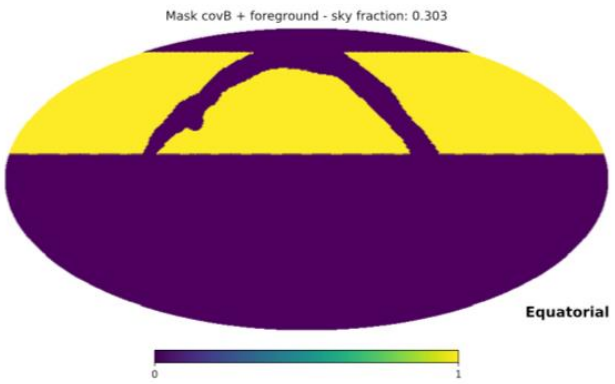

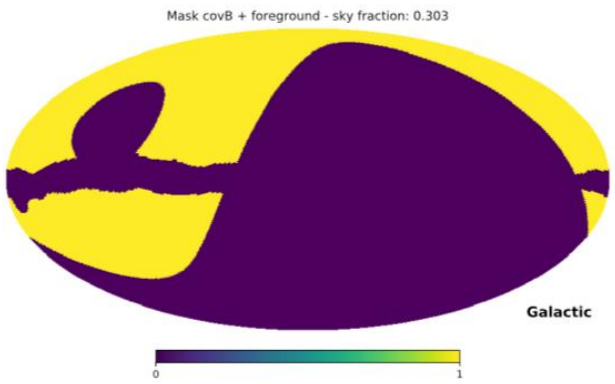

Credit L. Pagano, F. Piacentini

LSPE-STRIP in a nutshell

- Survey TeneRIfe Polarimeter
- Target: Polarized Synchrotron
- Two arrays of coherent polarimeters: 49 @44 GHz (QUIET) plus 7 @ 90 GHz.
- The measured response of the corrugated feedhorns confirms the expected performance down to -55 dB
- 1.5 m telescope (Clover)
- PI M. Bersanelli UNIMI

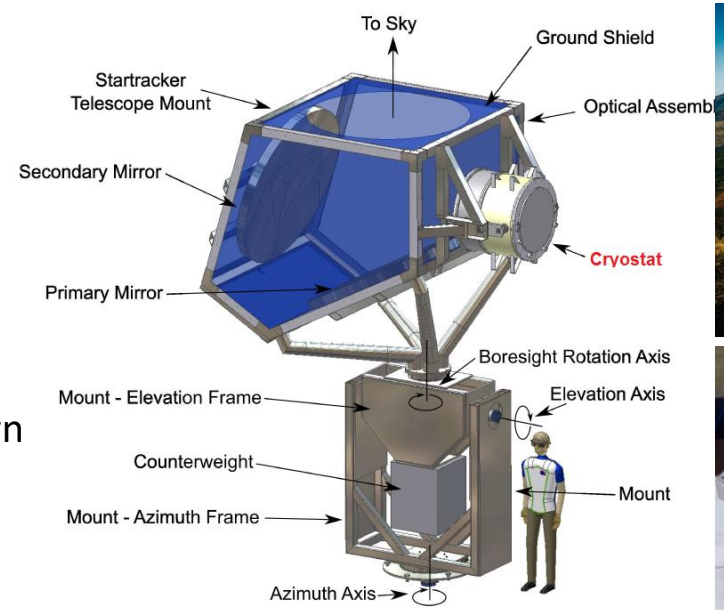

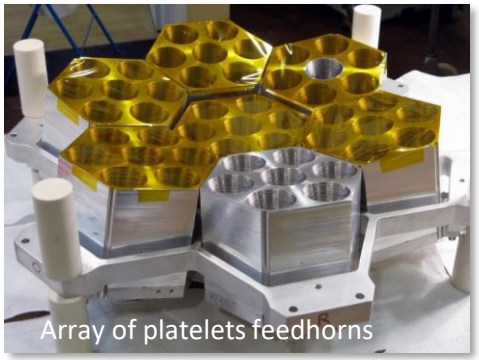

Instrument	STRIP	
Site	Tenerife	
Freq (GHz)	43	90
Bandwidth	17%	8%
Angular resolution FWHM (arcmin)	20	10
Detectors technology	HEMT	
Number of detectors N_{det}	49	6
Detector NET ($\mu K_{CMB}\sqrt{s}$)	515	1139
Mission duration	2 years	
Duty cycle	50%	
Sky coverage f_{sky}	37%	
Map sensitivity $\sigma_{Q,U}$ (μK_{CMB} · arcmin)	102	777
Noise power spectrum $(\mathcal{N}_\ell^{E,B})^{1/2}$ (μK_{CMB} · arcmin)	171	1330

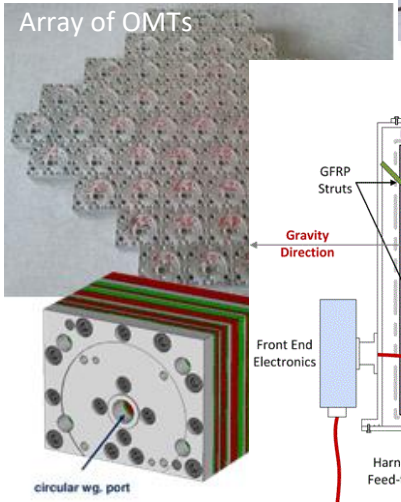

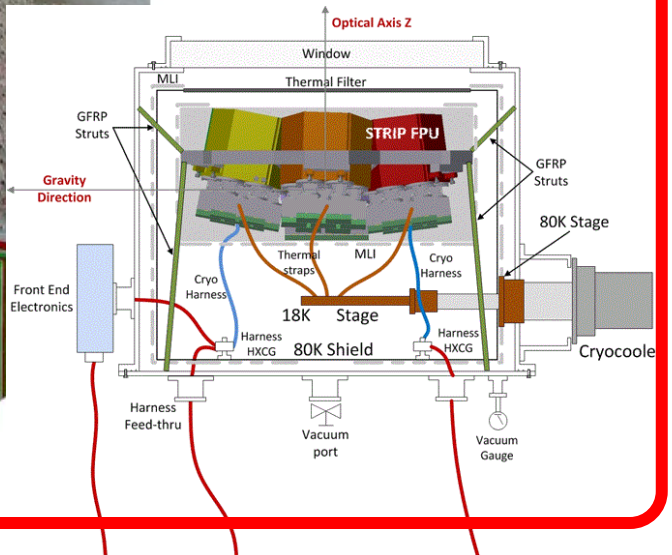

Provides essential information on polarized synchrotron

LSPE-SWIPE in a nutshell

- SWIPE is a multiband (145, 210, 220 GHz) array of Stokes polarimeters (163).
- Is flown on a stratospheric **balloon,** to avoid atmospheric noise at high *f,* including polarized radiation from ice crystals in tropospheric clouds (e.g. Takakura et al. 2018). **38%** of the sky covered in a 15d flight.
- SWIPE uses 326 **multimoded detectors** to improve the sensitivity wrt to Planck-HFI. The focal planes collect 8800 radiation modes. The resolution of each multimoded beam is 1.4° FWHM.
- Combined sensitivity: **10 μK arcmin per flight**
- SWIPE uses a **HWP-based polarization modulator as the first optically active element,** to solve several issues important at large scales (beam asymmetry leakage, bandpass mismatch, 1/f noise ... etc.)
- SWIPE uses a **single *large* polarizer, common** to the entire focal plane, to define the main axis of the polarimeter with high precision (< 0.1°): accurate absolute reconstruction of the pol. directions.
- PI P. de Bernardis (Sapienza)

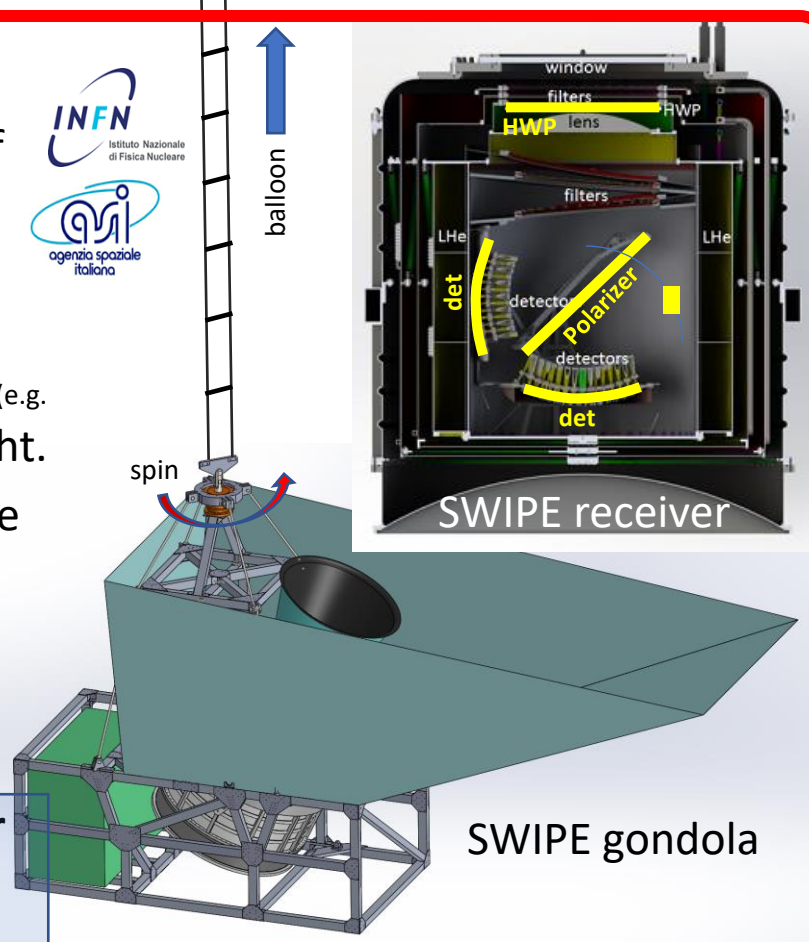

Instrument	SWIPE		
Site	balloon		
Freq (GHz)	145	210	240
Bandwidth	30%	20%	10%
Angular resolution FWHM (arcmin)	85		
Detectors technology	TES multimoded		
Number of detectors N_{det}	162	82	82
Detector NET ($\mu K_{CMB}\sqrt{s}$)	12.7	15.7	30.9
Mission duration	8 - 15 days		
Duty cycle	90%		
Sky coverage f_{sky}	38%		
Map sensitivity $\sigma_{Q,U}$ (μK_{CMB} · arcmin)	10	17	34
Noise power spectrum $(N_\ell^{E,B})^{1/2}$ (μK_{CMB} · arcmin)	16	28	55

LSPE/SWIPE: photon background

To fully exploit the low radiative background: thin window

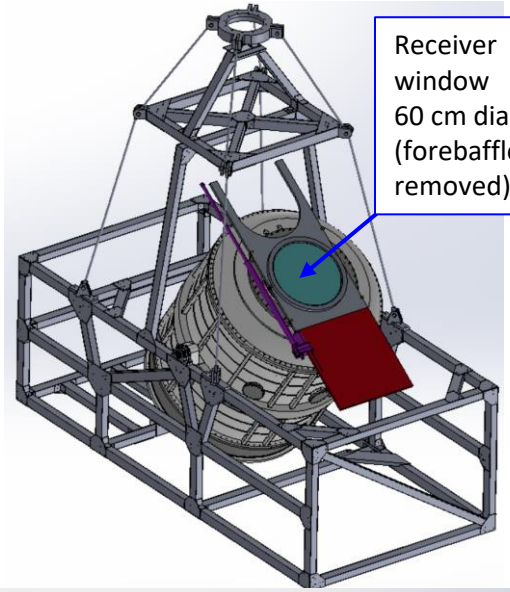

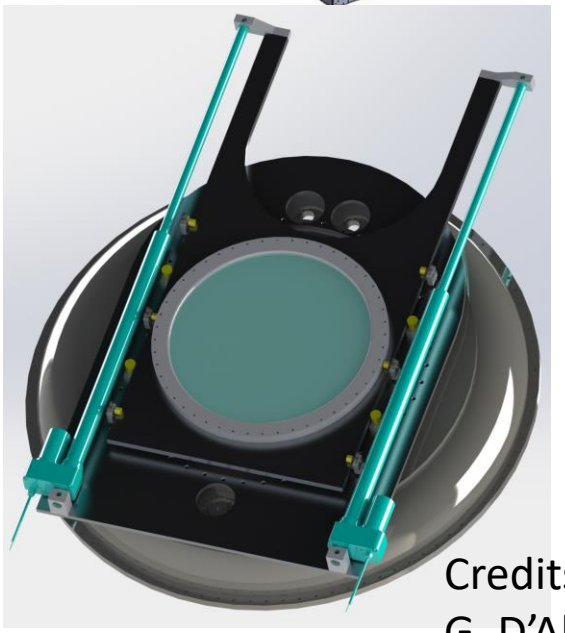

Credits:
G. D'Alessandro

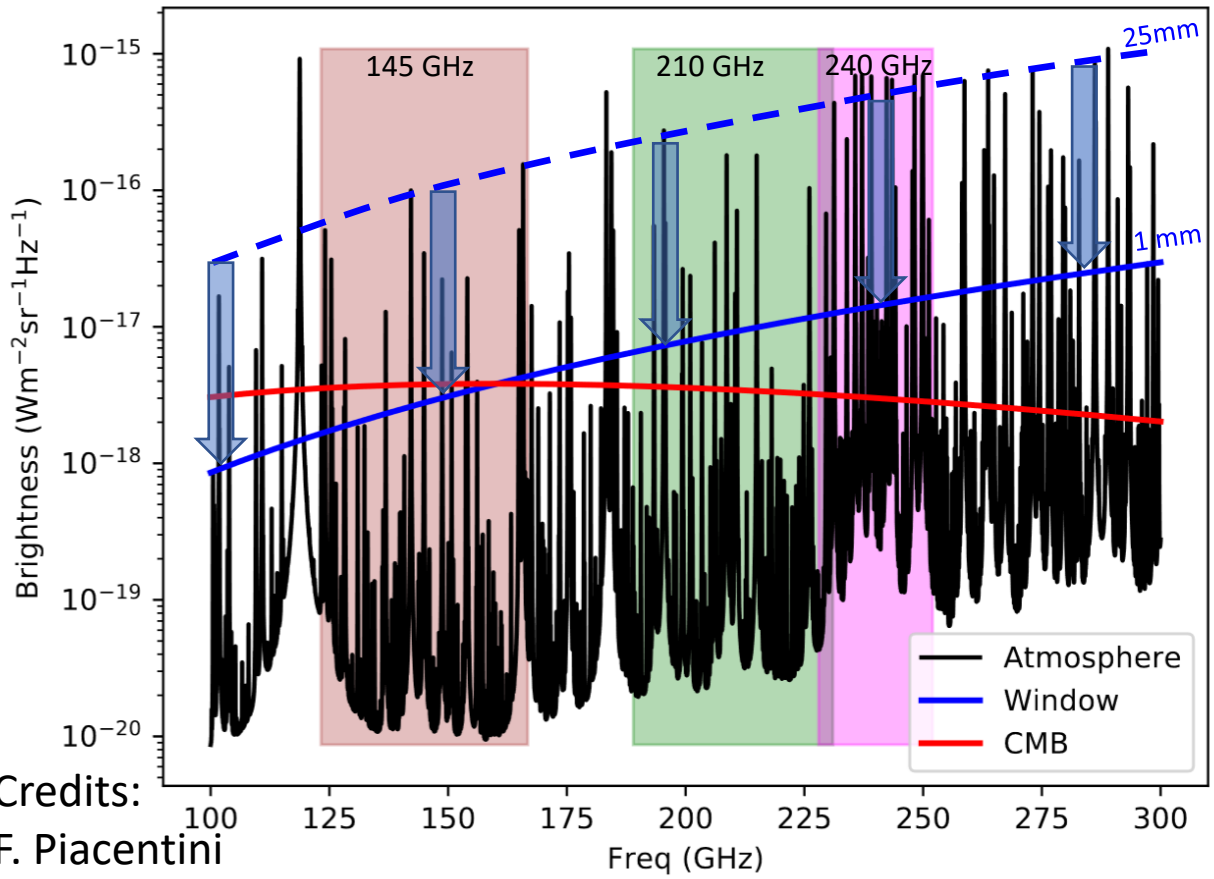

Credits:
F. Piacentini

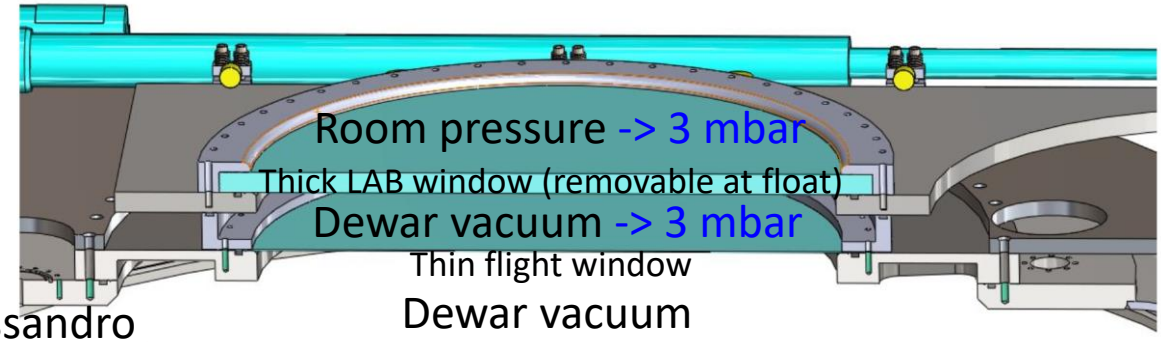

Reduction of the amplitudes of HWP-synchronous systematic effects

In a real Stokes polarimeter, the optical devices produce polarized emission, which can be in part modulated by the rotation of the HWP (e.g. Salatino & de Bernardis 2010, Columbro et al. 2019)

- Polarized emission/transmission of the lens, stop, field optics: mitigated using the HWP as the first optical element skywise.
- The HWP can have slightly different efficiencies for the fast and slow axes. This results in polarized emission & transmission of the HWP, modulated by the polarizer, i.e. a **$2f_{HWP}$** signal **(5 mK !)**. Mitigated by filtering the output signal (bandpass around $4f_{HWP}$)
- The polarizer emission can be reflected by the HWP and modulated: this results in a small **$4f_{HWP}$** signal. Mitigated by reducing the temperature of the polarizer (here 1.6K, so **few μK**). Can be removed by a dedicated pipeline (e.g. Ritacco & 2017).
- The polarized emission of the HWP can be reflected by the polarizer and by the HWP. This is a small $4f_{HWP}$ signal. In our case is very small, since the polarizer is tilted 45° wrt the HWP.

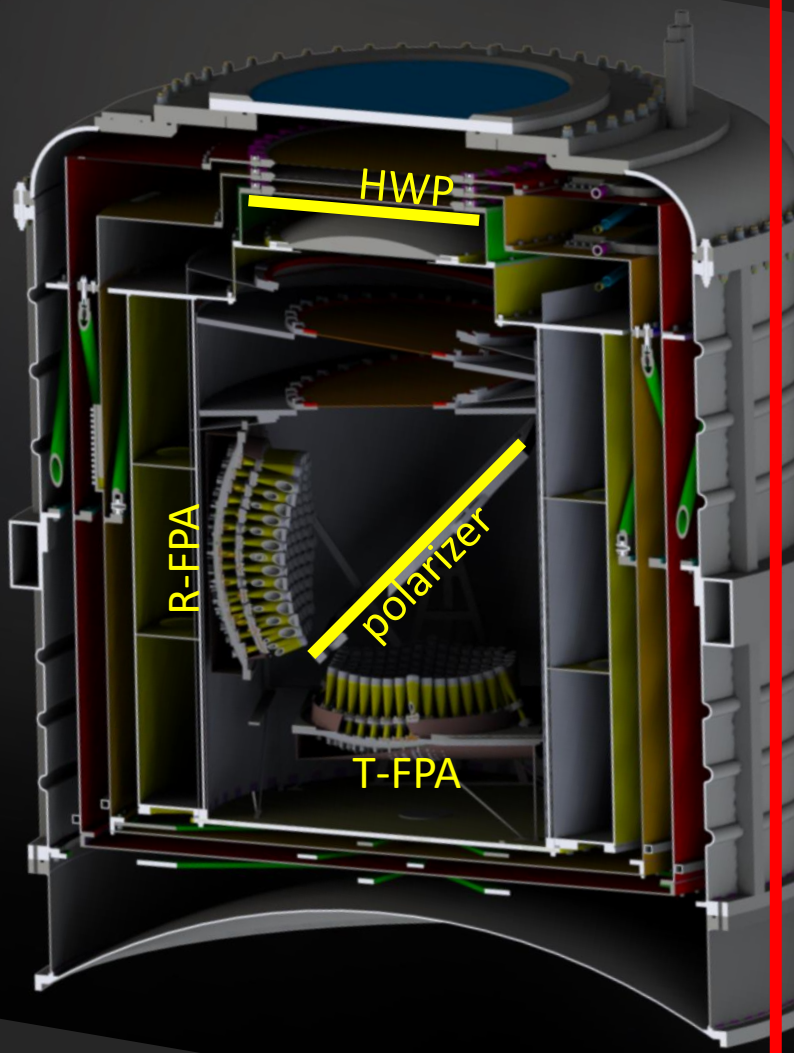

Reduction of the amplitudes of HWP-synchronous systematic effects

- There are other subtle systematic effects, an additional ones will be discovered.
- One of the main reasons of interest for this experiment is that we have the opportunity to study experimentally the performance of a Stokes polarimeter with cryogenic spinning HWP, a configuration which will be used in several ultresensitive experiments, including LiteBIRD.
- Real experimental tests are badly needed, in addition to simulations, to validate a very difficult meaurement !

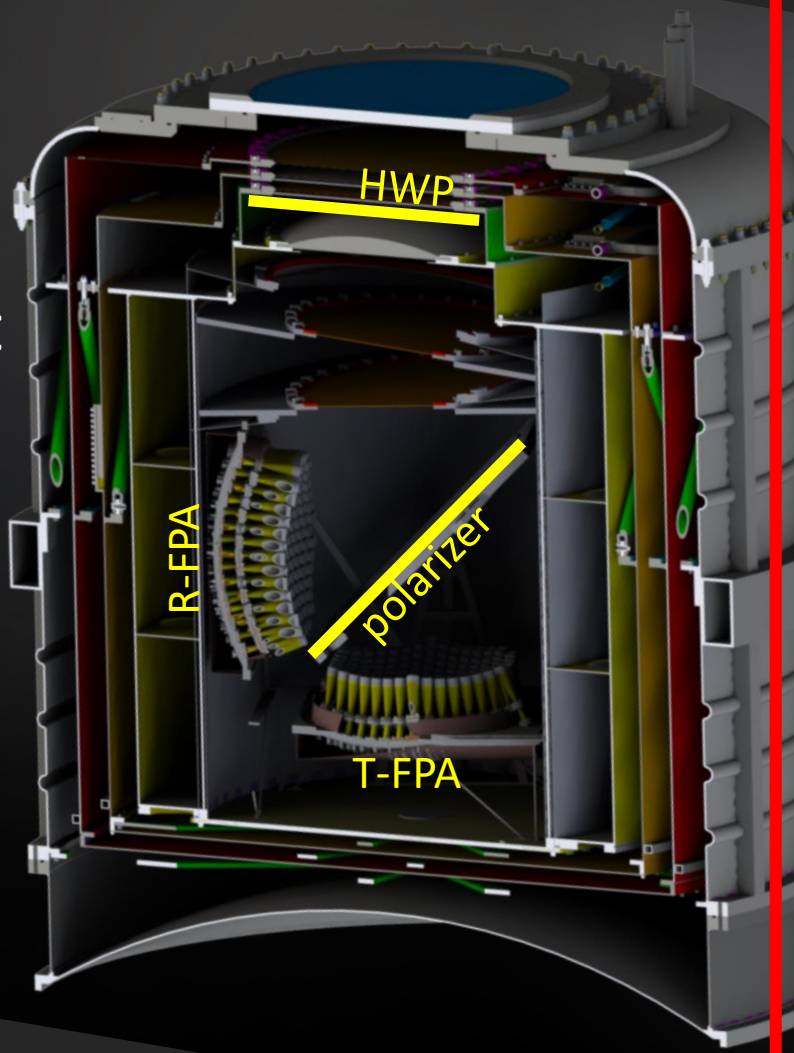

LSPE/SWIPE : polar night flight

- Uses the winter stratospheric polar vortex
- Less stable than the summer vortex used in Antarctica
- Reliable forecast tools needed

16/Dec/2019: polar vortex

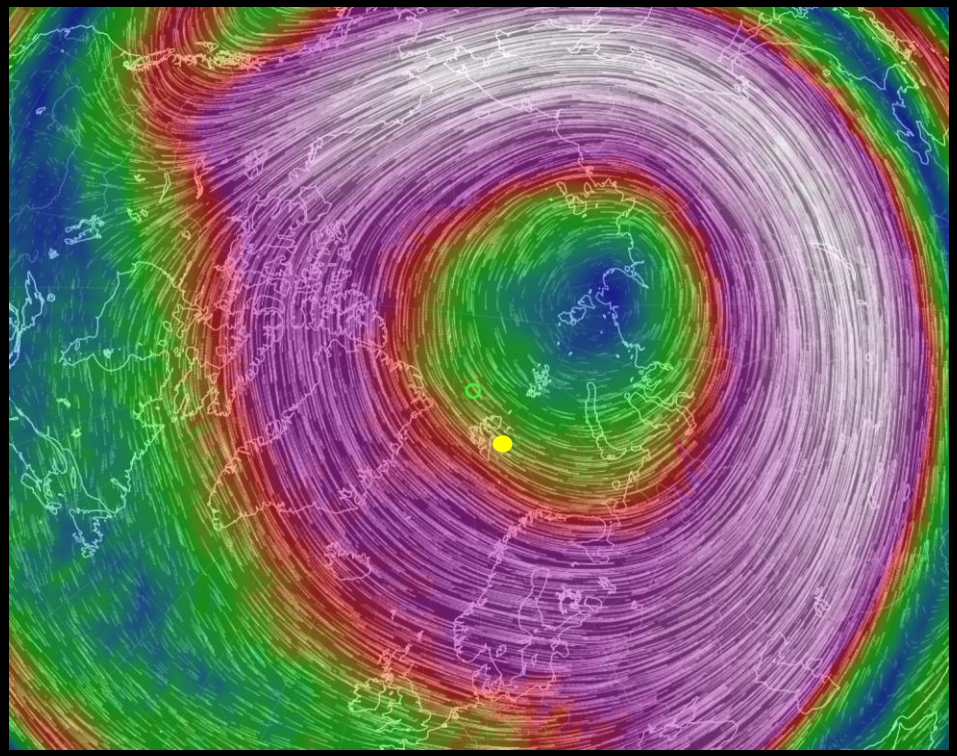

Credit: earth.nullschool.net

16/Dec/2019: flight forecast: 14 days

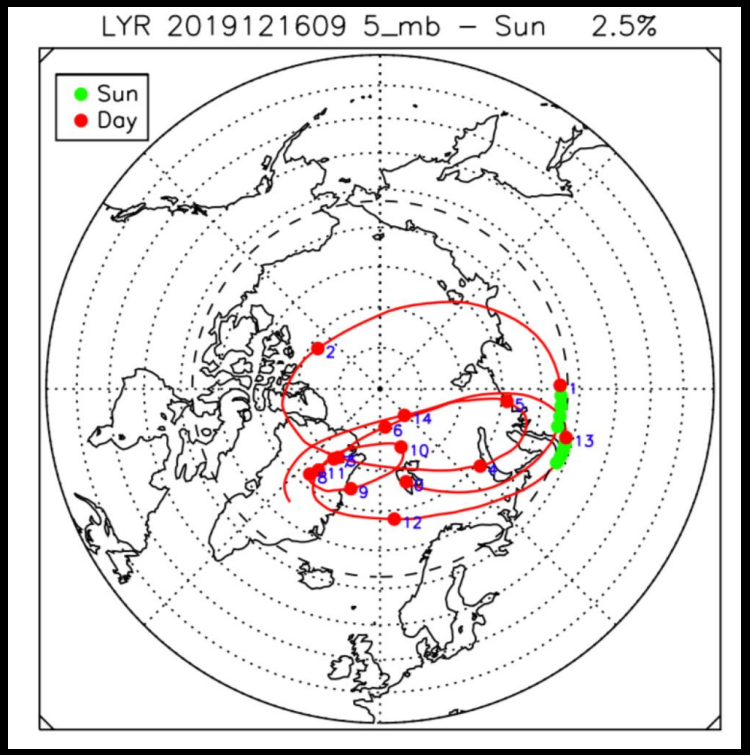

Credit: Piacentini

LSPE/SWIPE : night polar flight

- Flight managed by ASI, scheduled for end of 2023
- Longyearbyen – Svalbard or Kiruna Sweden
- Several test flights already carried out

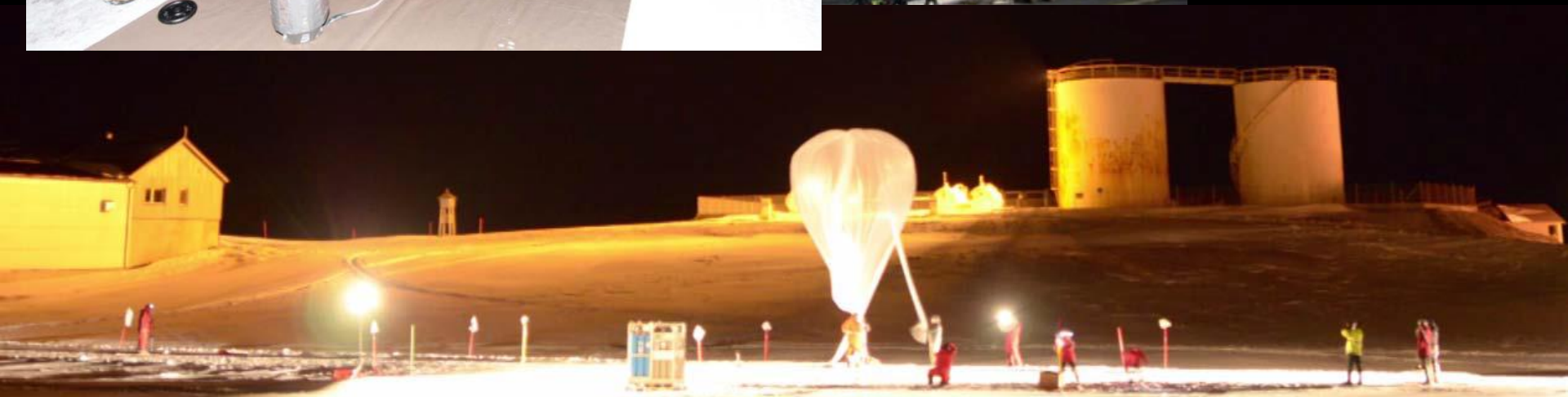

SWIPE: solar illumination issues

- With a careful choice of the launch date and launch site the length of the illuminated portions of the flight can be minimized
- We do not plan to carry out science measurements during these periods, but the instrument should be prepared to survive short solar illumination periods.

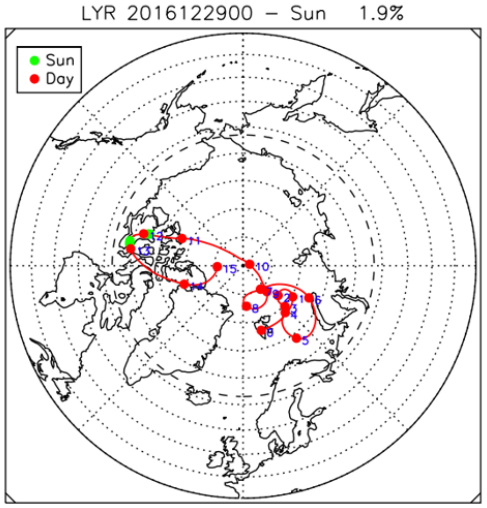

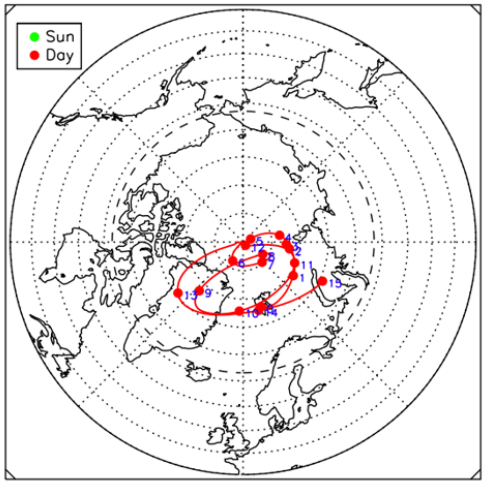

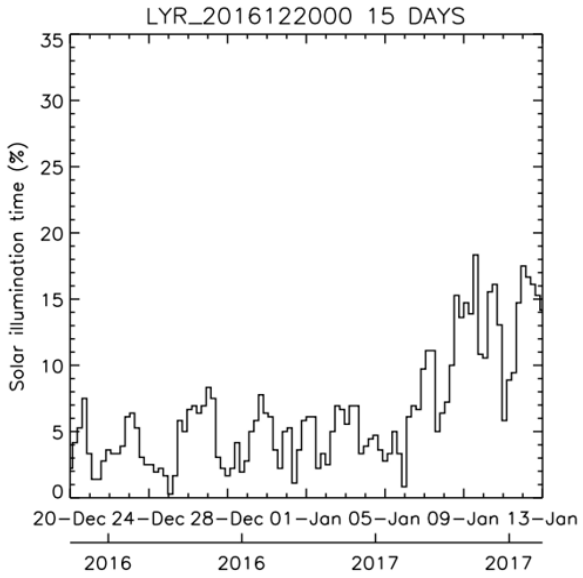

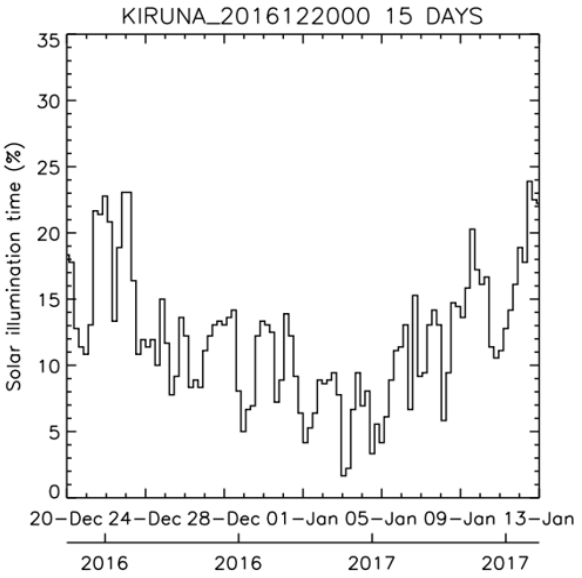

F. Piacentini

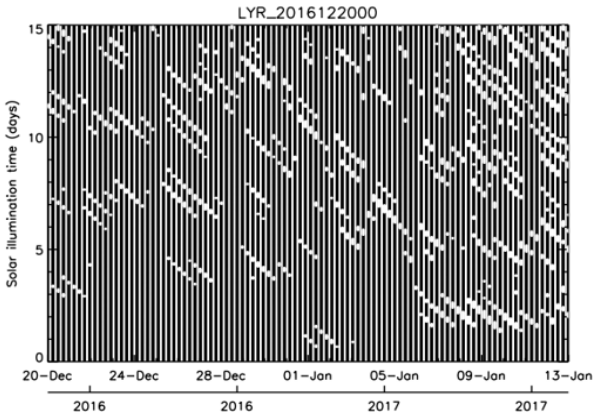

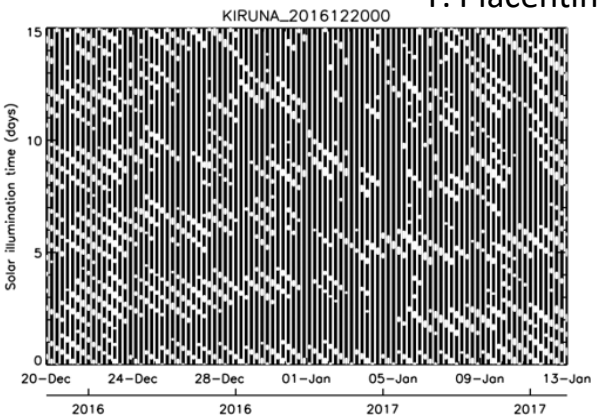

SWIPE - receiver

- A Stokes (HWP + polarizer + power detector) polarimeter, panoramic
- Simple implementation
- Two large focal planes (8800 modes), at 0.3K, in a large cryostat, cooling also the lens (490mm diam. and a 460 mm diam. cold stop) and the polarization modulator (HWP at about 10-15 K).
- FOV: 20° split by a 500mm diam., 45° tilted wire grid into 2 Focal Planes 300 mm diam (f/1.75)
- **Most components being machined, some ready**

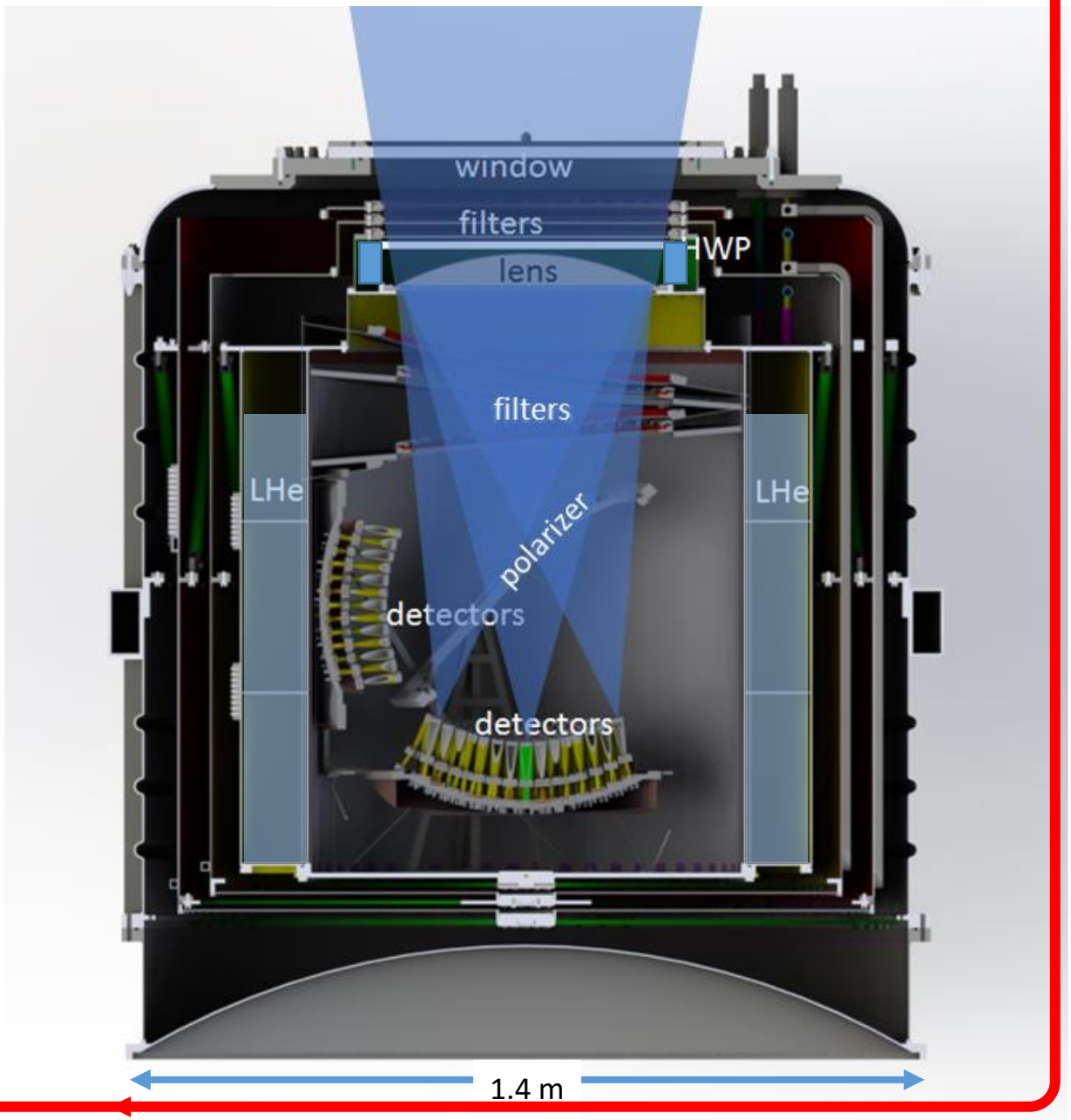

SWIPE – HWP

- Is a cold (2K), large (50 cm useful dia.), wide-band meta-materials HWP, placed immediately behind the window and thermal filters stack.
- HWP characteristics for the ordinary and extraordinary rays are well matched: $(T_o-T_e)/T_o < 0.001$, $X_{pol}<0.01$, over the 100-300 GHz band.
- Simulations show that continuous rotation has advantages in terms of 1/f noise mitigation and angles coverage.
- A custom superconductive rotator has been developed.

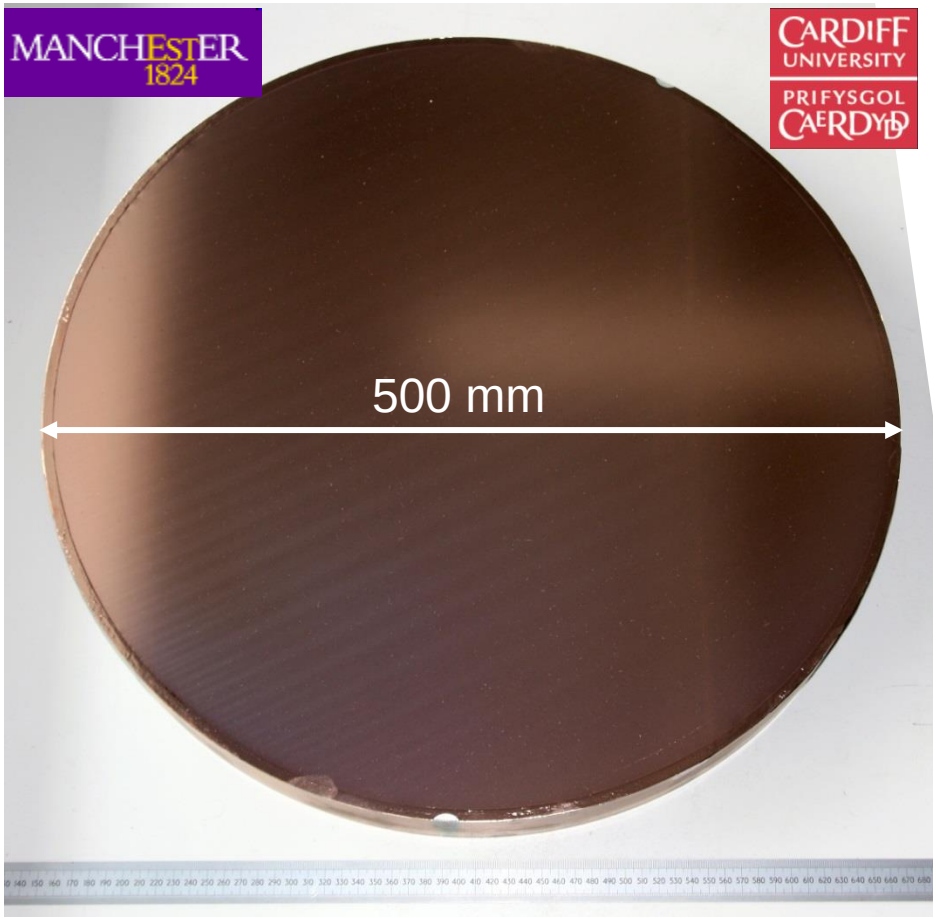

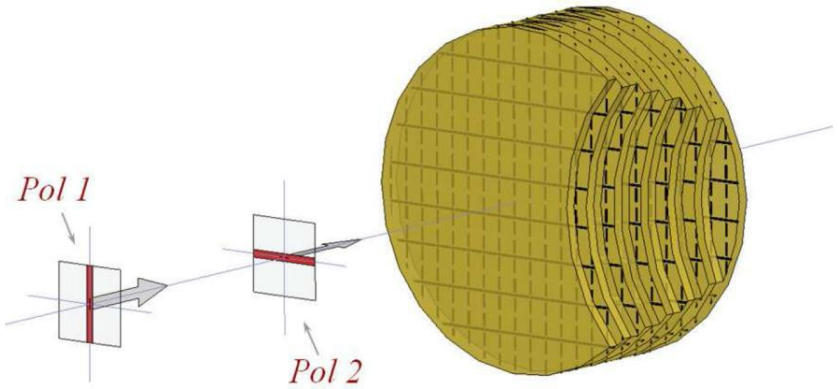

Pisano et al., Proc. SPIE, Vol. 9153, id. 915317 (2014)

SWIPE – HWP rotator

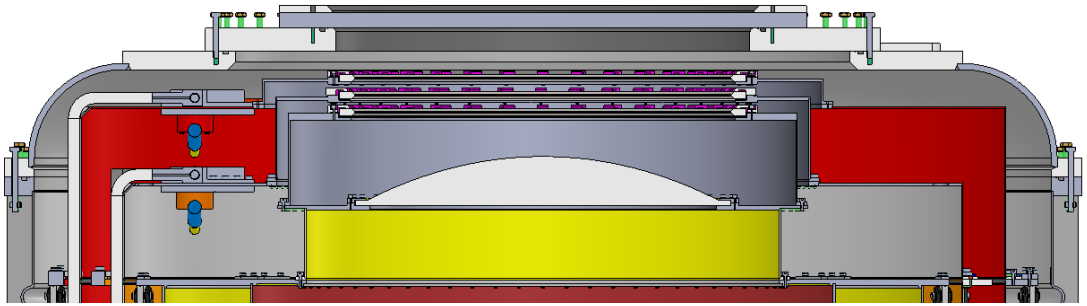

~670mm

Permanent magnet ring

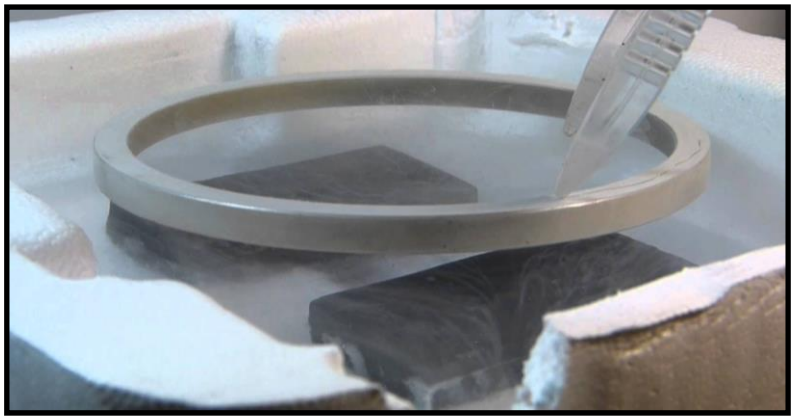

High Temperature Superconductors

Pros

- NO stick-slip friction
- NO extra-effort to cool HTSs
- Passive stable levitation
- Low Coefficient of friction
- Continuous rotation (0-10Hz)

Cons

- Variable magnetic field
- Clamp mechanism at 4K

S. Hanany et al., IEEE Trans.Appl.Supercond. 13 (2003) 2128-2133

T. Matsumura et al., IEEE Trans.Appl.Supercond. 26 (2016)

SWIPE – HWP rotator - General layout

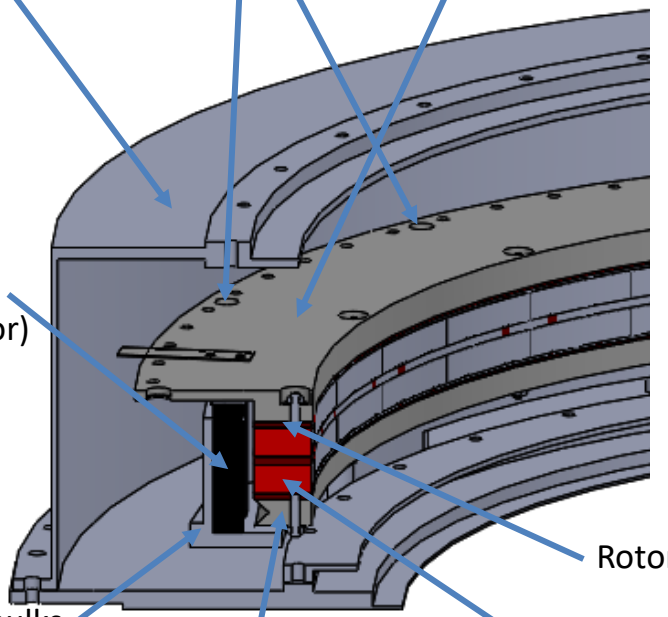

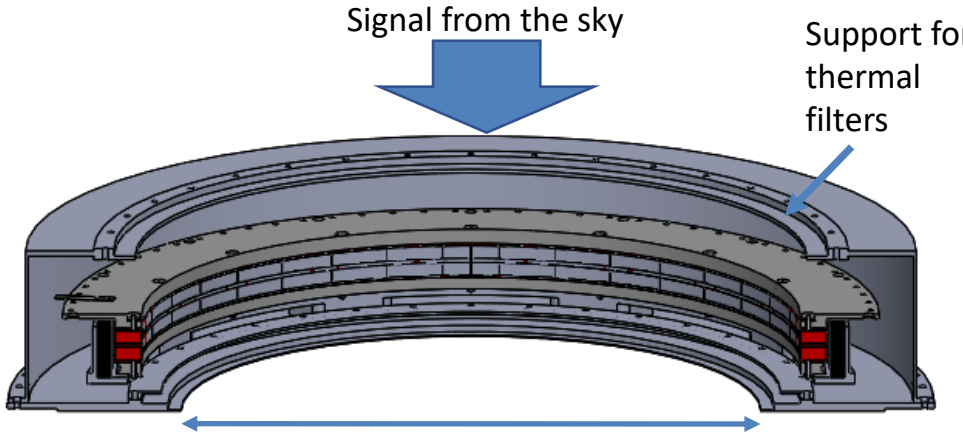

1T field strength in the gap. Total mass 9 kg.

SWIPE – HWP rotator – parts procured

Groove ring for C/R

Stator with YBCO bulks

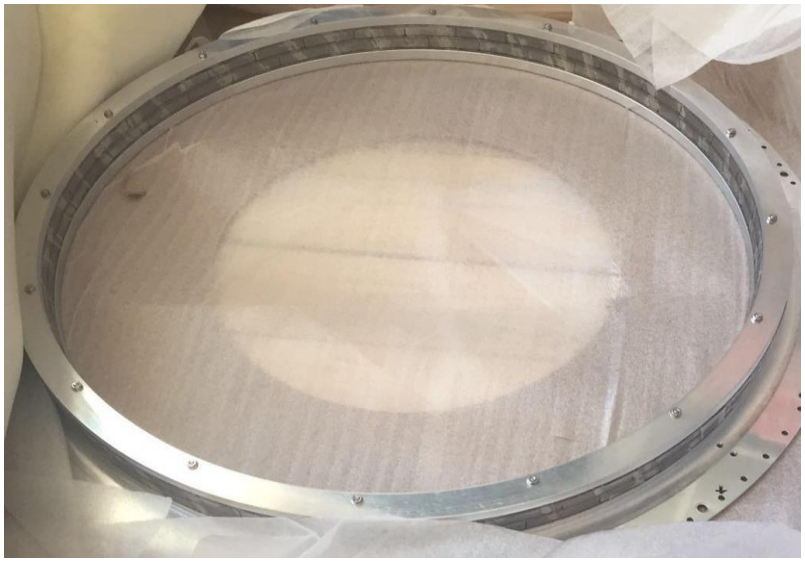

Rotor with permanent magnets

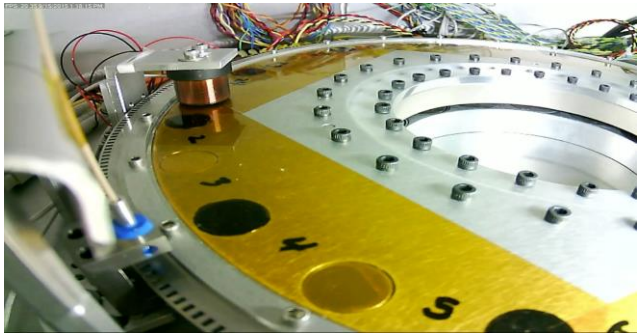

smaller diameter Prototype
arXiv:1706.05963v3

SAPIENZA UNIVERSITÀ DI ROMA

SWIPE – HWP rotator – clamp/release

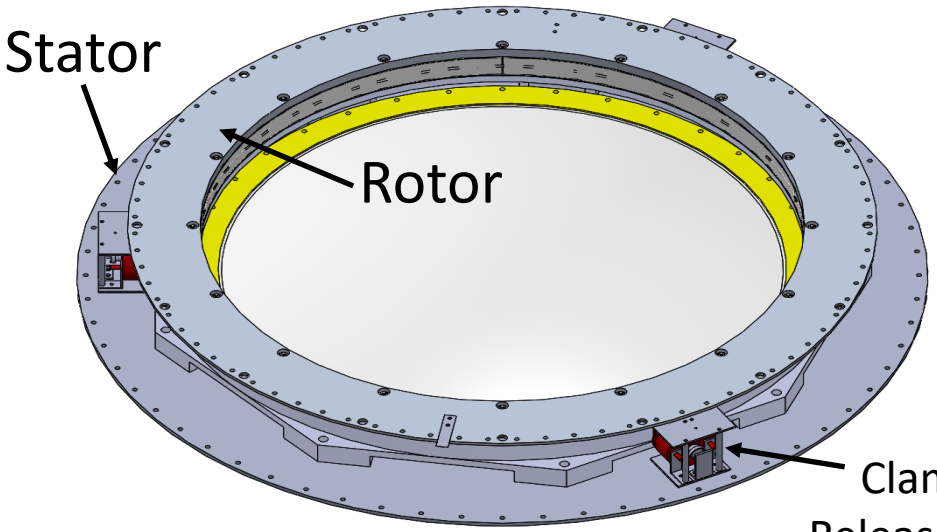

Frictionless actuator for operation @ 2K

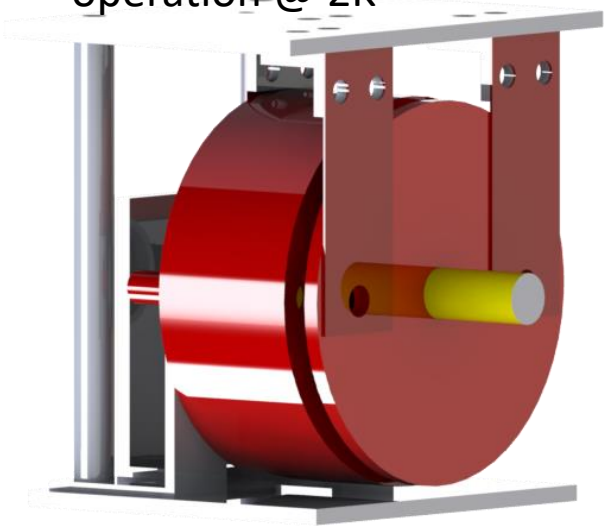

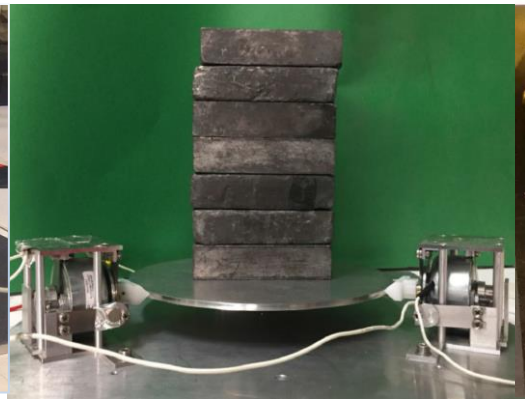

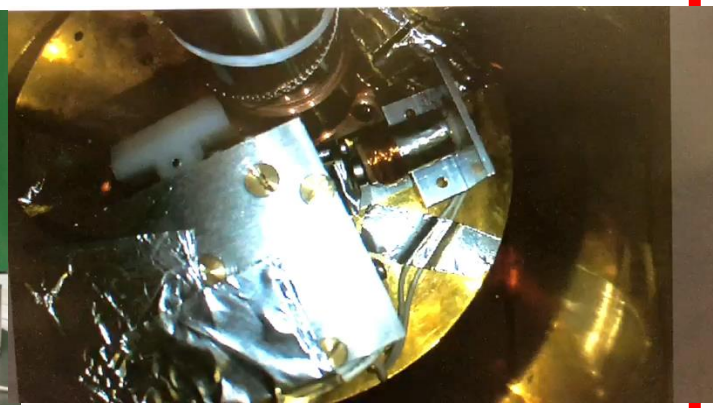

Fabio Columbro, Paolo de Bernardis, and Silvia Masi
A clamp and release system for superconducting magnetic bearings
Review of Scientific Instruments 89, 125004 (2018)

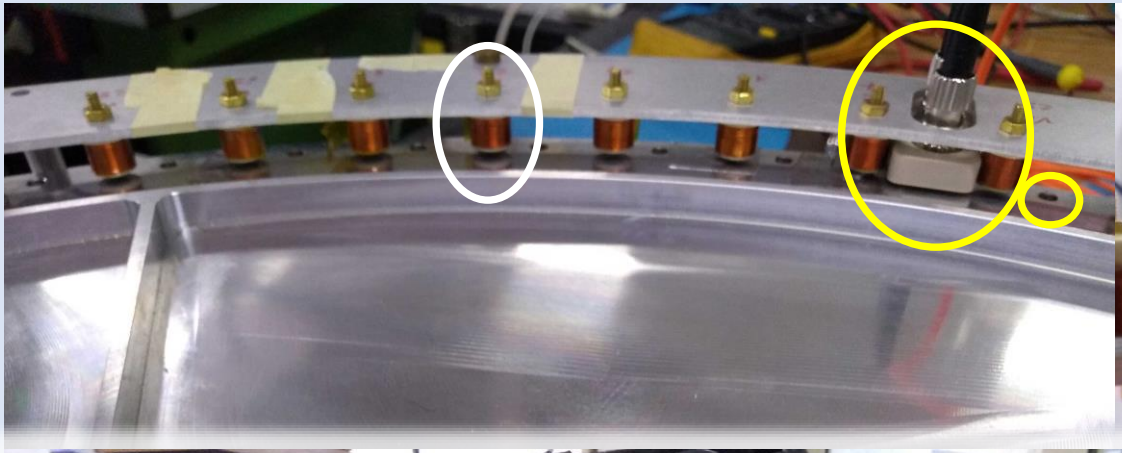

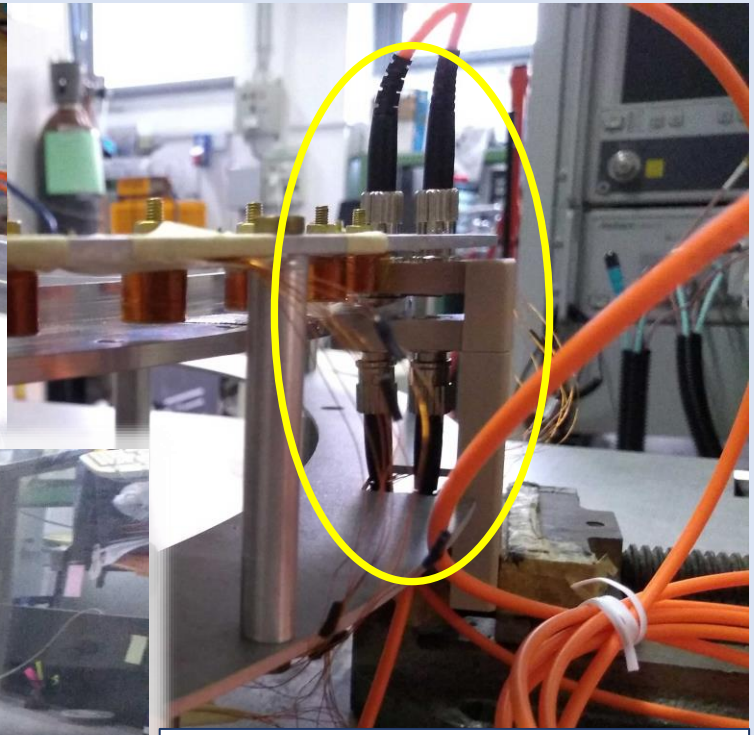

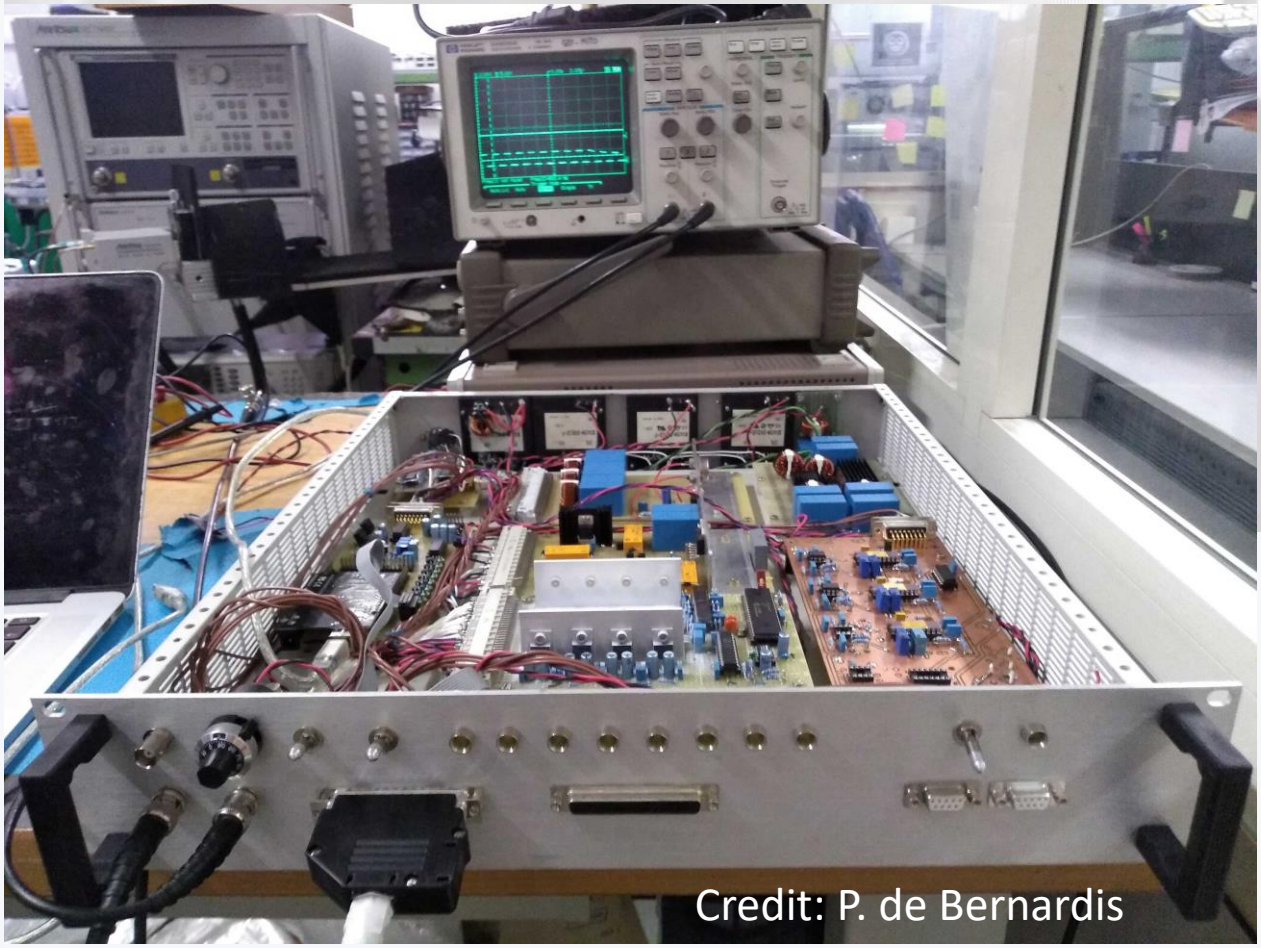

Custom brushless synchronous motor & control electronics:

- 8 phases
- 64 equalized coils (stator)
- 8 magnets (rotor)
- Smooth phased currents to minimize EMI & induced eddy currents
- 64-slits optical encoder
- High accuracy optical fibers readout ($\Delta t=50\mu s$)

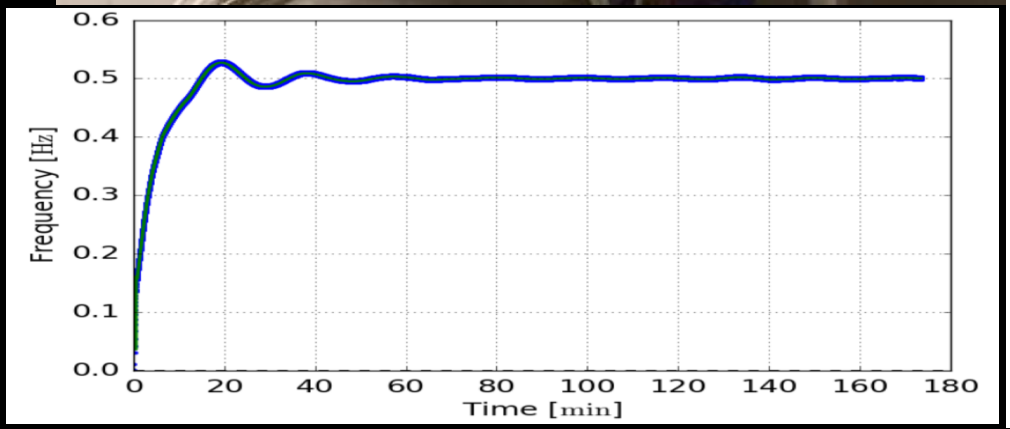

Room-T testbed for motor & control: OK

Working for :

- Optimization of start
- Optimization of feedback algorithm (frequency, phase and amplitude)
- Minimization of driving currents
- FPGA board for precision time stamping
- Thermal/vac test

SWIPE: Focal Planes real estate

- The distribution of colors in the pixels has been optimized with a simplified scheme for foregrounds (dust) removal.
- This distribution provides sufficient precision to extrapolate the dust signal from high frequency down to 150 GHz
- This configuration totalizes 4400 radiation modes for each focal plane (transmitted and reflected).

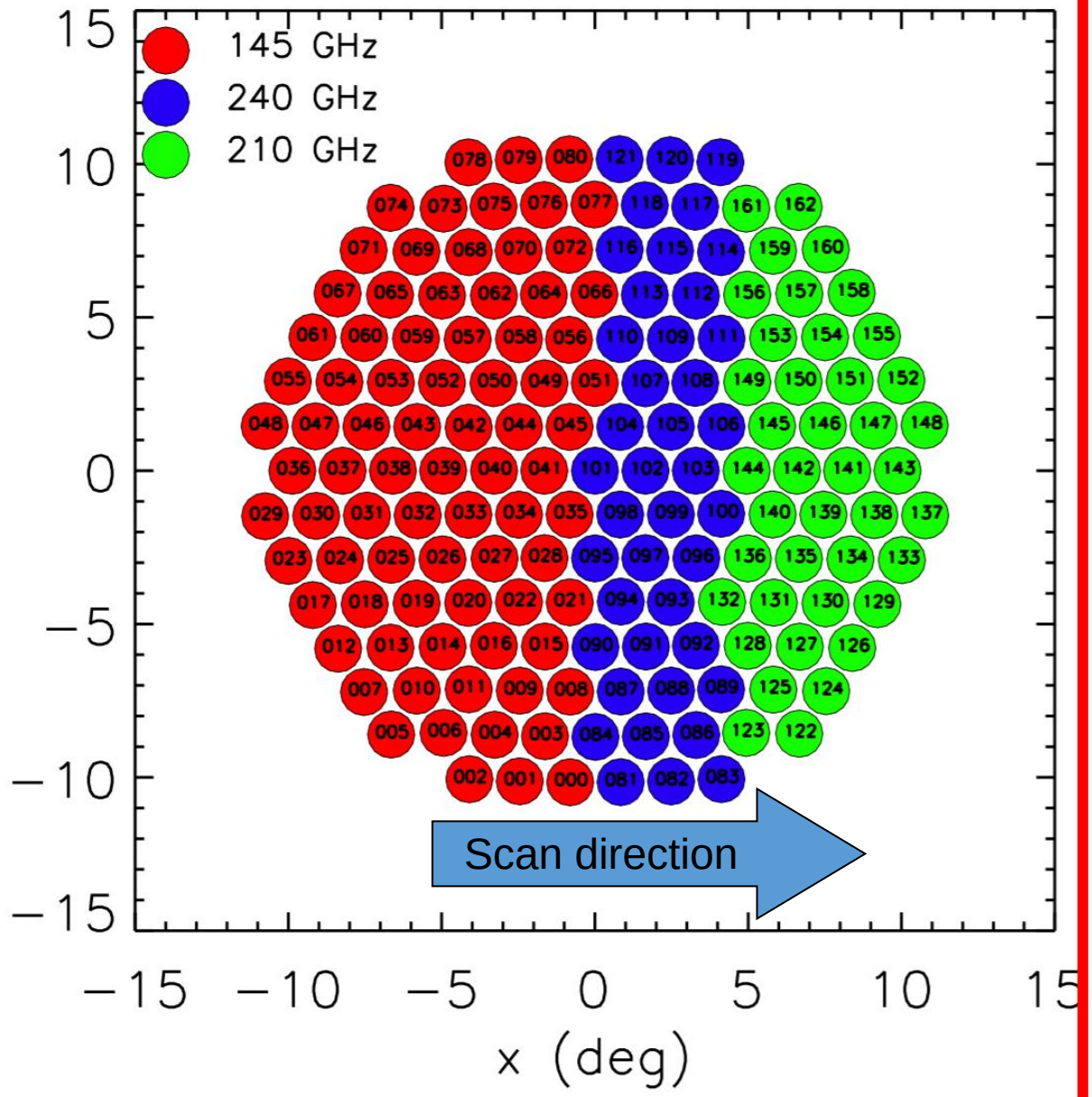

LSPE horns & bolo holders

Large Throughput multimode detectors: 8800 modes collected by 330 sensors

Focal plane detector flanges (gold plated Al6061, 40 cm side).

LSPE horns & bolo holders

Large Throughput multimode detectors: 8800 modes collected by 330 sensors

Focal plane detector flanges (gold plated Al6061, 40 cm side).

In May 2019, LiteBIRD has been selected for JAXA's strategic L-class mission!

Official announcement at
http://www.isas.jaxa.jp/home/rikou/godo/2019/0602/gbi7uzhxfxmz/misison_selection_announcement_may2019.pdf

2. LiteBIRD Overview

- JAXA's L-class mission #2
- Expected launch in 2027
- Observations for 3 years (baseline) around Sun-Earth Lagrangian point L2
- Millimeter-wave all sky surveys (34–448 GHz, 15 bands) at 70–20 arcmin.
- Mission: $\delta r < 0.001$ in $2 \leq l \leq 200$ w/ CMB B-mode observation

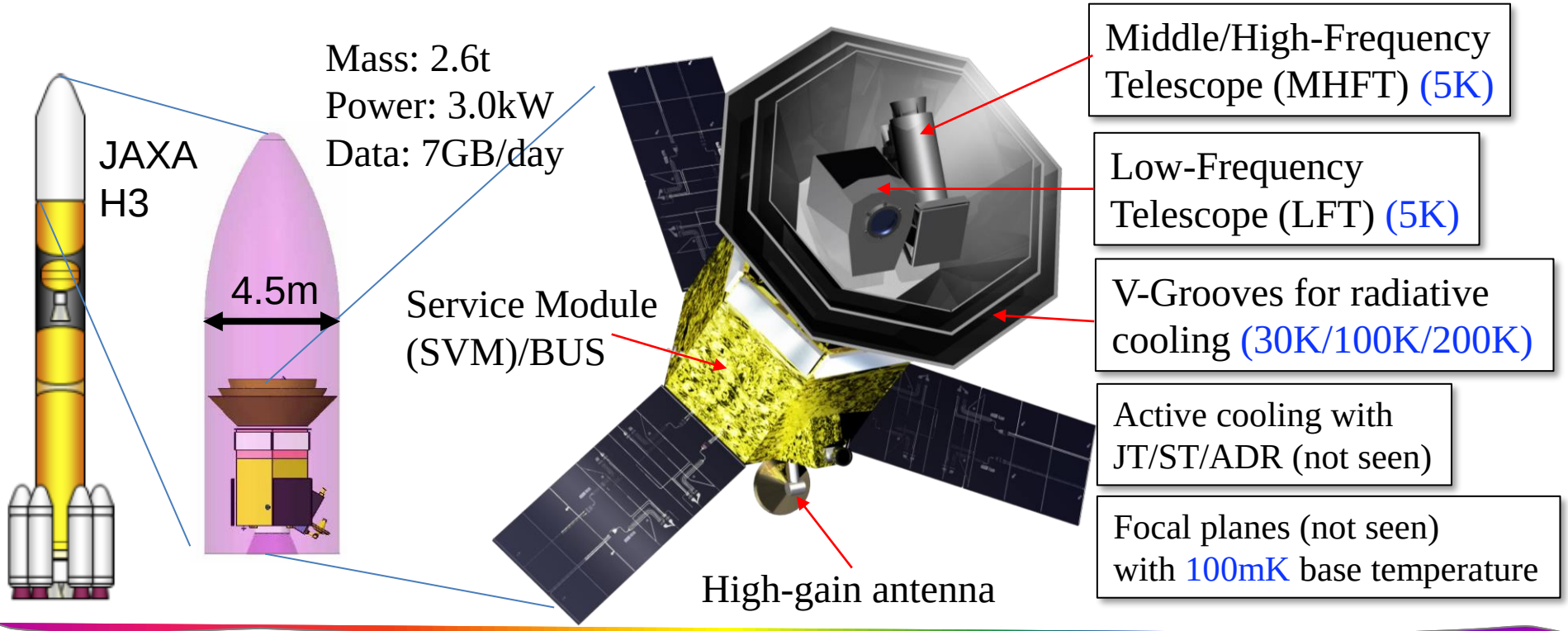

Operation

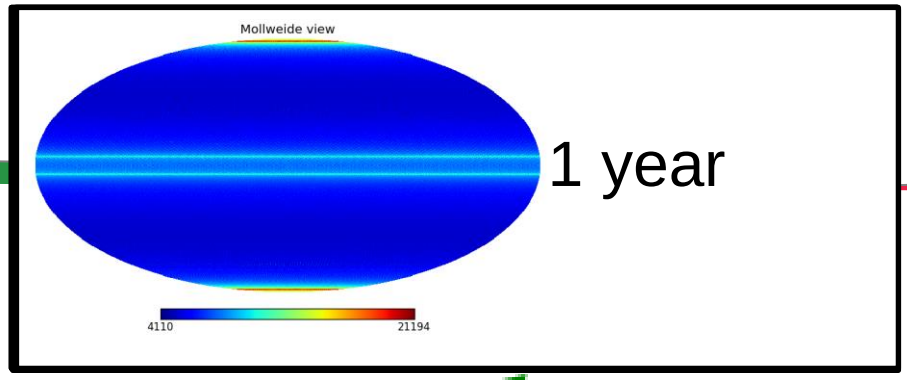

1 year

Orbit:
Sun-Earth L2 Lissajous

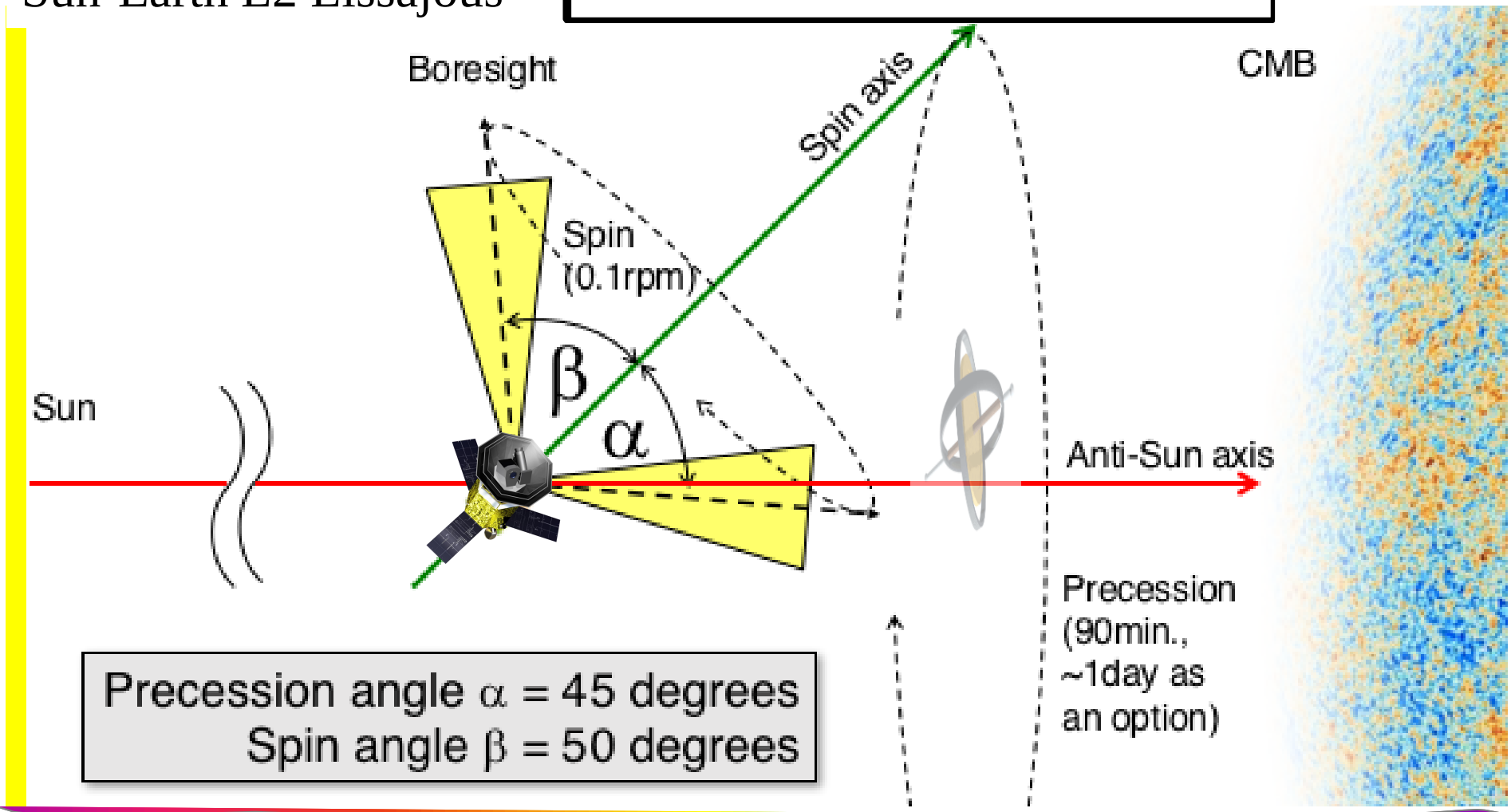

LiteBIRD mission instrument

Three features

1. Two telescopes w/ TES arrays
2. Polarization modulator for 1/f noise & systematics reduction
3. Cryogenic system for 0.1K base temperature

Component tree

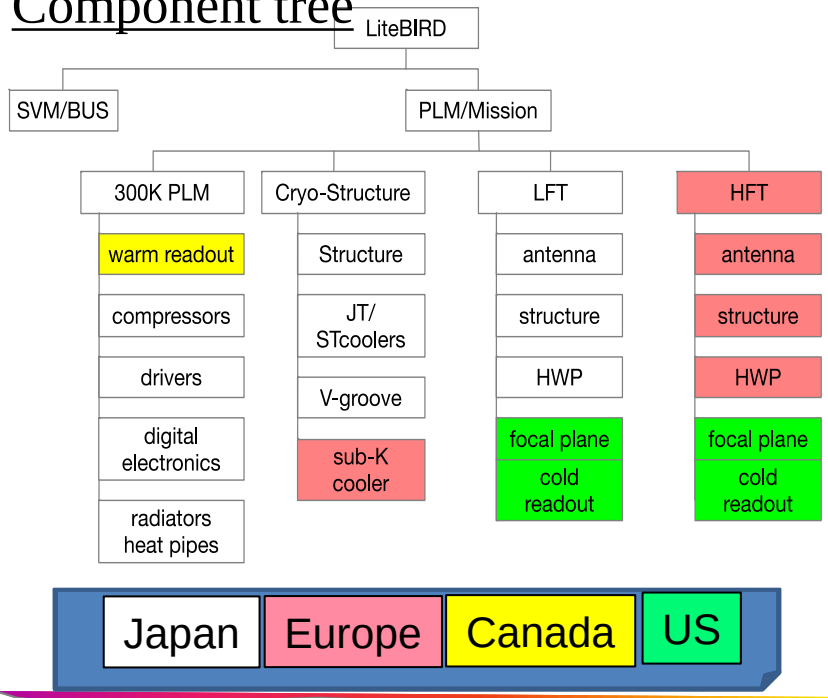

1. Two telescopes w/ TES arrays

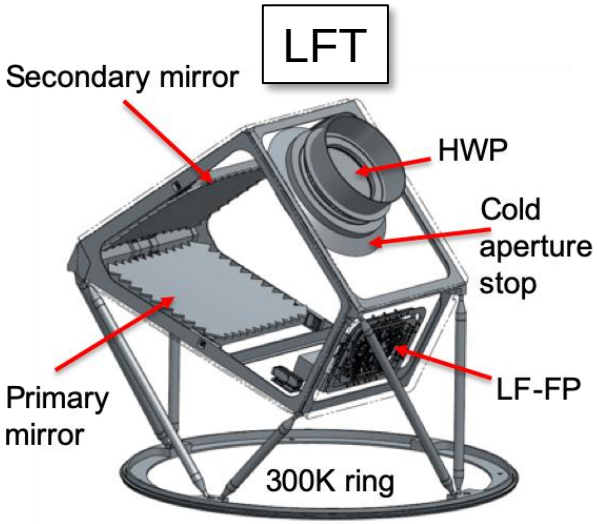

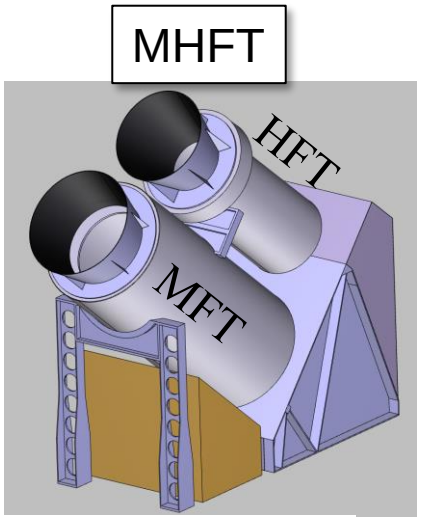

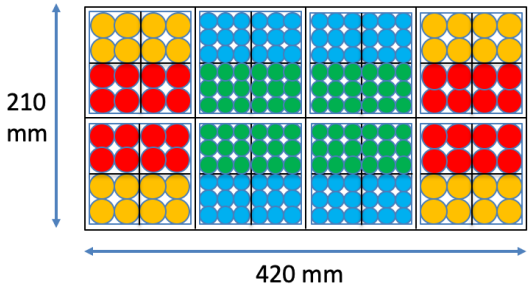

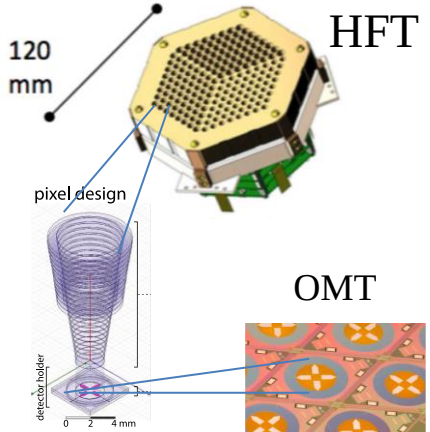

Sinuous Antenna for broadband trichroic pixels

Silicon platelet Corrugated horn

LiteBIRD mission instrument

2. Polarization modulator for 1/f noise & systematics reduction

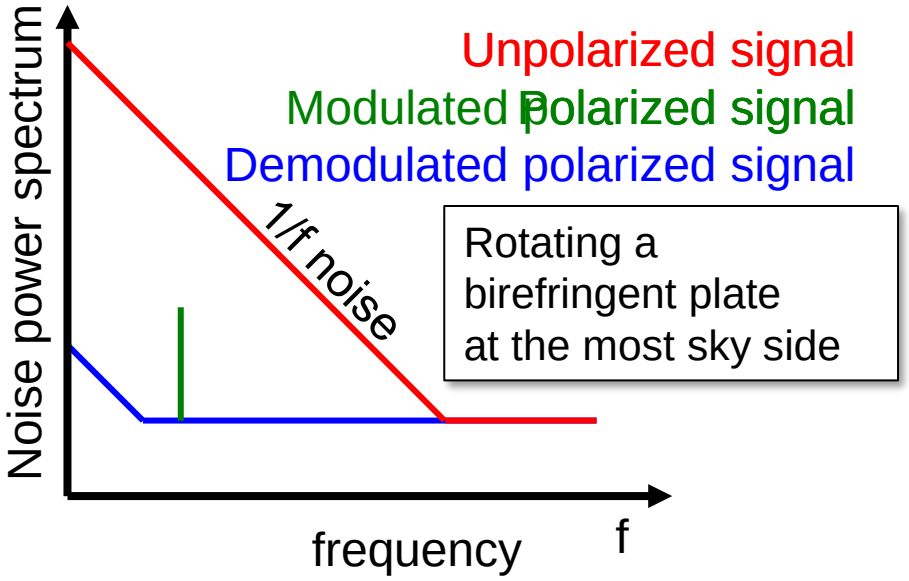

Rotating a birefringent plate at the most sky side

3. Cryogenic system for 0.1K base temperature

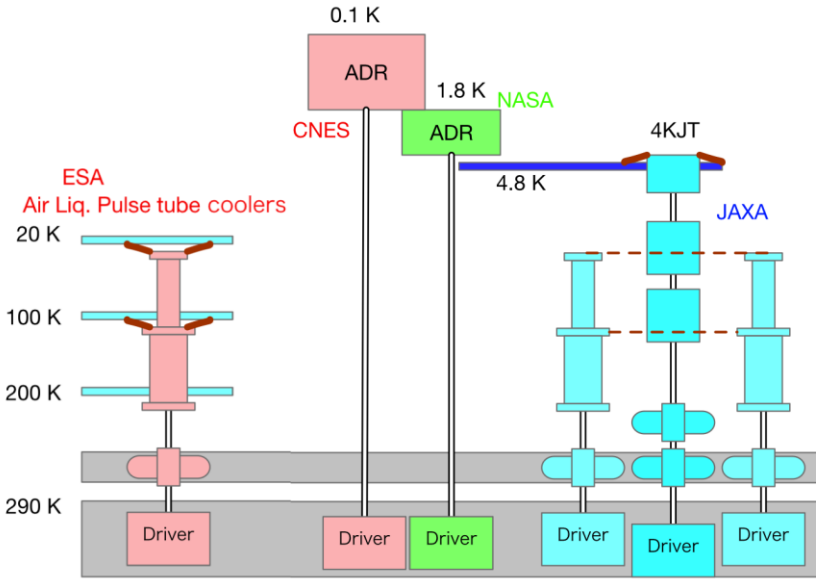

Superconducting magnetic bearing system operational in a 4K cryostat.
We observed the stable rotation at cryogenic temperature (<10K).

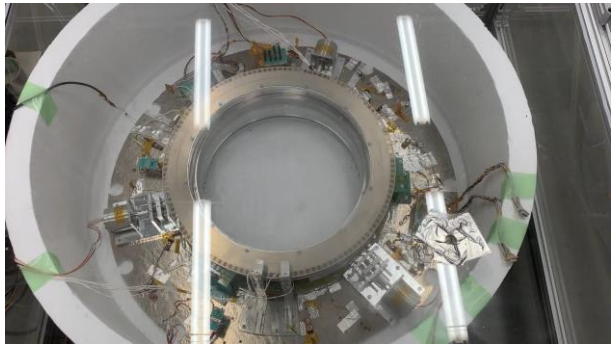

Scientific goal and challenges

Full Success :
$\delta r < 1 \times 10^{-3}$ (for r=0)
$2 \leq \ell \leq 200$

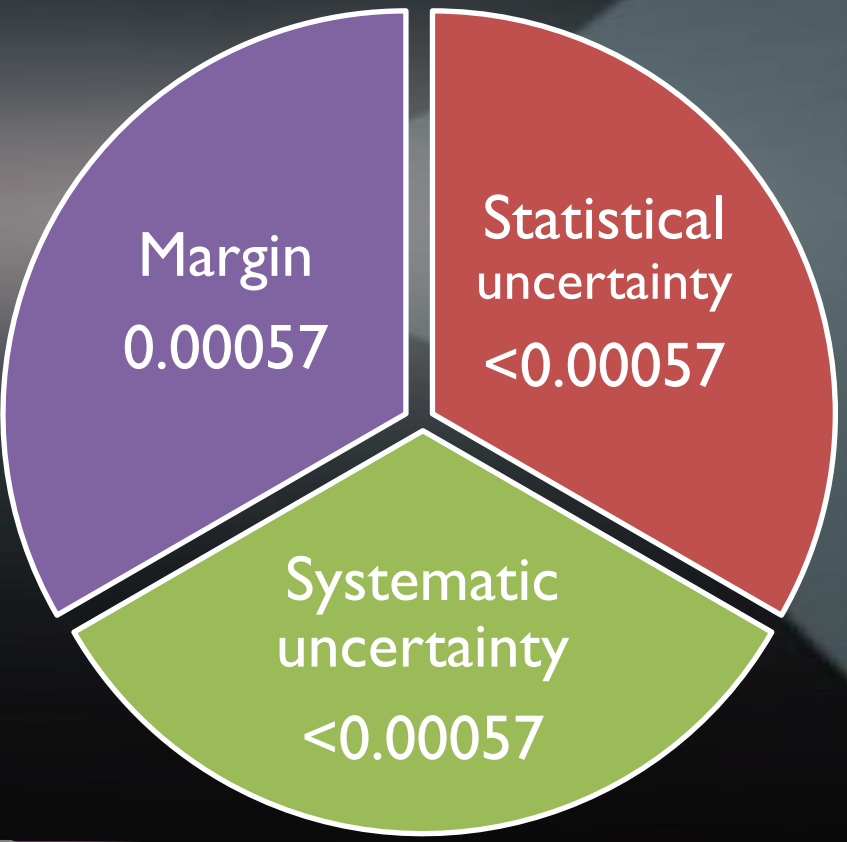

δr : Total uncertainty

Statistical uncertainty includes
- foreground cleaning residuals
- lensing B-mode power
- 1/f noise

Systematic uncertainty includes
- Bias from 1/f noise
- Polarization efficiency & knowledge
- Disturbance to instrument
- Off-boresight pick up
- Calibration accuracy

Foreground cleaning

Methodology

Synchrotron: $[Q_s, U_s](\hat{n}, \nu) = [Q_s, U_s](\hat{n}, \nu_*) \left(\frac{\nu}{\nu_*}\right)^{\beta_s(\hat{n}) + C_s(\hat{n}) \ln(\nu/\nu_*^C)}$

- AME is effectively absorbed by synchrotron curvature

Dust: $[Q_d, U_d](\hat{n}, \nu) = [Q_d, U_d](\hat{n}, \nu_*) \left(\frac{\nu}{\nu_*}\right)^{\beta_d(\hat{n})-2} \frac{B[\nu, T_d(\hat{n})]}{B[\nu_*, T_d(\hat{n})]}$

(8 parameters in each sky region) x (12 x $N_{\rm side}^2$)

= 6144 parameters w/ $N_{\rm side} = 8$

to take spatial variations into account

Results

"Multipatch technique" (extension of xForecast)*

- σ(r=0) = 0.0006
- Negligibly small bias

Consistent results from COMMANDER!

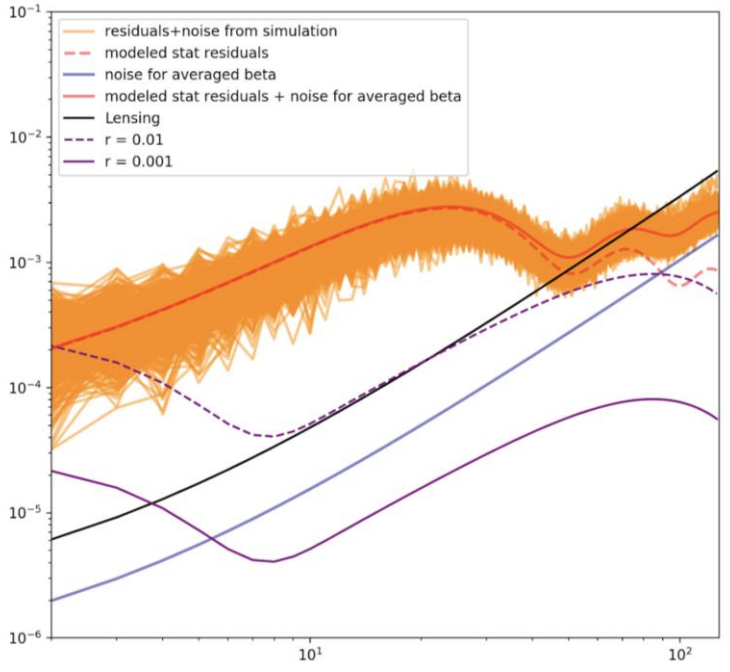

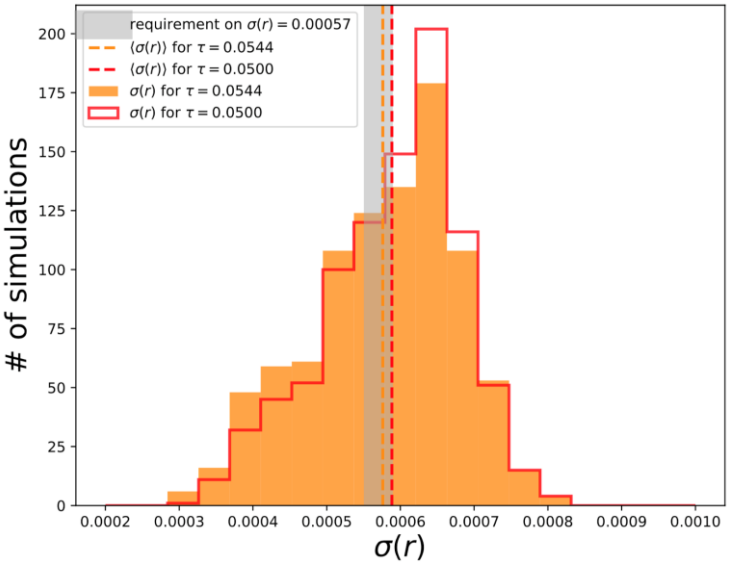

* Errard and Stompor, Phys.Rev. D99 (2019) no.4, 043529

Systematics and calibration

- One of the largest study groups at LiteBIRD
- Systematic approach for systematic uncertainties
  - List systematic error items → 14 categories, 70 items listed
  - Assign each item $\sigma(r)_{sys} < 5.7 \times 10^{-6}$ as the budget (1% of total budget for systematic error)
  - Derive a requirement for each item, define method (incl. calibration methods) and estimate $\sigma(r)_{sys}$
  - Assign special budget allocations for outstanding items
  - Sum each contribution on map base to estimate total $\sigma(r)_{sys}$ (some studies even on TOD basis) to take positive correlations into account
  - Iterate procedure
- Example: studies of systematic errors due to HWP imperfection
  - Mueller matrix from RCWA simulations of electromagnetic wave propagation through realistic HWP for different frequencies and incident angles
  - 4f component from M_{IQ}, M_{IU} ~10^{-4} in the worst case
  - Obtain leakage maps and BB power to estimate $\sigma(r)_{sys}$

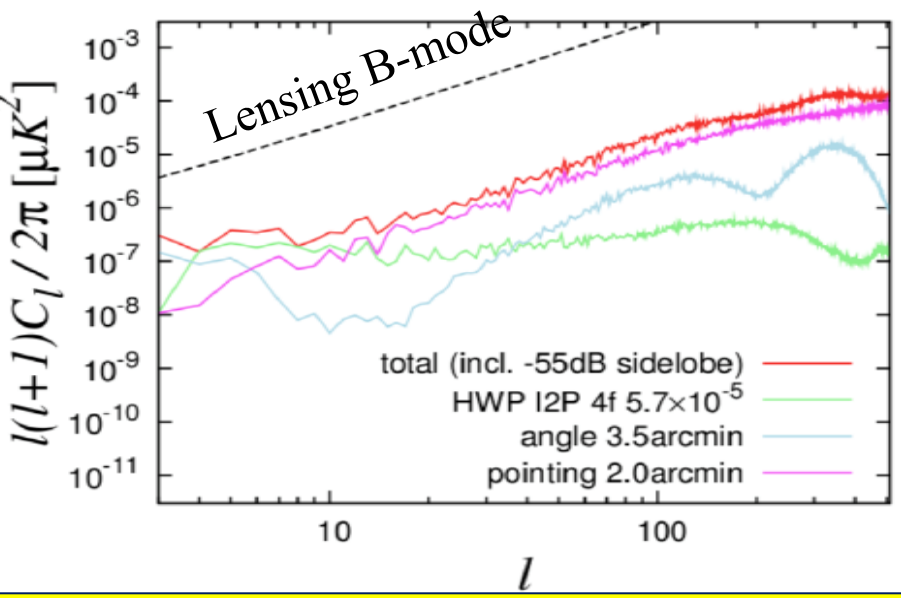

All known systematics will be adequately mitigated!

Further improvement with external data (extra success)

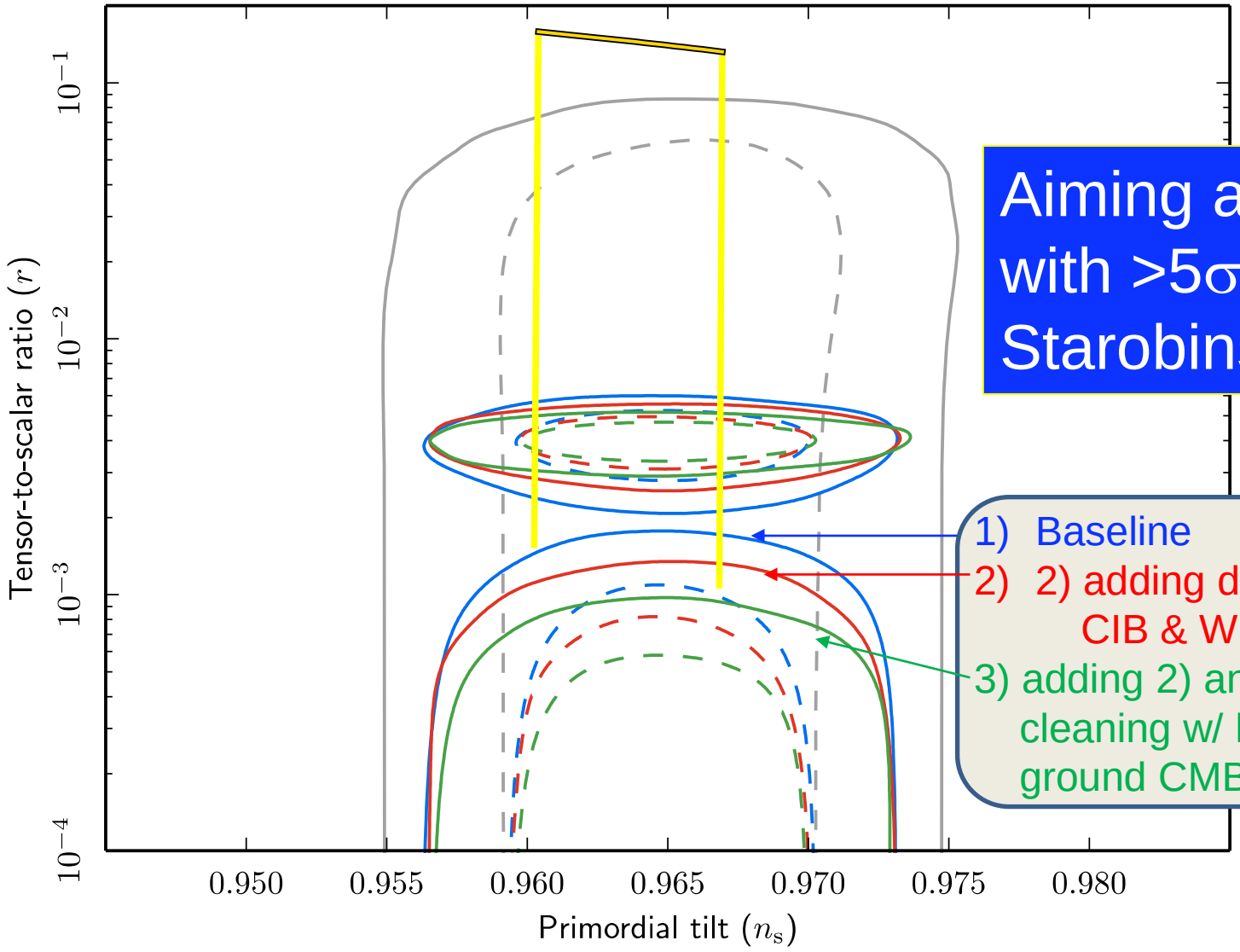

Aiming at detection with >5σ in case of Starobinsky model

1) Baseline
2) 2) adding delensing w/ Planck CIB & WISE
3) adding 2) and extra foreground cleaning w/ high-resolution ground CMB data

LiteBIRD science outcomes

1. Full success

System requirements from 1. only

2. Extra success (see previous page)
3. Characterization of B-mode
   (e.g scale-invariance, non-Gaussianity, and parity violation)
4. Large-scale E mode and its implications
   for reionization history and the neutrino mass
5. Birefringence
6. Power spectrum features in polarization
7. SZ effect (thermal and relativistic correction)
8. Anomaly
9. Cross-correlation science
10. Galactic science

3. – 10. almost guaranteed if full success is achieved.

LiteBIRD Summary

- Selected for JAXA's L-class mission #2
- Expected launch in 2027
- Observations for 3 years around Sun-Earth Lagrangian point L2
- Millimeter-wave all sky surveys (34–448 GHz, 15 bands) at degree scales

Full Success :
$\delta r < 1 \times 10^{-3}$ (for r=0)
$2 \leq \ell \leq 200$

- Detailed foreground cleaning studies yield $\sigma(r=0) = 0.5 \times 10^{-3}$
- Thorough systematic error studies yield total uncertainty $\delta r < 1.0 \times 10^{-3}$

CMB B-mode from primordial gravitational waves generated during Inflation would provide

- Direct evidence for Inflation, and knowledge on when it happened
- (Arguably) First evidence for quantum fluctuation of space-time
- Knowledge on the Inflation energy scale

PTEP paper of LiteBIRD

Astrophysics > Instrumentation and Methods for Astrophysics

[Submitted on 6 Feb 2022]

Probing Cosmic Inflation with the LiteBIRD Cosmic Microwave Background Polarization Survey

LiteBIRD Collaboration: E. Allys, K. Arnold, J. Aumont, R. Aurlien, S. Azzoni, C. Baccigalupi, A. J. Banday, R. Banerji, R. B. Barreiro, N. Bartolo, L. Bautista, D. Beck, S. Beckman, M. Bersanelli, F. Boulanger, M. Brilenkov, M. Bucher, E. Calabrese, P. Campeti, A. Carones, F. J. Casas, A. Catalano, V. Chan, K. Cheung, Y. Chinone, S. E. Clark, F. Columbro, G. D'Alessandro, P. de Bernardis, T. de Haan, E. de la Hoz, M. De Petris, S. Della Torre, P. Diego-Palazuelos, T. Dotani, J. M. Duval, T. Elleflot, H. K. Eriksen, J. Errard, T. Essinger-Hileman, F. Finelli, R. Flauger, C. Franceschet, U. Fuskeland, M. Galloway, K. Ganga, M. Gerbino, M. Gervasi, R. T. Génova-Santos, T. Ghigna, S. Giardiello, E. Gjerløw, J. Grain, F. Grupp, A. Gruppuso, J. E. Gudmundsson, N. W. Halverson, P. Hargrave, T. Hasebe, M. Hasegawa, M. Hazumi, S. Henrot-Versillé, B. Hensley, L. T. Hergt, D. Herman, E. Hivon, R. A. Hlozek, A. L. Hornsby, Y. Hoshino, J. Hubmayr, K. Ichiki, T. Iida, H. Imada, H. Ishino, G. Jaehnig, N. Katayama, A. Kato, R. Keskitalo, T. Kisner, Y. Kobayashi, A. Kogut, K. Kohri, E. Komatsu, K. Komatsu, K. Konishi, N. Krachmalnicoff, C. L. Kuo, L. Lamagna, M. Lattanzi, A. T. Lee, C. Leloup, F. Levrier, E. Linder, G. Luzzi, J. Macias-Perez, B. Maffei, D. Maino, S. Mandelli, E. Martínez-González et al. (87 additional authors not shown)

LiteBIRD, the Lite (Light) satellite for the study of B-mode polarization and Inflation from cosmic background Radiation Detection, is a space mission for primordial cosmology and fundamental physics. The Japan Aerospace Exploration Agency (JAXA) selected LiteBIRD in May 2019 as a strategic large-class (L-class) mission, with an expected launch in the late 2020s using JAXA's H3 rocket. LiteBIRD is planned to orbit the Sun-Earth Lagrangian point L2, where it will map the cosmic microwave background (CMB) polarization over the entire sky for three years, with three telescopes in 15 frequency bands between 34 and 448 GHz, to achieve an unprecedented total sensitivity of 2.2μK-arcmin, with a typical angular resolution of 0.5° at 100 GHz. The primary scientific objective of LiteBIRD is to search for the signal from cosmic inflation, either making a discovery or ruling out well-motivated inflationary models. The measurements of LiteBIRD will also provide us with insight into the quantum nature of gravity and other new physics beyond the standard models of particle physics and cosmology. We provide an overview of the LiteBIRD project, including scientific objectives, mission and system requirements, operation concept, spacecraft and payload module design, expected scientific outcomes, potential design extensions and synergies with other projects.

Comments: 155 pages, submitted to PTEP

Subjects: **Instrumentation and Methods for Astrophysics (astro-ph.IM)**; Cosmology and Nongalactic Astrophysics (astro-ph.CO)

Cite as: arXiv:2202.02773 **[astro-ph.IM]**

(or arXiv:2202.02773v1 **[astro-ph.IM]** for this version)